4-2016

Assessing the performance of a soy methyl ester - polystyrene topical treatment to extend the service life of concrete structures

D'Shawn G. Thomas
Purdue University

Graduate School Form
30 Updated 12/26/2015

PURDUE UNIVERSITY
GRADUATE SCHOOL
Thesis/Dissertation Acceptance

This is to certify that the thesis/dissertation prepared

By D'Shawn Gregory Thomas

Entitled
Assessing the Performance of a Soy Methyl Ester –Polystyrene Topical Treatment to Extend the Service Life of Concrete Structures

For the degree of Master of Science in Civil Engineering

Is approved by the final examining committee:

Jason Weiss
Chair

Pablo Zavattieri

Bernard Tao

To the best of my knowledge and as understood by the student in the Thesis/Dissertation Agreement, Publication Delay, and Certification Disclaimer (Graduate School Form 32), this thesis/dissertation adheres to the provisions of Purdue University's "Policy of Integrity in Research" and the use of copyright material.

Approved by Major Professor(s): Jason Weiss

Approved by: Dulcy Abraham 4/26/2016
Head of the Departmental Graduate Program Date

ASSESSING THE PERFORMANCE OF A SOY METHYL ESTER – POLYSTYRENE TOPICAL TREATMENT TO EXTEND THE SERVICE LIFE OF CONCRETE STRUCTURES

A Thesis

Submitted to the Faculty

of

Purdue University

by

D'Shawn G. Thomas

In Partial Fulfillment of the

Requirements for the Degree

of

Master of Science in Civil Engineering

May 2016

Purdue University

West Lafayette, IN

ACKNOWLEDGMENTS

This thesis includes research from a study titled “Assessing The Performance of a Soy Methyl Ester –Polystyrene Topical Treatment to Extend the Service Life of Concrete Structures” conducted by the School of Civil Engineering at Purdue University, which has been sponsored by the Indiana Soybean Alliance (ISA). Foremost, I would like to express my sincere gratitude to my advisor Dr. Jason Weiss for his continuous support, unrelenting patience, enthusiasm and guidance during my time at Purdue University. Besides my advisor, I would like express gratitude to the Indiana Soybean Alliance for their financial support of this research and to Dr. Bernard Tao and Dr. Pablo Zavattieri for serving as members of my thesis defense committee. I am extremely thankful for all the hard work, dedication and assistance provided to this research project by many of the graduate and undergraduate researches that I had the opportunity to work with over the course of this project. Lastly, to my family and my mother, without your continual support, spiritual leadership and encouragement none of this would have been possible.

TABLE OF CONTENTS

Page

Page

Page

Page

LIST OF TABLES

Table Page

Appendix Table Page

LIST OF FIGURES

Figure Page

Figure Page

Figure Page

Figure Page

Appendix Figure Page

Appendix Figure Page

Appendix Figure Page

NOTATIONS

The following symbols are used in this thesis:

A	= air content (percentage of voids) in the concrete
a	= area specimen
AE	= air entrained
B	= tortuosity of the material
CAI	= Center for Aging Infrastructure (CAI)
C (x, t)	= total chloride content at a depth x at time t (mass % concrete)
Cl^-	= total chlorides by % weight of concrete (%)
Cl^- Conc.	= total chlorides by % weight of concrete (%)
Co	= initial chloride concentration in concrete
Cs	= chloride concentration at the surface x=0 (mass % concrete)
D	= diffusion coefficient (m^2/s)
d	= days
D_o	= diffusion of ionic species in solution (m^2/s)
Do	= the initial degree of saturation for sample in volume fraction
Dapp	= apparent diffusion coefficient (m^2/s)
DOS	= degree of saturation
E	= salt exposure condition
erf	= the error function
F	= formation factor of the porous material
F-T	= freeze-thaw
f’c	= cylinder compressive strength of concrete (Mpa/Psi)
g	= grams
i	= normalized absorbed fluid volume (mm^3)
i_0	= intrinsic fluid absorption (mm)

M_{DM} = the demolded mass of an 8-in by 4-in specimen
m_o = initial mass of the specimen before exposure
M_{OD} = the oven dry mass of an 8-in by 4-in specimen
m_{OD} = the oven dry mass of a 2-in by 4-in specimen
m_{SSD} = the saturated surface dry mass of a 2-in by 4-in specimen
m_t = change in the specimen mass at time t
NAE = non-air entrained
OPCC = ordinary portland cement concrete
S1 = Initial Sorptivity Secondary
S2 = Secondary Sorptivity
SME = soy methyl ester
SME-PS = soy methyl ester-polystyrene
t = the duration of exposure
V_{filled} = volume of pores filled with a fluid the total pore volume ($V_{total)}$
V_{total} = the total pore volume
w/c = water-to-cement ratio
x = the distance from the concrete surface (m)
σ = bulk conductivity of the porous material in Siemens/meter (S/m)
σ_o = conductivity of the pore solution in Siemens/meter (S/m)
ρ = bulk resistivity of the porous material
ρ_o = resistivity of the pore solution
Φ = porosity of the material
ρ = density of absorbed fluid (1000 kg/m^3 at 23˚C for water)
γw = the surface tension for water (N/mm)
γs = the surface tension for solution (N/mm)
ηw = the viscosity for water (Pa·s)
ηs = the viscosity for solution (Pa·s)
Φ = the porosity of the sample in volume fraction

ABSTRACT

Thomas, D'Shawn. M.S.C.E., Purdue University, May 2016. Assessing The Performance of a Soy Methyl Ester –Polystyrene Topical Treatment to Extend the Service Life of Concrete Structures. Major Professor: W. Jason Weiss.

Experimental results show that soy methyl ester (SME), a derivative of soy bean oil, along with the incorporation of polystyrene (PS) is a non-toxic, biodegradable and renewable material that can be used effectively as a topical concrete surface treatment. While, concrete sealants and topical surface treatments can be used to extend to durability of concrete structures, it is difficult to predict the durability of concrete structures sealed with a sealant or topical surface treatment. This is due to a lack of necessary model inputs that can be used to address the durability of concrete structures treated with these materials. In general, this thesis expands upon previous research in exploring the use of SME-PS blends as a topical treatment used to enhance concrete durability and presents a sound theoretical framework for modeling the durability of concrete structures topically treated with SME-PS using Fick's 2nd Law of diffusion. Using experimental data generated in this study, fluid transport tests have been carried out to investigate how SME-PS changes fluid absorption and chloride ingress into concrete. The results show that the diffusion of chloride ions into concrete treated with SME-PS can be modeled by using a fractional amount (in this case 60% is recommended) of the value of Cs that is used for conventional concrete when Fick 2nd Law is used. This is critically important from a design and cost prospective, since tests do not need to be conducted with SME-PS to determine the benefits of surface treatment.

CHAPTER 1. INTRODUCTION, OBJECTIVES AND ORGANIZATION

1.1. Introduction

The need to increase sustainable infrastructure within the construction industry is largely driven by the need to use financial and environmental resources more economically and to preserve the structural systems we have in place. While, concrete is inherently quite strong and durable, concrete can be damaged by physical damage and chemical damage (i.e., chloride, carbonation, sulfate attack). One method that has been utilized to extend the service life of concrete structures is the use of concrete sealers or topically applied surface treatments. The primary purpose of a sealer or topical treatment is to limit the ingress of water and chemicals such as deicing salts. Reducing the ingress of water/deicing salts can potentially increase the service life of concrete structures. The use of conventional sealants such as siloxane and silicone to extend the service life of concrete structures and for construction applications are common in today's industry [2]. However, an alternative to these commonly used sealants is a soy methyl ester based topical treatment. Research has shown the use of SME along with the incorporation of polystyrene materials has shown the potential to be an economical solution to increasing the durability of concrete structures by mitigating chloride and fluid ingress. However, tests conducted on SME-PS blends has general have been geared towards understanding how SME-PS performs as "concrete sealant", and have solely focused on the short term performance of how SME-PS blends alter fluid transport and chloride ingress into concrete. Additionally, previous work on SME-PS has focused on tests performed in controlled laboratory settings. However, little has been done to establish a long term field observation program

to measure the effects and durability of SME-PS blends under true field conditions. This research is the initial phase of a long term study to address these needs.

1.2. Research Objectives

The material presented in this study serves as a continuation of previous research on the use of SME-PS blends as a topical concrete treatment used to enhance concrete durability. This thesis addresses the long term performance of SME-PS blends quantifies how SME-PS blends change fluid absorption and chloride ingress into concrete. The main objectives of this research program are to:

- Develop an extensive outdoor study to investigate the use of SME-PS blends in concrete mixtures with varying water to cement binder ratios.
- Conduct fluid transport tests on cementitious materials as a characterization tool for portland cement-based materials.
- Present a fluid transport study on SME-PS treated cementitious materials exposed to accelerated testing conditions.
- Highlight a series of factors that affect the measurements, including sample conditioning, exposure time, salt type, water to cement binder ratios, surface chloride concentration, diffusivity, SME-PS application rate and material composition.
- Develop a methodology to predict the service life of cementitious materials topically treated with SME-PS.

1.3. Research Organization

This thesis presents an approach for modeling concrete durability in the presence of SME-PS. The first phase of this study utilized a fundamental approach to characterize the constituent materials used in this investigation. It is important to characterize the constituent materials (i.e., concrete mixture designs) in order to effectively compare the durability of untreated specimens with that of SME-PS treated specimens to determine the benefits of surface treatment. The first phase

of work was divided into four main tasks, which has been laid out in Chapter 3 of this thesis. To complete the work, four different concrete mixtures were selected for this experimental investigation, one specified by the Indiana Department of Transportation (INDOT) and three variations of that mixture. The mixtures were selected to demonstrate how SME-PS blends extend the service life of mixtures exposed to accelerated exposure conditions. The second phase of this study, outlined in Chapter 4 of this thesis, evaluates how SME-PS influences fluid and chloride ingress in cementitious systems and investigates how to predict the service life of concrete materials that have been treated with SME-PS.

CHAPTER 2. LITERATURE REVIEW ON SME-PS BLENDS AND RELATED WORK

2.1. Introduction

This chapter offers a background on the use of SME-PS topical treatments and incorporates information discovered during the literature review. The literature review focuses primarily on the "Evaluation of Soy Methyl Ester Polystyrene Blends for Use in Concrete" by Coates [3], and "The Use of Soy Methyl Ester-Polystyrene Sealants and Internal Curing to Enhance Concrete Durability" by Golias [4]. Both studies provide an extensive summarization of work on SME-PS blends. Articles and technical reports by Farnam [5, 6] and Jones [7] were also considered in this study.

2.2. Topical Sealants

Topical concrete sealants and surface treatments are often used to limit the ingress of aqueous fluids and chemicals from entering into a cementitious system such as concrete [8]. After the initial hydration and hardening of concrete has taken place, water that enters the concrete can have adverse effects on the integrity of the system [8]. Aqueous fluids are able to readily dissolve and transport deleterious chemicals such as oxygen, sulfates and carbon dioxide [8]. While, it is often thought that the fluid in concrete pores is water, this is not true [8]. Many durability problems that are associated with concrete structures are caused by the transport of fluid containing chloride ions [8]. Water and other chemicals can enter the pores of cementitious systems by various different means such as diffusion and capillary action [8]. Therefore, many seek to predict the durability of concrete structures by using fluid transport models such absorption (i.e., ASTM C1585) models and Fick's 2nd law of diffusion to assess the service life of concrete

structures. However, sealing concrete systems can effectively slow down the processes that are dependent upon exposure to water and other chemicals that can be deleterious to concrete and steel reinforcement [8]. Furthermore, topical concrete sealants and surface treatments can reduce the moisture in concrete systems from reaching critical levels that enable deterioration processes to take place or accelerate [8]. For newly constructed concrete systems, modern mixture designs and adequate air entrainment can help to mitigate water permeability and the expansion of water undergoing freezing and thawing processes [8]. However, construction practices and the placement of concrete can cause variability in the durability of concrete materials [8]. Moreover, early age cracking is often a problem that is noted to take place in newly placed concrete structures. In effect the sealing of concrete can extend the service life of cementitious systems [8]. Furthermore, studies have shown that topical sealers applied to old concrete systems that are in a low to moderate stages of deterioration also have the potential to extend the service life of those systems by slowing the process of deterioration [8].

2.3. Deicing Salts

Deicing salt, which is typically used on the surface of concrete structures in order to depress the temperature at which water freezes can increase safety and help with snow removal. However, deicing salts can induce damage in concrete structures [4]. As the deicing salts, which contains chlorides ions, are absorbed into the concrete, they induce corrosion in the reinforcing steel, cause surface scaling, and form salt crystals within the pore matrix, which can cause damage to the concrete [4]. Deterioration is accelerated in environments where concrete structures are subjected to aqueous salt solutions, and environments subjected to freezing and thawing cycles [5,8]. When an aqueous salt solution comes into contact with concrete that undergoes ponding or a wetting and drying process, the concentration of salt can build up over time [8]. As salt travels through cementitious systems, salt is able to crystalize inside the pore system [8]. Furthermore, as water enters concrete and freezes, the expansive ice along with the salt crystals, can

cause a buildup in pressure in the system which can lead to deterioration by method of cracking [8]. Different chloride based salts can influence the transport properties of cementitious materials in different ways. Aqueous solutions containing $CaCl_2$ and $MgCl_2$ can cause the formation of chemical phase changes such as calcium oxychloride and magnesium oxychloride. Sealers have traditionally been used to coat concrete structures such as pavements and bridge decks [17]. Research has shown that soy based sealers can reduce deterioration and extend the overall life expectancy of concrete elements [3, 4].

2.4. Conventional Sealer Application Requirements

Many factors can affect the performance of concrete sealers such as the rate of application the sealer is applied to the surface of concrete, climatic conditions, the condition of the concrete and surface preparation [8]. Typically, manufacturers provide specific application requirements for different types of concrete sealers in order to achieve the best performance [8]. The condition of the concrete can greatly affect the performance of the sealer [8]. Typically, sealers are the most effective on concretes that have experienced no more than a low to moderate stage of deterioration [8]. If a sealer is applied to the surface of concrete that has experienced a substantial amount of deterioration the effectiveness of the sealers diminishes [8].

2.5. Background on Soy-Methyl-Ester Polystyrene Blends

Many industries have moved towards sustainable solutions, driven in part by the need to address environmental concerns, which has prompted the use of more environmentally friendly materials such as soy beans. Soy bean derivatives have proven to be prime examples of biodegradable, non-toxic, non-corrosive, renewable and economical resources [3]. The extracted oils from soybeans have many uses from soaps, cosmetics, paints, solvents, resins, pesticides, and plastics [11]. Recent studies have shown that soy methyl esters, which are derived from soy bean oils have the potential to be to be used in the construction industry as

both an asphalt remover and as a topical concrete sealant [4,9]. Soy methyl esters, which are a byproduct of the esterification of soy bean oils consist of long fatty acids that are esterified to a methyl group [4]. To create a soy methyl ester material, soy bean oil is usually mixed which a methanol alcohol and alkaline catalyst such as sodium hydroxide [4]. The process by which the soy bean oil becomes a soy methyl ester is called transesterification [4]. The result of the transesterification is a fatty acid methyl ester molecule [4].

2.5.1. Creating a SME-PS blend

SME has a high solvent capacity, enabling the material to be able to hold dissolved components such as polymers, which can alter the physical properties of the SME [11]. Adding a polymer such as polystyrene influences the fluid behavior by altering the viscosity of the material [11]. Although any form of polystyrene can be used, it is advantageous to use waste or recycled polystyrene for the reasons that there could be potential environmental benefits, reduced cost, and the abundance of recycled materials [11]. Polystyrene is a thermoplastic, long chain-like molecule that can be used to increase the viscosity of SME when added [3,4]. Polystyrene can be easily added to SME by heating and mixing the SME and polystyrene [3,4]. This can significantly influence the sealant's ability to adhere to the walls of the concrete which in effect can influence the efficiency of the sealant's ability to mitigate the transport of fluids [3,4]. Ideal conditions for sealing concrete involve limiting the polystyrene content to 2-10%PS to ensure that SME does not penetrate too far into the concrete and to ensure that SME is absorbed quickly into the concrete [3]. In this experimental investigation, only one SME blend was used for all experiments. Unless otherwise noted, the SME blend reported throughout this study is an SME blend that incorporates 2% by mass polystyrene [3].

2.5.2. Dispersion of SME-PS in Cementitious Mixtures

Mixing SME in aqueous solutions that contain hydraulic cement powder presents a practical problem because that SME-PS blended solutions contain hydrophobic agents [4]. Due to the hydrophobic nature of SME particles, SME-PS is able to quickly separate when water is added, as shown in Figure 2.1.

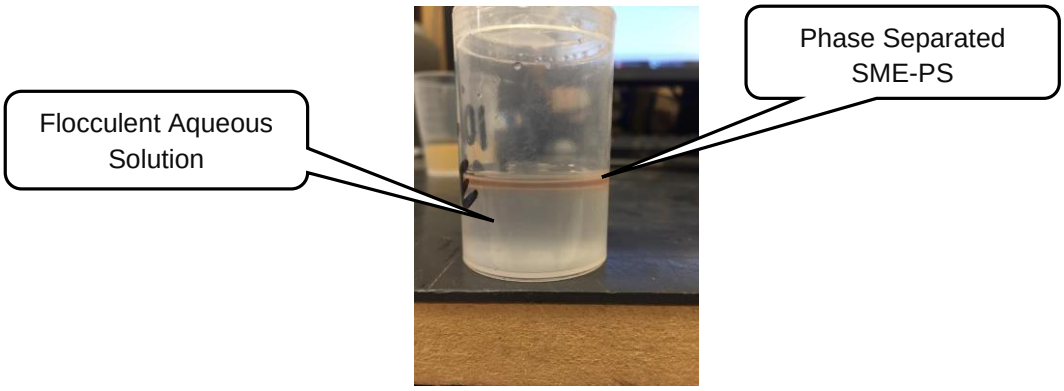

Figure 2-1: Phase Separation of Soy Methyl Ester Polystyrene Blend in Water

In Coates [3] investigation of SME-PS blends in concrete, it was observed that when SME came into contact with dry constituent materials (i.e., un-hydrated cement power, fine aggregates, etc.) before being added to an aqueous solution, the particles tended to coat the SME-PS and would tend to agglomerate throughout the mixing process [4]. Once absorbed onto the surface of the cement, the SME-PS will only separate from the surface under high shear rates which is not achieved under normal mixing speeds [4]. Golias [4] proposed that before adding SME to the constituent materials, the materials should be mixed with the aqueous solution before the addition of SME-PS. This proposed method found that large particle agglomeration did not form, resulting in a more homogeneous mixture.

2.5.3. Penetration of SME into Concrete

The rate of penetration of SME-PS into concrete is a function of the concrete moisture level, size of the polystyrene molecules, and time [4]. As the concrete

moisture level increases, the rate of absorption of the SME-PS blend will decrease [4]. Likewise, as the polystyrene chain length increases, the rate of absorption of the SME-PS will also decrease [4]. Furthermore, when SME is first exposed to concrete, the rate of absorption will be relatively quick, but over time the rate of absorption of the SME-PS into the concrete will decrease [3,4]. Research by Golias [4] recommends that the dosage of SME applied to concrete specimens should also be maximized in order to attain a higher resistance to deleterious mechanisms. This can be accomplished by ensuring that the concrete surface is free from moisture before applying the topical treatment and allowing ample time for the sealant to penetrate the concrete. Therefore, it is also important, that application not occur when temperatures are below the dew point, which is the point at which liquid water will condense on solid surfaces. This ensures the pores of the concrete are open and available to absorb the applied SME-PS.

2.5.4. Cold Weather Behavior of SME-PS

Typically, most materials undergo a phase change as the material reaches its freezing or melting point [4, 12]. Water, for example, considered to be a single phase liquid, experiences a phase change for the entire system as the temperature changes from 1°C (33.8°F) to 0°C (32°F) [4, 12]. On the other hand, SME, a multi-phase material, does not behave in the same manner [4, 12]. SME, which consist of Fatty Acid Methyl Esters (FAME) derived from the transesterification of the soy bean oil with methanol, each have their own unique temperature that can result in a phase change [4, 12]. When SME reaches a temperature of 0°C, known as the “cloud point” the FAMEs will begin to lose their solubility and will come out of solution [4]. The cloud point of SME with 5% and 10% PS is typically accepted to be 5°C. Furthermore, as the SME reaches this “critical” temperature a second solid phase will begin to form in solution, which appears as conglomerations of waxy crystals that give a cloudy appearance [4, 12]. The appearance of ‘cloudiness’ indicates that some components have changed into a solid phase while others remain in a liquid state. To achieve greater penetrating performance of the SME-

PS sealant, it becomes important to monitor the temperature at which SME is applied to the concrete. It is recommended that SME-PS be applied to concrete specimens in warmer months. If SME-PS nears the could point temperature, the SME-PS will lose its ability to penetrate the concrete [9]. At temperatures below 0°C, more FAMEs will precipitate out of solution and become a waxy gel like substance [4, 12]. Eventually, SME will lose its ability to flow like a liquid once its reaches what is known as the “pour point” at -4°C [4, 12]. The pour point of a liquid is the temperature at which the material becomes semi solid and loses its flow characteristics.

2.5.5. Effect of SME-PS on Concrete Durability

Previous work addressing the use of SME-PS as a “concrete sealer” by Coates [3] and Golias [4] have demonstrated SME-PS blends are economical alternatives to conventional sealers. The hydrophobic nature of SME makes the material ideal to be used as a water reducing sealant that can be used to enhance the durability of concrete [3,4]. SME has been shown to be capable of reducing water absorption (up to 75%), preventing damage caused by freezing and thawing (reduces damage by 66%) processes, and is able to prevent the formation of calcium oxychloride in cementitious systems exposed to Calcium Chloride salt [3-5]. Recent studies by Farnam et al. (2015a), have suggested that use of SME can be used to effectively seal concrete systems to prevent aqueous solutions containing $CaCl_2$ from entering the concrete [5]. $CaCl_2$ can cause a considerable amount of damage in concrete resulting from the formation of calcium oxychloride [5].

$$3Ca(OH)_2 + CaCl_2 + 12H_2O \rightarrow CaCl_2{\cdot}3Ca(OH)_2{\cdot}12H_2O \quad Equation\ [2.1]$$

Calcium Oxychloride

The formation of calcium oxychloride is suggested to be a chemical phase transition, characterized by using low temperature differential scanning calorimetry (LT-DSC) [5]. Farnam *et al.* (2015a), cited that using LT-DSC (see Figure 2-2) on

plain mortar samples treated with SME showed no peak or phase transformation corresponding to the formation of calcium oxychloride [5]. Farnam *et al.* (2015a), cited that using LT-DSC (see Figure 2-2) on plain mortar samples treated with SME showed no peak or phase transformation corresponding to the formation of calcium oxychloride [5]. On the other hand, a considerable amount of calcium oxychloride formation was observed for plain mortar samples not treated with SME [5]. In cementitious systems containing calcium hydroxide $Ca(OH)_2$, the formation of calcium oxychloride has been reported to be very destructive [5]. It has been suggested that the formation of calcium oxychloride in concrete results in a large volume structure that is characterized to be more expansive than water undergoing freezing and thawing cycles within the pore network of a concrete system [5]. Since, SME contains hydrophobic agents, SME-PS sealants have the ability to repel fluid which makes them very suitable and ideal to be used as a topical sealant to prevent the formation of calcium oxychloride [5].

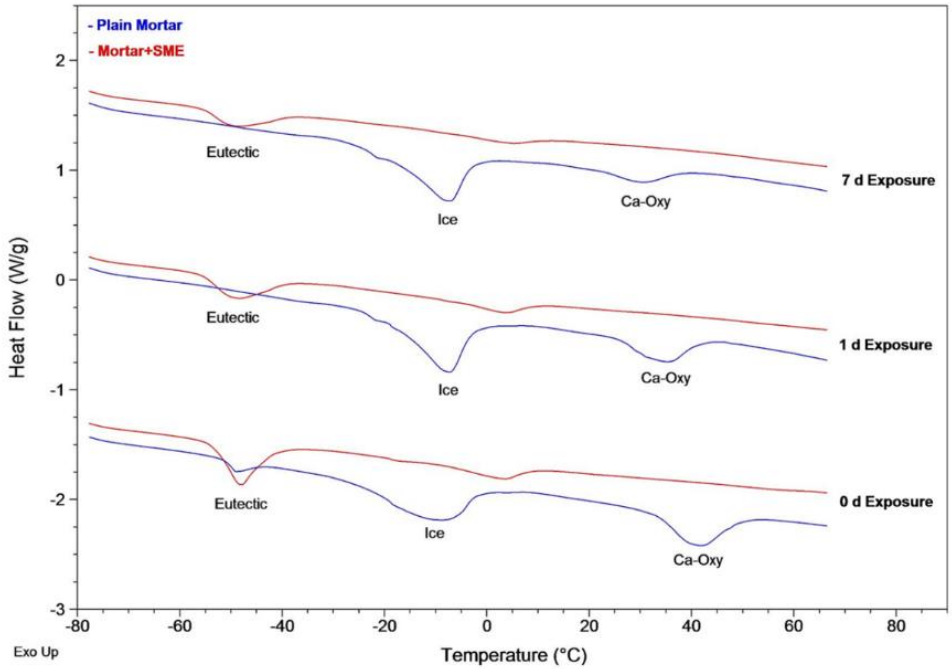

Figure 2-2: Low temperature differential scanning calorimetry (LT-DSC) for plain mortar sample and mortar sample with SME at different exposure times to 29.8% CaCl2 solution (calcium oxychloride is shown as Ca-Oxy in the figure) [5]

2.6. Summary and Conclusions

This chapter briefly reviews methods to predict and extend the service life of concrete elements in the presence of fluid or aqueous solutions containing chlorides. The chapter reviews background on use of SME-PS blends as an alternative method to reduce deleterious mechanisms in concrete. Finally, a brief overview of some precautions is detailed that should be understood about the use of SME-PS as a topical concrete surface treatment before application of material in the field. Based on the literature review, the following conclusions and observations may be summarized as follows:

- First, the absorption of fluid into concrete can be assessed by using transport models such absorption (i.e., ASTM C1585). The diffusion of chloride ions will be assessed using Fick's second law of diffusion.
- Second, there is a critical temperature known as the "cloud point" at which SME and SME-PS blends will have a greatly reduced ability to penetrate into concrete. Therefore, it is important to monitor the temperature at which SME-PS is applied to concrete specimens in the field. For SME this temperature is generally accepted as 0°C and for SME-PS blends with 5% to 10% PS, it is 5°C.
- Third, to maximize the performance of SME-PS blends used for field applications, it is also important that application of SME-PS not occur when temperatures at the time of application are below the dew point. This enables the pore structure of the concrete to be open and available to absorb the applied SME-PS.
- Finally, the dosage of SME-PS applied to concrete specimens should also be maximized in order to attain a higher resistance to deleterious mechanisms. This can be accomplished by ensuring that the concrete surface is free from moisture before applying the topical treatment and allowing ample time for the SME-PS to penetrate the concrete.

CHAPTER 3. CHARACTERIZATION OF MATERIALS: AN ANALYSIS OF THE DURABILITY OF UNTREATED ORDINARY PORTLAND CEMENT CONCRETE

3.1. Introduction

The goal of applying topical concrete treatments to the surface of concrete is to extend the service life of concrete pavements and structures by limiting fluid and chemical ingress. However, before further assessing the performance of SME-PS, it is necessary to understand the concrete to which the topical surface treatment is applied. This chapter characterizes the concrete mixture designs that are used in this study. Furthermore, this chapter intends to establish a conceptual framework and to discuss the experimental methods and procedures used to characterize the concrete materials used in this investigation.

3.2. Background: A Brief Assessment of Concrete Properties and the Use of Non-Destructive Testing to Quantify the Durability of Concrete Materials

3.2.1. Critical Degree of Saturation

Many studies have indicated that as the DOS (degree of saturation) increases in low temperature environments, the likelihood of deterioration by method of freeze thaw damage increases [4]. Concrete experiences damage once it reaches a critical DOS and undergoes temperature cycles that enable freezing and thawing [4]. Damage that occurs from the result of freezing and thawing can cause premature deterioration and early replacement of concrete infrastructural elements [4]. When water freezes, it is capable of expanding up to 9% of its original volume. The ice puts pressure on the surrounding concrete which causes damage to the

concrete when the DOS exceeds what is known as the critical degree of saturation (~86-88%) [4]. Once concrete reaches the critical DOS or when the pores inside the cementitious system are around 86%-88% full, deterioration by freeze thaw damage is inevitable [4]. Freezing and thawing damage can result in costly repairs which is why concrete is frequently air entrained in order to decrease the chances of concrete experiencing freeze thaw damage [4].

3.2.2. Porosity and Initial Degree of Saturation

Porosity (Φ) and DOS can govern many aspects of the durability of a cementitious material from strength, corrosion, facture and shrinkage [13]. The DOS can be defined as the volume of pores filled with a fluid (V_{filled}) and the total pore volume (V_{total}) as shown in Equation 3.1.

$$DOS = \frac{V_{filled}}{V_{total}} \qquad Equation\ [3.1]$$

The porosity of hardened cement paste of a cementitious system from a chemistry standpoint is defined by Powers and Brownyard (1947) as the fraction of the volume of a saturated material (i.e., concrete) that is occupied by evaporable water [14]. Concrete porosity can be primarily thought of as the space or voids in concrete that can be filled with air or water. The tortuosity of concrete is a geometric property of the porous medium that characterizes the complex pathways of fluid diffusion and electrical conductivity through a porous medium [15, 16]. Researchers, have verified the greater the tortuosity, the longer fluid will take to flow through a porous medium, which correlates to lower permeability [15, 16]. Furthermore, as the porosity of a material decreases the tortuosity of the material likely increases [16]. Porosity in the cement paste includes large and small pores (i.e., gel pores, capillary pores, and air voids). Air voids (i.e., entrapped and entrained air) are slightly larger than both capillary and gel pores and range in diameter from 0.5 mm to 1.25 mm [13]. Air voids are penetrable, but since they

appear to be isolated in the microstructure and do not form a continuous pathway for flow, it is often assumed that they make little to no contribution to the transport of fluid in concrete. The smallest of the pores, the gel pores, which range in diameter from about 0.5 nm to 10nm, are an intrinsic part of the hydrated cement that form in the reacted hydrated product [13]. Capillary porosity, which is slightly larger than gel porosity, ranges in diameter from about 10nm to 10μm [13]. Capillary porosity is dependent on the w/c (water to cement ratio). As concrete hardens, the water that has not reacted with cement leaves voids inside the cementitious system [13]. As the degree of hydration (DOH) increases (i.e., the amount of cement that has reacted with water in the cementitious system) capillary porosity decreases. Differences in pore sizes can also influence how quickly concrete can absorb fluids [13]. Typically, smaller pores generate high capillary pressure which causes a rapid uptake of water [13]. On the other hand, larger pores generate low capillary pressure and remain air filled without the presence of water till the smaller pores become saturated [13].

3.2.3. Electrical Resistivity and Formation Factor

Electrical resistivity can be directly related to fluid transport properties which can be used to obtain information on ion and fluid transport, the speed at which fluid and other ionic species move through the concrete [17]. Electrical resistivity measurements can also provide an indication as to how concrete will perform throughout its service life [17]. The resistivity, or its inverse conductivity, of a porous material can be related to diffusion by a material property called the formation factor [17]. The formation factor is determined from the measurement of the bulk electrical properties (e.g., resistivity or conductivity) of a porous material [17]. As defined in Equation 3.2-3.3, the formation factor is a function of the total liquid filled porosity of the concrete and the connectedness of the concrete pore network [17]. In other words, the formation factor can be thought of as a measurement of the volume of pores and their connectivity. For a nonconductive porous material such as concrete, that contains a conductive pore solution, the

formation factor is the ratio of the pore solution conductivity σ_O to the bulk conductivity (σ) of the material [18]. Studies have proposed that the concept of the formation factor can be used to create service life specifications for porous cementitious materials [13]. Furthermore, the formation factor, which provides a link between conductivity and diffusion is used to characterize the pore structure of a material and its ability to mitigate ions from entering a saturated system [17]. Lower formation factors (implying conductivity increases) can be interpreted as having more pore connectivity and pore volume. On the other hand, a higher formation factor (implying decreasing conductivity) can be interpreted as less interconnected and having less pore volume. However, unlike the determination of the bulk resistivity of a specimen which can vary even with a specimen of the same tortuosity, the formation factor will remain the same [17].

$$F = \frac{\sigma}{\sigma_O} = \frac{\rho}{\rho_O} = \frac{1}{\Phi\beta} \qquad Equation\ [3.2]$$

$$D = \frac{D_O\sigma}{\sigma_O} = \frac{D_O\rho}{\rho_O} \qquad Equation\ [3.3]$$

Where, F = Formation factor of the porous material, σ = bulk conductivity of the porous material in Siemens/meter (S/m), σ_o = conductivity of the pore solution in Siemens/meter (S/m), ρ = bulk resistivity of the porous material, ρ_o = resistivity of the pore solution, D= Diffusion coefficient (m^2/s), D_o =Diffusion of ionic species in solution (m^2/s), Φ= porosity of the material, β= pore connectivity of the material. The resistivity of concrete is a function of the porosity of the concrete, the DOS, the connectivity of the pore network and the resistivity of the pore solution in the concrete. However, Spragg [17] has shown factors such as variations in geometry and temperature alter the resistivity of the concrete. Therefore, in order to compare specimens with varying geometries and temperatures resistivity needs to be corrected to obtain, geometry and temperature independent resistivity [17].

Specimens that were considered for this experiment were not conditioned in an environmental chamber but started from a sealed condition. Specimens from each concrete mixture design were used to test the materials electrical resistance for a period of 2 months and for a period lasting less than 2 weeks using an EIS (Electrochemical Impedance Spectroscopy) machine and Wenner probe. Before testing the electrical resistance of the materials, a synthetic pore solution was created using a pore solution conductivity calculator by NIST (National Institute of Standards and Technology) and the cement chemistry to prevent the leaching of alkalis that exist in concrete. The first type of ions that exist in concrete are called free chloride ions which are the chloride ions that are dissolved in the pore water inside concrete [17] and the second type of chloride ions are the ions that are chemically bound to the cement paste [17]. The last type of ions are chloride ions that are chemically bound within the aggregate [17].

3.2.4. Water Absorption Test

ASTM C1585-13 (Standard Test Method for Measurement of Rate of Absorption) is used to determine the rate of water absorption (sorptivity) of hydraulic cement concrete by measuring the increase in the mass of the specimen resulting from the absorption of water as a function of time [19]. The intersection point where initial sorptivity terminates and secondary sorptivity commences on the absorption curve is known as the nick point. The nick point corresponds to the stage where all the small pores (i.e., capillary pores and gels pores) are completely water filled (air voids unfilled) [19]. Due to the considerable amount of capillary suction generated by the small pores, the pores are able to become saturated within a short period of time [19]. The water absorption that occurs after the nick point corresponds to the gradual water filling of the large pores [19]. The gradual water filling of the large pores in a cementitious system is slower than that of smaller capillary pores due to large pores not generating as much capillary suction as smaller pores [19]. In order to compensate for variable changes in the cross sectional areas of the

specimens used in this study the amount of absorbed water is normalized by the cross sectional area of the specimens exposed to the fluid [19] using Equation 3.4:

$$i = \frac{m_t - m_o}{(a \cdot \rho)}$$

Where, i is the normalized absorbed fluid volume (mm^3), m_t is the change in the specimen mass at time t, m_o is the initial mass of the specimen before exposure, a is the area of the unexposed bottom surface of the specimen exposed to water, and p is the density of the absorbed water (taken to be 1000 kg/m^3 at 23˚C).

3.3. Materials and Methods

The raw materials used in this study were selected based on the following criteria: 1) The raw materials be locally available and 2) the raw materials be approved by INDOT for use on pavement projects. Unless noted otherwise, the following materials were utilized for all experiments described in this thesis. Ordinary Portland Cement (OPC) was used for each mixture design that was considered in this study, with a Blaine fineness of 395 m^2/kg and estimated potential phase composition of 65.5% C_3S, 6.6% C_2S, 8% C_3A, 9.0% C_4AF, and a Na_2O equivalent of 0.67% by mass. The fine aggregate that was utilized in all experiments had a specific gravity of 2.65 and absorption of 1.20%.

A Super Air Meter (SAM) device was used to assess the quality of the air void distribution of the fresh concrete cast in the field [20]. The SAM device is a testing meter that measures both the air content of fresh concrete and outputs a SAM number which is believed to correlate to air void distribution [20]. The air void spacing in concrete has shown to be a better predictor of concrete F-T durability than air content [20]. Powers and Brownyard (1949) developed the concept of the spacing factor, which is recognized as a measurement of the quality of the air voids in a cementitious system [21]. Rapid laboratory F-T studies by Backstrom et al. (1958) found that a spacing factor of 0.008 in was needed to provide proper F-T durability [22]. Furthermore, the ACI (American Concrete Institute) 201 committee

[23] on the concrete durability and ACI 212 committee on concrete admixtures [23] also recommends a spacing factor of 0.008 in. Although, a spacing factor less than 0.008-in is suitable [23], a spacing factor of 0.008 in is indicative of frost resistance concrete [23]. Typically, a lower SAM number indicates a well distributed air void system, which is defined by a low spacing factor and a higher specific surface [13, 20]. SAM numbers less than or equal to 0.20 have shown to be relatively good indicators of adequate air void systems, with a spacing factors lower than 0.008 in and specific surface values above 600-in^{-1} [13, 20]. The amount of variability for the SAM numbers presented in Table 3-1 is not available for the mixtures considered in this investigation. However, the SAM number over a sequence of measurements is expected to vary with each mixture design.

The experimentation was divided into several different sections as described in Table 3-1. Porosity and DOS test were performed to measure the voids in concrete that can be filled with air and fluid. Compressive strength tests were performed as a basis for quality control of concrete proportioning and mixing. Electrical resistivity measurements were performed to provide an indication as to how concrete materials will potentially perform throughout its service life. Water absorption and chloride ion penetration tests were performed in order to understand how SME-PS changes fluid absorption and chloride ingress into samples treated with SME-PS versus samples that were left untreated.

TABLE 3-1 Overview of Experimental Testing Program

Property	Test Method	Specimen Size	Quantity	Description	Deliverable
Porosity	ASTM C642	2-in. X 4-in. cylinders	2 cylinders per w/c	No-SME	φ
Degree of Saturation (DOS)	Degree of Saturation (DOS) Test	2-in. X 4-in. cylinders	2 cylinders per w/c	No-SME	DOS
Compressive Strength (f'c)	ASTM C39	4-in. X 8-in. cylinders	3 cylinders per w/c	No-SME	f'c
Resistivity of Concrete	Uniaxial EIS Machine & Wenner Probe	4-in. X 8-in. cylinders	2 cylinders per w/c	No-SME	F, Po, P
Water Absorption Test (23°C)	ASTM C1585	2-in. X 4-in. cylinders	2 cylinders per w/c	2%SME-PS, No-SME	S1, S2
Chloride Ion Penetration	Ponding Test & Visible & Chemical Titration Test	3-in. x 4-in. cylinders (Ponding Test) 5-ft. x 6-ft. x 6-in. Pavements (Field Test)	36 cylinders (Ponding Test) 36 Pavements Total (Field Test)*	2%SME-PS No-SME	Cs, Dapp, Cl^- Conc.

3.3.1. Mixture Proportions

The study assessed four different concrete mixture designs with three different w/c (0.42, 0.49 and 0.56) that were air entrained and a similar w/c (0.49) mixture that was non-air entrained. The concrete mixtures for this experimental investigation were used to construct concrete pavements using a sidewalk mixture design specified by the Indiana Department of Transportation (INDOT) as well as several other variations. The mixture design specified by INDOT was made in accordance to a Class C concrete as per section 702.02 of the 2016 INDOT standard specification for concrete. The concrete mixture design that was specified by INDOT is denoted as mixture No.1, in Table 3-2. The INDOT mixture design as well as the other three variations were all provided by the ready mixture plant Irving Material, Inc. (IMI). The INDOT mixture design was prepared using a 6.6% air entrained, 0.42 w/c mixture with 29% fine aggregates and 39% coarse aggregates.

Mixture No.2 was prepared using a 7% air entrained, 0.49 w/c mixture with 28% fine aggregates and 38% coarse aggregates. Mixture No.3 was prepared using a 6% air entrained, 0.59 w/c mixture with 28% fine aggregates and 37% coarse aggregates and mixture No.4 was prepared using a non-air entrained, 0.49 w/c mixture with 30% fine aggregates and 40% coarse aggregates with a measured air content of 1.7%.

TABLE 3-2. Mixture Proportions and Naming Conventions

Concrete Mixture ID	Mixture 1	Mixture 2	Mixture 3	Mixture 4
Materials	lbs./yd^3	lbs./yd^3	lbs./yd^3	lbs./yd^3
Cement	564	564	550.4	573
Sand	1312	1268	1238	1333
Coarse Aggregate	1800	1740	1699.5	1829
Water	237	275	308	281
w/c	0.42	0.49	0.56	0.49
Air Content	6.6%	7.0%	6.0%	1.7%
SAM Number	0.14	0.23	0.20	0.55
Σ	3913	3847	3796	4016

3.3.2. Mixture Procedures

The mixing procedure for the design mixtures that were used in this investigation were prepared and carried out by Irving Material, Inc. (IMI). Prior to the cast of each of the four mixture designs considered in this study a batch of aggregates were taken from the IMI ready mix plant to be oven dried at 105°C and cooled. Oven drying and cooling the aggregates was done to account for any additional water absorbed by the aggregate to correct for the amount of water added to the mixture design by the ready mix plant. Upon arrival of the ready mix truck in the field, a slump and air content test were performed in accordance to ASTM C143 (Standard Test Method for Slump of Hydraulic Cement Concrete), and ASTM C231 (Standard Test Method for Air Content of Freshly Mixed Concrete by the Pressure

Method), respectively. Fabrication of compressive strength cylinders and other cylinders for fluid transport tests were started immediately upon the arrival of the read mix truck (see Figure 3-1.). All cylindrical specimens were cast in plastic molds which is considered a sealed (constant moisture) condition, and consolidated by rodding. The cylinders were allowed to cure inside the containers for 28 days.

Figure 3-1: Laboratory Concrete Test specimens in the Field.

3.3.3. Compressive Strength

The compressive strength (f'c) of the materials used in this experiment were determined in accordance with ASTM C39 (2012a). For each mixture design that was considered in the evaluation of the SME-PS, a set of three 4-in. by 8-in. cylinders were cast to study the f'c of the materials for a testing age of 28 days. The cylinders were cast in two lifts and rodded 25 times after each lift before placing a lid on the containers. The specimens were kept in the field for one day and then taken to a lab and stored in a lab environment at room temperature before being demolded at a material age of 28 days. At 28 days, after the demolding the cylinders, three cylinders were tested to determine the compressive strength at 28 ± 1 days. Using neoprene end caps the cylinders were loaded at rate of 35 ± 2 psi/s in a 700-kip hydraulic compression machine. The fracture pattern and compressive strength (f'c) were recorded, and an average compressive strength

was taken for each of the three cylinders from each mixture design (Table 3-2). The cylinders were all cast at the Center for Aging Infrastructure. Experimental results can be seen in Figure 3-2.

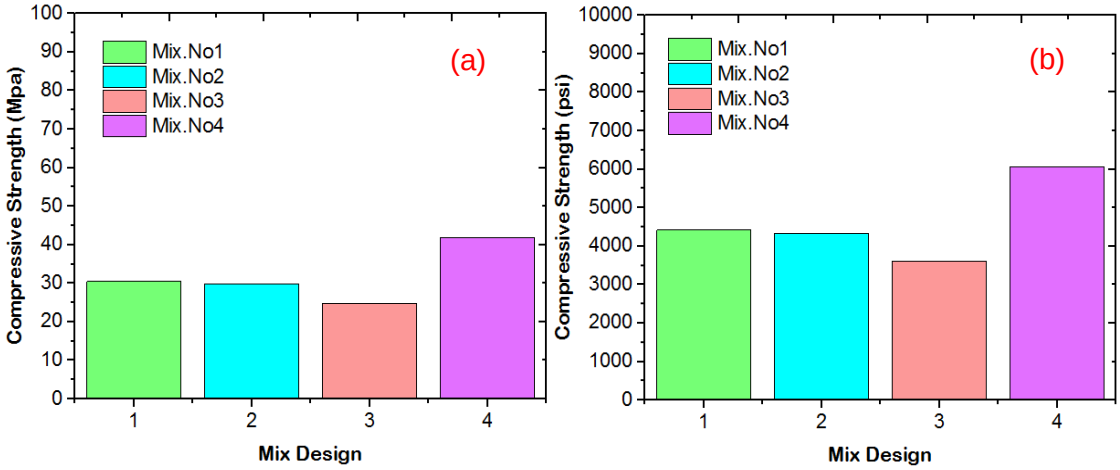

Figure 3-2: Compressive Strength Experimental Results. (a) Mpa, (b) Psi.

Typically, specimens that do not meet f'c requirements have issues dealing with improper rodding. Generally, materials with higher w/c exhibit lower compressive strengths at 28 days than materials that have lower w/c. This is consistent with the results presented in Figure 3-2. The numerical compressive strength values for each mixture at a material age of 28 days is also listed in Appendix A of this thesis.

3.3.4. Field Testing

The field component of this research is limited in duration (only one year has elapsed), however research is ongoing. The same topical treatment applied in the field was also applied to specimens in the laboratory. The SME-PS was applied to field pavement specimens using a backpack sprayer in November 2014 at the Center for Aging Infrastructure (CAI), a new field exposure site that was installed south of Purdue University's Campus on South River Road (see Figure 3-3.,3-4.).

Figure 3-3: Panorama View of the Center for Aging Infrastructure: Slabs Covered for 28-day Curing

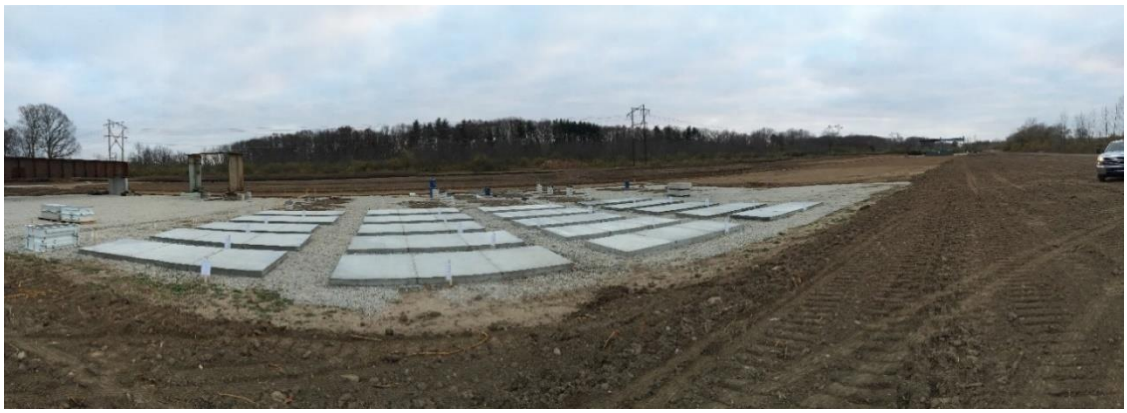

Figure 3-4: Panorama View of the Center for Aging Infrastructure: Slab Exposure Site

The concrete pavements fabricated from each mixture design that was cast for this investigation each consisted of fifteen, 5 ft. x 6 ft. by 6-inch-thick slabs as shown in Figure 3-4. 20 Slabs were left untreated with SME-PS. The remaining 40 slabs were topically treated using one or two applications of SME-PS and exposed to continuous salting using a backpack sprayer. In total, 60 slabs were placed (i.e., 15 slabs per mix design) in the field. However, for this investigation only 36 slabs were considered (24-selaed specimens and 12-plain/untreated reference specimens). A general layout of the field exposure site is shown in Figure 3-5.

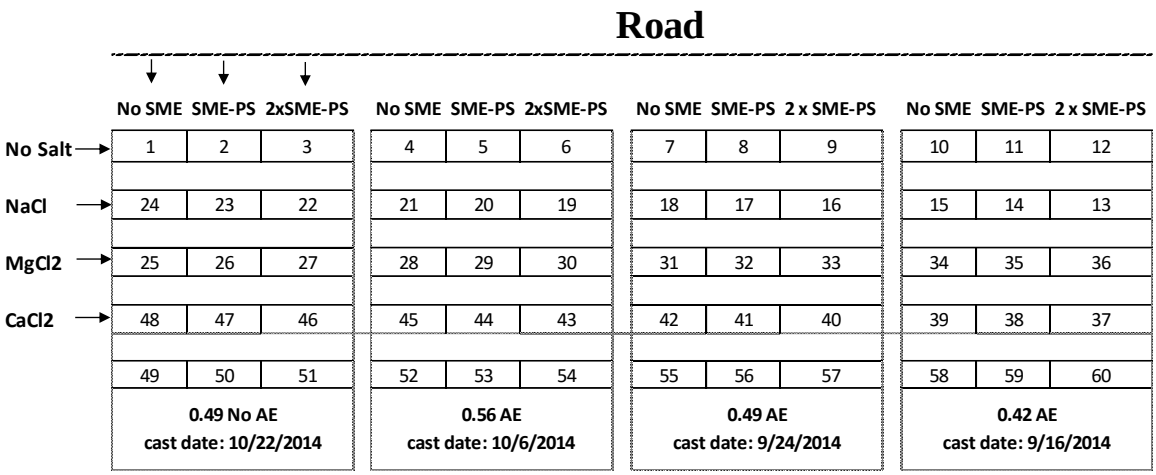

Figure 3-5: General Site Layout of the Exposure Site at CAI (1)

Cored specimens were later extracted from treated and untreated areas 4 and 9 months after initial salt exposure in December 2014 to determine the chloride depth of penetration and the long term effectiveness of the SME-PS blend. The pavement slabs treated with the SME-PS and without the SME-PS were exposed to freezing and thawing cycles in Indiana, as shown in Figure 3-6. Therefore, the slabs were continuously examined for surface scaling and freeze thaw damage.

Figure 3-6: Pavement slabs undergoing freezing cycles at the CAI exposure site

3.3.4.1. Deicing Salt Application Requirements

Prior to the application of applying non-reagent grade salt solutions to the slabs, the rate of application of the salt solution and the time frame for applying salt to the

slabs was determined. Commercial grade deicing salts was applied the sidewalk pavements (see Figure 3-4.), twice a week at the CAI site at an application rate of 23.1 g sol/ft^2 as shown in Table 3-3. Deicing salts were applied to slab surfaces both with and without a coating of SME-PS. Using a backpack sprayer, as shown in Figure 3-7, to apply aqueous salt solutions is suggested for exposing sidewalk pavements to chlorides.

Table 3-3: Salt Application Rate Applied to Concrete Surface Using a Backpack Sprayer

Rate of application of Salt: 23.1 grams. sol/ft^2.		
salt	Amount of salt needed per backpack sprayer per week (grams)	Amount of water needed per backpack sprayer per week(gallons)
$MgCl_2$	832	2.2
NaCl	832	2.2
$CaCl_2$	1664	4.4

Note: Application rate is based on the area of pavements sprayed and making side to side passes. The amount of material listed is based on salting pavements twice per week.

Figure 3-7: RL Pro Backpack Sprayer Used in Field Application of Deicing Salts.

The procedure used to salt the sidewalk pavements is to start at the beginning of each slab pavement and make side to side passes with the wand and sprayer nozzle while moving forward to cover all the unexposed regions of the pavement

using the aqueous salt solution. The procedure was completed using full spraying pressure, at a walking pace. The spraying nozzle used in the experiment used a “fan spray” nozzle, attached to a spraying wand. An elevation between 3-6 inches was maintained between the spraying wand and the concrete surface for proper coating.

3.4. Laboratory Testing

The laboratory investigations focused on characterizing the concrete mixture designs and their ability to resist water penetration, chloride ion penetration and outdoor weathering action such as surface scaling. Research was conducted to collect data on some of the properties of each of the specimens. Tests to evaluate these properties include: Electrical resistivity test, water absorption test, chloride ion penetration test, and salt water ponding tests. Samples used for laboratory testing utilized 4x8 inch cylinders that were fabricated at the CAI site. Furthermore, the laboratory investigations included standard test methods to evaluate mechanical and fluid transport properties.

3.4.1 Casting Samples

As mentioned, to simulate concrete used in Indiana, field and laboratory specimens were cast using the same sidewalk mixture design specified by INDOT as well as several other variations. Appendix A, contains information regarding aggregate gradations (coarse and fine), air content, casting dates, and compressive strength. Each batch of cylinders cast from the four mixture designs, the slump, air content and 28-day compressive strength (3 cylinders per batch) were recorded.

3.4.2. Electrical Resistivity and Formation Factor

To determine the formation factor, the electrical resistivity of the four mixture designs was monitored over time. The concept of the formation factor extends from

geological research on saturated porous materials [18]. Therefore, it should be noted that the definition for the formation factor is defined only at saturation. For a partially saturated concrete, a correction factor denoted S^n is needed in order to account for the effects of partial saturation. As the level of saturation in concrete decreases (i.e., assuming the pore solution remains constant) the conductivity of the concrete also decreases. This is attributed, in part, to a decrease in the conductive pore solution volume and changes to the tortuosity and pore solution inside the system [24]. Furthermore, the correction factor S^n accounts for changes in saturation due to chemical shrinkage and allows for the comparison of the results of different conditioning methods and to fully saturated concrete specimens [13]. The expression for the correction factor is defined in Equation 3-6:

$$F = \frac{\rho}{\rho_O} \cdot S^n \qquad Equation\ [3.6]$$

Where, F = Formation factor of the porous material, ρ = bulk resistivity of the porous material, ρ_o = resistivity of the pore solution, and S^n is a function that describes the degree of saturation, where S is taken as 1.0 for a fully saturated system. The expression n is a fitting parameter called the saturation coefficient, that is typically of the order of 3.5-5 for cement and concrete [25]. The saturation coefficient for this study was taken as 3.2. It should be noted that an additional correction factor is needed for concentrated solutions [25]. Using the cement chemistry, the theoretical pore solution composition and resistivity of the test specimens was determined using a pore solution conductivity calculator made available online by NIST (National Institute of Standards and Technology), as shown in Figure 3-8 [26].

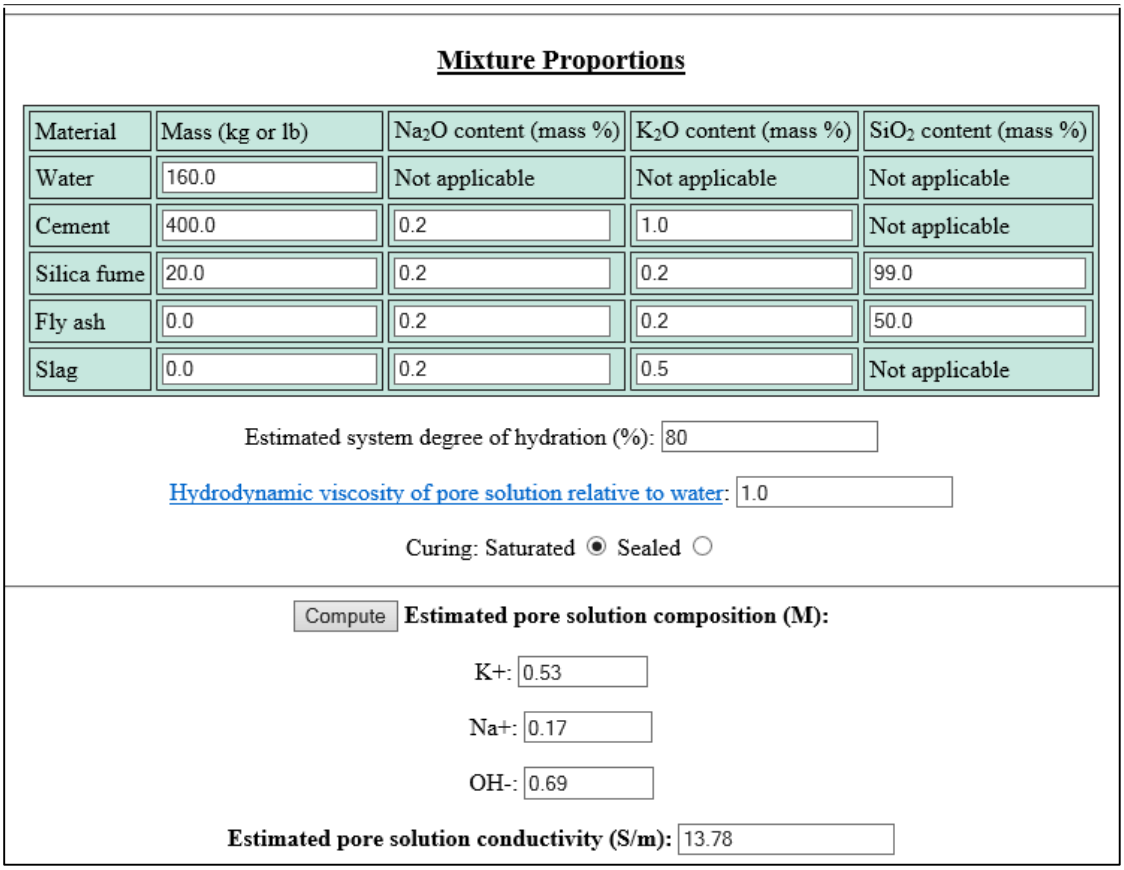

Mixture Proportions

Material	Mass (kg or lb)	Na_2O content (mass %)	K_2O content (mass %)	SiO_2 content (mass %)
Water	160.0	Not applicable	Not applicable	Not applicable
Cement	400.0	0.2	1.0	Not applicable
Silica fume	20.0	0.2	0.2	99.0
Fly ash	0.0	0.2	0.2	50.0
Slag	0.0	0.2	0.5	Not applicable

Estimated system degree of hydration (%): 80

Hydrodynamic viscosity of pore solution relative to water: 1.0

Curing: Saturated ◉ Sealed ○

Compute **Estimated pore solution composition (M):**

K+: 0.53

Na+: 0.17

OH-: 0.69

Estimated pore solution conductivity (S/m): 13.78

Figure 3-8: Screenshot of Pore Solution Conductivity Calculator [26]

TABLE 3-4: Pore Solution Chemistry

Concrete Mixture #	Mixture ID. (w/c-A)	W/C	NaOH (g/L)	CaOH (g/L)	Pore Solution Resistivity (k·ohm/cm)
Mix.No.1	0.42-6.6%	0.42	22.8	2.0	0.009
Mix.No.2	0.49-7.0%	0.49	18.4	2.0	0.011
Mix.No.3	0.56-6.0%	0.56	15.2	2.0	0.013
Mix.No.4	0.49-1.7%	0.49	18.4	2.0	0.011

Note: A = air content (percentage of voids) in the concrete

To determine the theoretical pore solution composition and resistivity, the amount of water, mass of the cement and the chemical properties of the cement was entered into the calculator. From the cement chemistry, the Na_2O equivalent number was entered for mass % content of Na_2O for cement. In this experimental study, not supplementary cementitious materials were used, therefore the amount of silica fume, fly ash, slag, mass % content of Na_2O, K_2O, and SiO_2 entered into

the calculator was zero. The estimation of the pore solution conductivity calculator requires that the system DOH of the concrete be provided. It was estimated that the system for each concrete mixture design was between 70-90% hydrated therefore a value of 80% was used for the estimated DOH. In order to estimate the constituent materials that make up the unique synthetic pore solutions, for each mixture the estimated molar concentrations for K+ and Na+, were multiplied by the molar masses of KOH (56.12 g/mol.), and NaOH (39.99 g/mol.) respectively, and the amount of water to be used to estimate the amount of sodium hydroxide, and potassium hydroxide needed. 26 grams of lime or CaOH (Calcium Hydroxide) was added to each of the pore solutions for each mixture design. Two cylinders from each mixture design were tested. Each test was started at a material age of 28 ± 2 days for each test specimen. Samples were taken from their sealed condition, massed and labeled accordingly. The surface resistivity and uniaxial resistivity were measured for the sealed condition.

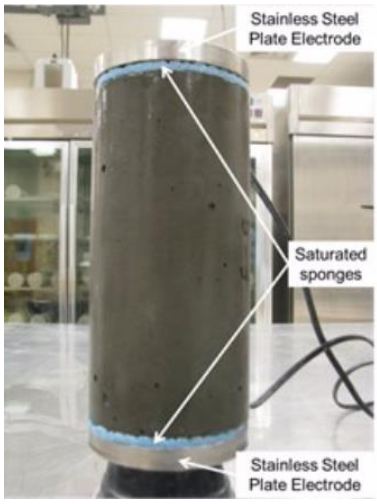

Figure 3-9: Measuring the resistance of the system. The test cylinder is a standard 8-in. by 4-in. (200 mm x 100 mm) specimen [31].

Denoted the storage condition approach, two cylindrical specimens, with dimensions 4-in. by 8-in. from each mixture were then submerged in 5-gallon buckets with synthetic pore solution for a period of 10 and 60 days. The reason why the specimens were placed in pore solutions is to stop the leaching of alkalis

in the concrete matrix, which can influence the conductivity of the pore solution. The mass, surface resistivity and uniaxial resistivity were measured at 0 h, 18 h, 24 h,42 h,48 h,3 d,4 d,5 d,7 d, 9 d,10 d, 14 d, 21 d, 28 d, 35 d, 42 d, 49 d,56 d and 60 days. Upon the completion of the test, the samples were then oven dried at 105°C until the change in mass was less than 0.05%. The 8-in. by 4-in. specimens were cut into three 2-in. by 4-in. disc specimens, oven dried and then vacuum saturated under a residual pressure of 6-10 torr for 3 hours. After 3 hours of vacuuming, water was introduced into the vacuum system. The samples remained under vacuum for an additional h, and left in the fluid for 24 hrs., before the fully saturated (100% degree of saturation) mass was taken to determine the DOS using Eq. 3-7:

$$DOS\ (2x4in) = \frac{\frac{M_{DM(8x4)} - M_{OD(4x8)}}{M_{OD(8x4)}}}{\frac{m_{SSD(2x4)} - m_{OD(2x4)}}{m_{OD(2x4)}}} x\ 100 \qquad Equation\ [3.7]$$

Where, DOS is the degree of saturation of the sample, M_{DM} is the demolded mass of an 8-in by 4-in specimen, M_{OD} is the oven dry mass of a 4-in by 8-in specimen, m_{OD} is the oven dry mass of a 2-in by 4-in specimen, and m_{SSD} is the saturated surface dry mass of a 2-in by 4-in specimen. The formation factor was determined by taking the corrected resistivity values and dividing it by resistivity of the pore solution.

3.4.3. Water Absorption Test

To prepare the samples for water absorption testing 4x8 inch cylinders were prepared to the four mixture designs given in Table 3-2. Two different sets of specimens were used in this study. The first set of samples was used to evaluate the effect of material composition and sample conditioning on water absorption. The second set of samples, used for water absorption testing were topically treated with one and two applications of SME-PS. Samples were cured for 28 days, before being demolded and epoxied as shown in Figure 3-9.

Figure 3-10: Epoxied Concrete Test Specimens

Specimens were then vacuum saturated in a lime water solution, massed and then placed in environmental humidity chambers to be conditioned at 23°C and 50%±2% RH and at 23°C and 75%±2% RH for 6-8 months prior to testing. In the testing series, all samples were tested for 7-day water absorption. Prior to immerging the samples in a water bath, one side surface of the sample was covered with plastic and secured with an elastic band. The specimens were then massed again and placed on a support device at the bottom on the water bath inside a container. The fluid levels were maintained 2±1 mm above the top surface of each sample. Samples were removed from the container, towel dried and weighed the first 60s after immersion and placed back in the container. This procedure was repeated 5 min,10 min, 20 min, 30 min, 1 h, 2 h, 3 h,4 h, 5 h, 6 h, 1 d, 2 d, 3 d, 4 d, 5 d, 6 d and 7 d after the time of immersion, denoted time zero. The absorbed fluid volumes are plotted as a function of the square root of time. The initial sorptivity of the absorption curve is defined as the slope of the curve during the first 6 hours of testing while the secondary sportively is noted to be the slope of the curve after 1-8 days as specified by ASTM C1585-13.

3.4.3.1. Sample Conditioning

The purpose of conditioning the samples is to bring the internal RH (relative humidity) of the samples to 50% and 75% RH. The samples are weighed every 15 days to determine if the internal moisture condition has reached equilibrium. Once the samples have reached the specified internal moisture condition the samples are ready for testing. However, pervious research has shown that standard conditioning methods may not be adequate in order to bring specimens to equilibrium. In this experimental investigation specimens were considered to have reached equilibrium when the mass change was less than 2% for three consecutive measurements. After specimens reached equilibrium the top surface of the samples was sealed using a plastic sheet and tapped on the sides. The purpose of sealing the top of the samples is to prevent or reduce the amount of drying the specimen may experience over the duration of the experiment.

3.4.4. Chloride Diffusion Test (Fick's 2nd Law of Diffusion)

As previously discussed, chloride penetration is a well-known problem that can lead to a variety of deleterious mechanisms that induce damage in concrete, such as the corrosion of reinforcement bars. Therefore, it is thus very important to understand the extent of chloride penetration into concrete, in order to predict the service life of concrete structures. The most common approach to modeling the ingress of chloride ions into concrete elements is to use Fick's second law of diffusion, as defined by equation 3.8:

$$\frac{C_{(x,t)-}C_O}{C_{S-}C_O} = 1 - \mathrm{erf}\left(\frac{x}{\sqrt{4 \cdot D \cdot t}}\right) \qquad Equation\ [3.8]$$

Where, Co is the initial chloride concentration in concrete, C (x, t) is the total chloride content at a depth x at time t (mass % concrete), Cs is the chloride concentration at the surface x=0 (mass % concrete), D is the apparent diffusion coefficient (m^2/s), erf is the error function, x is the distance from the concrete

surface (m) and t is the duration of exposure (s). Due to the complexity of modeling the mechanisms that contribute to chloride ion diffusion into concrete, models are typically based on assumptions and tend to be empirical. Furthermore, Fick's second law of diffusion is only valid for a constant diffusion coefficient and a constant surface chloride concentration; however, in real life exposure conditions D and Cs change over time. Therefore, apparent values for chloride diffusion and Cs are used to account for these assumptions. On the other hand, solving Fick's second law can provide a close approximate solution to how chlorides diffuse into concrete. ASTM C1556-11a was performed to determine the values of D and Cs for the four cementitious mixtures shown in Table 3-2. These values were determined experimentally by fitting chloride concentration profiles developed from titration curves using Fick's 2nd law. The results analyzed in this experimental investigation evaluated data compiled from samples extracted from the CAI site and samples that were ponded in an aqueous salt solution.

3.4.4.1. Determination of Chlorides in Concrete by Titration

Titration is a process that can be used to determine the concentration of chlorides in concrete. To prepare specimens for titration, samples are first broken in halves. The first half of the specimen is used to visibly determine the chloride depth of penetration by spraying silver nitrate ($AgNO_3$) solution onto the sample as shown in Figure 3-10.

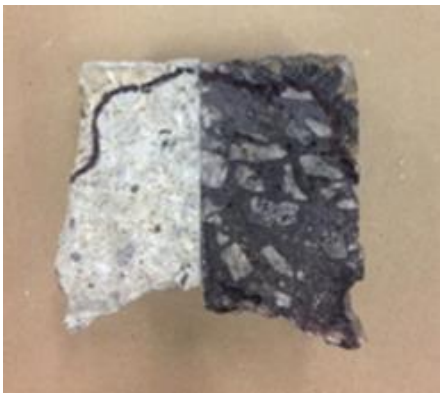

Figure 3-11: Core split in half with silver nitrate applied. Black sharpie outline indicates the approximate chloride depth of penetration [9].

If chlorides are present in the specimens the $AgNO_3$ solution will chemically react with the chlorides forming a white solution where the reaction has taken place. This indicates how far the salt has penetrated into the sample and is used to approximate how deep to grind the second half of the sample into a powder for titration. To account for any chlorides that cannot be visibly seen, it is suggested that all specimens are ground 5mm beyond the outermost maximum depth of chloride penetration that was determined from the visible depth of chloride penetration test. In this study, samples were ground in incremental depths of 2mm from the top most depth of the specimen that was exposed to deicing salts and then titrated to find the concentration of chlorides at each incremental depth. 3.0000 ± 0.0005 g of ground concrete powder from each incremental depth of 2mm was added to a 250 ml beaker with 10 ml ±2 ml of pre-heated deionized water and then stirred using a glass stirring rod. After stirring the solution, 3 ml of nitric acid and an additional 40 ml of pre-heated deionized water was added to each solution. Each solution is then boiled, cooled at room temperature and placed in plastic titration cups and titrated using a titration machine. Fick's second law of diffusion is then used to fit the data from the titration tests to find Cs and Dapp.

3.4.4.2. Chloride Diffusion Test (Field Samples)

Two different sets of specimens were cored from the CAI site to evaluate the effect of external chlorides on the value of the apparent chloride diffusion coefficient (Dapp) and surface chloride concentration (Cs) for the cementitious mixtures shown in Table 3-2. The first set of samples was used to evaluate the effect of material composition and exposure to different salting conditions on Dapp and Cs. The second set of samples that were used for chloride diffusion tests, were samples topically treated with one and two applications of SME-PS. The concrete mixtures that were used for these tests are shown in Table 3-2. To prepare the specimens for chloride diffusion testing, small cores, approximately 6-in by 4-in were extracted from the pavement sections at the CAI site using a drilling rig. However, due to the time associated with coring samples using a drilling rig, only

one sample per pavement section was extracted from the site. The first batch of cored specimens that were extracted from the CAI site began April 2015 and the second batch September 2015. Each of the concrete cores that were extracted from the concrete slabs followed a standard procedure for preparing the samples for titration and analysis.

3.4.4.3 Salt Water Ponding Test

ASTM C1543-10a was performed to determine the penetration of chloride ions into concrete by ponding. The purpose of this test is to determine the surface chloride concentration (Cs) and apparent chloride diffusion coefficient (Dapp) of concrete mixtures. The concrete mixtures that were used for these tests are shown in Table 3-2. Two different sets of specimens were used in this study. The first set of samples was used to evaluate the effect of material composition and sample conditioning on chloride diffusion. The second set of samples, used for salt water ponding testing were topically treated with one and two applications of SME-PS. In each testing series, three samples were used for each mixture design. To prepare the samples for salt water ponding testing, the samples were cut into 3-in. by 4-in disc and then epoxied around the sides of the specimens. After the epoxy had hardened, the top portion of the samples were then encapsulated in a plastic container and then placed in an environmental relative humidity chamber to be conditioned at 50% ± 2% RH, 23°C and ponded in a 10% by mass NaCl salt solution for 136 days. To determine the surface chloride concentration and apparent chloride diffusion coefficients of the four concrete mixtures, the plastic and epoxy surrounding the samples were removed and the samples were prepared for titration following the standard titration procedure as outlined in section 3.4.4.1.

3.4.5. Porosity and Initial Degree of Saturation

The total porosity and degree of saturation (DOS) of concrete has been used as a tool to predict the properties of concrete. The objective of this experiment is to investigate the influence that porosity and DOS of test specimens has on the fluid transport properties of concrete. Samples were prepared to the four mixture designs given in Table 3-2. For each mixture design evaluated in this experiment a set of four 4-in by 8-in cylinders were tested after 28 days was allowed for curing. The samples were then massed from a sealed condition and oven dried till the change in mass was less than 0.02%. After oven drying the samples, the samples were then cut into 2-in thick by 4-in diameter disc and massed and oven dried again till the change in mass was less than 0.02%. Specimens were then vacuum saturated in a vacuum saturation machine for 4 hours. Once the samples were taken out the vacuum saturation machine the buoyant mass and saturated surface dry mass were recorded to calculated the DOS in each sample using equation 3.6. Sequentially, the porosity of each of the samples were calculated using ASTM C642. Table 3-5 shows the porosity and DOS of the four mixtures given in Table 3-2. Included in Table 3-5, are the results from an experimental model used to estimate the initial DOS and porosity of concrete materials [27].

TABLE 3-5: Experimental and Theoretical Initial DOS and Porosity

Mixture No.	Average Initial DOS (%)	Expected Initial DOS (%)	Average Porosity (%)	Expected Porosity (%)
1	66.1	63.2	18.5	17.7
2	65.7	67.3	21.5	19.9
3	72.8	70.4	22.3	21.9
4	89.2	87.3	13.8	15.8

3.5. Results and Discussions

3.5.1. Electrical Resistivity and Formation Factor

The bulk uniaxial resistivity measurements for the submerged cylinders measured over 60 days for the four mixture designs given in Table 3-2, is shown in Figure 3-

12. The first point on the curve corresponds to the uniaxial resistivity measurement for a cylinder that was measured from a sealed condition. It should be noted that the common trend observed in regard to resistivity is that the sealed resistivity is larger than the submerged resistivity measurement [28], which is consistent with the mixtures shown in Figure 3-12.

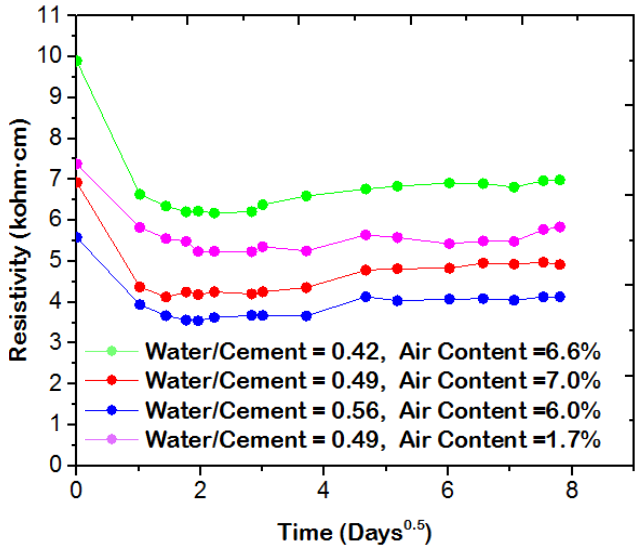

Figure 3-12: Resistivity Measurements for Submerged Cylinders for Mix No. 1-4

The submerged resistivity shown in Figure 3-12 is lower than the resistivity values measured from sealed condition for the reason that as fluid enters the cementitious system the DOS increases within the pore network, which thus increases the conductivity of the system. Since, conductivity is inversely proportional to resistivity, meaning that as the conductivity of a constituent material increases the resistivity of that material thus decreases. This explains the initial dramatic decrease in resistivity that is observed in Figure 3-12 after the specimens are submerged in the synthetic pore solution, which correspond to points after time zero on the curve. While drying effects were not monitored over time in this experiment, it is believed that fully sealed behavior was not present and that some degree of drying was suspected. It has been observed that specimens tested at later ages exhibit more drying and have higher sealed resistivity measurements

[28]. Todak (2015), has shown that after a material has reached its nick point, resistivity has been shown to slowly increase over time [28]. The mixtures in presented in Figure 3-12 collectively verify this observation. This trend is likely attributed to the continued hydration of the cementitious system [19]. As, water continues to hydrate a cement system it condenses the cement matrix, which thus decreases the conductivity. The reason why conductivity is higher, and inversely resistivity is lower in specimens with higher w/c as shown in Figure 3-12, is for the reason that these materials are more porous. Materials with higher w/c will have a higher DOH for a similar curing time (e.g., it has more water for hydration). But, it is likely a matter of the connectivity of pores that causes this decrease in resistivity as the w/c increases. Previous empirical test has shown RCPT (Rapid Chloride Penetration Test) such as ASTM C1202 (The Standard Test Method for Electrical Indication of Concrete's Ability to Resist Chloride Ion Penetration) and resistivity tests can be used to characterize the quality of concrete mixtures [29]. RCPT gives an indirect indication of the permeability of concrete and the risk of chloride permeability with regard to electrical charge passed. As shown in Figure 3-13, a table was developed to relate the values obtained from resistivity test to RCPT [30].

Relationships between values provided by different electrical test methods

ASTM C1202 Classification[1]	Charge Passed (Coulombs)[1]	Direct Resistivity (kOhm-cm)[2]	Berke Empirical (kOhm-cm)	Paredes Empirical (kOhm-cm)[3]	Apparent Surface Resistivity (102mm × 205mm) (kOhm-cm)[4]
High	>4,000	< 5.2	< 4.9	< 6.5	< 9.7
Moderate	2,000 – 4,000	5.2 – 10.4	4.9 – 8.76	6.5 – 11.3	9.7 – 19.3
Low	1,000 – 2,000	10.4 – 20.8	8.8 – 15.6	11.3 – 19.9	19.3 – 38.6
Very Low	100 – 1,000	20.8 – 207	15.6 – 105.9	19.9 – 136.6	38.6 – 386
Negligible	< 100	> 207	> 105.9	> 136.6	> 386

[1]from ASTM C1202-10 [15]
[2]calculated using Ohm's law and geometry
[3]corrected for geometry from Kessler, et al. [28]
[4]bulk resistivity multiplied by geometry factor

Figure 3-13: Relationship between RCPT and Electrical Resistivity Test [30]

As illustrated in Figure 3-13, the direct resistivity test, which is comparable to the experimental uniaxial resistivity test results in Figure 3-12, it can be roughly approximated that the materials used in this study will exhibit moderate to high

chloride ion penetrability. Where specimens with higher w/c, and air contents will exhibit higher chloride ion penetrability as indicated from Figure 3-12 and 3-13. Further, while the development of the table in Figure 3-13 can be a useful tool to quantify the quality of the design mixtures used in this study, the table is only used to approximately estimate how the mixture designs in this experiment might respond in the environment using the experimental resistivity results. This is for the reason that resistivity measurements can differ depending on conditioning methods, drying effects, and qualities such as differences in specimen geometries and temperature [31]. Previous research has suggested, that a standard resistivity test be developed. However, other research has specified that the more reliable approach to quantify the quality of design mixtures is to use the formation factor [32]. Furthermore, it is believed that higher formation factors typically indicate higher quality concrete. However, it should be noted that the manner in which samples are stored can have an impact on the electrical resistivity and computed formation factors [28]. Todak (2015), has suggested this is likely do to the effects of drying, self-desiccation and the leaching of the pore solution and alkalis into solution [28]. For computation of the formation factor, two curing conditions were considered: 1) sealed, and 2) curing in simulated pore solution (i.e., storage condition approach). The storage condition approach was used to determine the formation factor at the nick point. From previous studies, it is known and expected that specimens with lower w/c will exhibit higher strength as shown in Figure 3-2, are less permeable, and thus more durable. Therefore, it was expected that samples with lower w/c would exhibit higher formation factors. It was confirmed, that the formation factor for the two conditioning methods considered in this investigation were determined to be higher for specimens with lower w/c. This is likely attributed to the fact that the pore network for specimens with lower w/c, are not as connected as specimens with higher w/c, therefore are denser, and have less porosity as shown in Table 3-5. For both conditioning methods the pore solution corrections were taken into account in order to compute the formation factors as shown in Table 3-6. As the air content decreased, the formation factor

increased, which implies conductivity decreased. The lower conductivity (higher formation factor) for the mixture with an air content of 1.7% may likely be due to the mixture having a smaller amount of empty air voids. Furthermore, empty air voids can impede conductivity of the system by acting as an insulator, and therefore reducing the bulk conductivity of the material. The total percentage of air voids actually saturated in the system was lower for the mixture with the air content of 1.7%. This is due to the non-air entrained mixture with a w/c of 0.49 containing a smaller percentage of air voids (see Table 3-5). Therefore, the air entrained mixture with the air content of 7.0% and w/c of 0.49 has a larger percentage of empty air voids.

Table 3-6: Sealed, and Nick Point Formation Factor.

Concrete Mixture #	Concrete Mixture ID (w/c-A)	Sealed DOS (%)	Nick Point DOS (%)	Sealed Formation Factor*	Nick Point Formation Factor*
Mix.No.1	0.42-6.6%	65.6	74.4	285.2	268.0
Mix.No.2	0.49-7.0%	69.2	76.5	193.9	161.4
Mix.No.3	0.56-6.0%	70.3	79.0	139.0	131.2
Mix.No.4	0.49-1.7%	83.4	90.0	375.1	340.4

Note: A = air content (percentage of voids) in the concrete. *Based on a saturation coefficient of 3.2

3.5.2. Influence of Sample Conditioning and Material Composition on Water Absorption

The rate at which water is absorbed into concrete by the method of capillary suction can provide useful information in regards to the pore structure, permeation characteristics and the durability of the system [33]. Figures 3-14a and 3-14b presents normalized absorption data, the effects of w/c and sample conditioning on water absorption characteristics for mixture designs No.1 and No.2 (for reference see Table 3-2). Each point on the curve was normalized using Equation 3-4, as outlined in section 3.4.3.

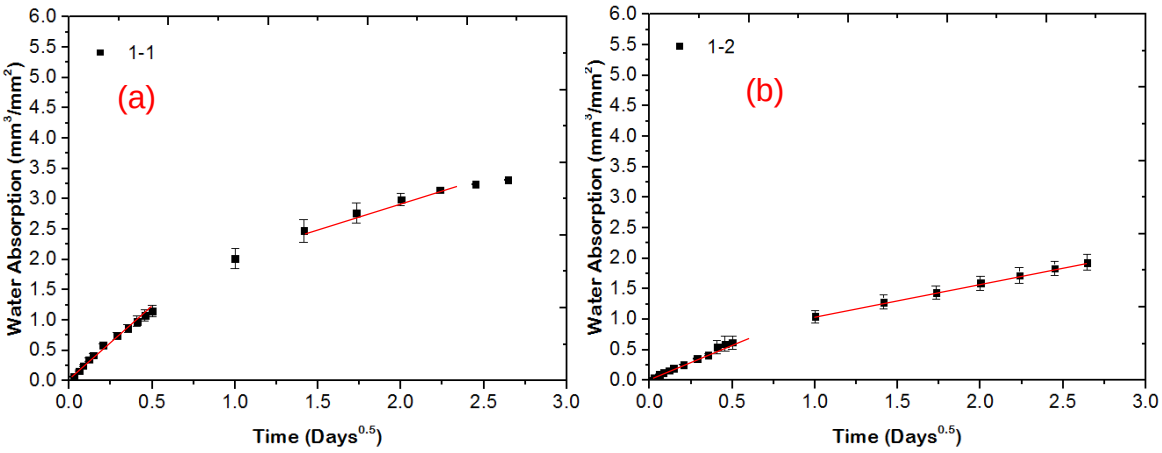

Figure 3-14a: Effect of w/c, and Conditioning on Water absorption. (a) Mix No.1 (50%RH), (b) Mix No.1 (75%RH)

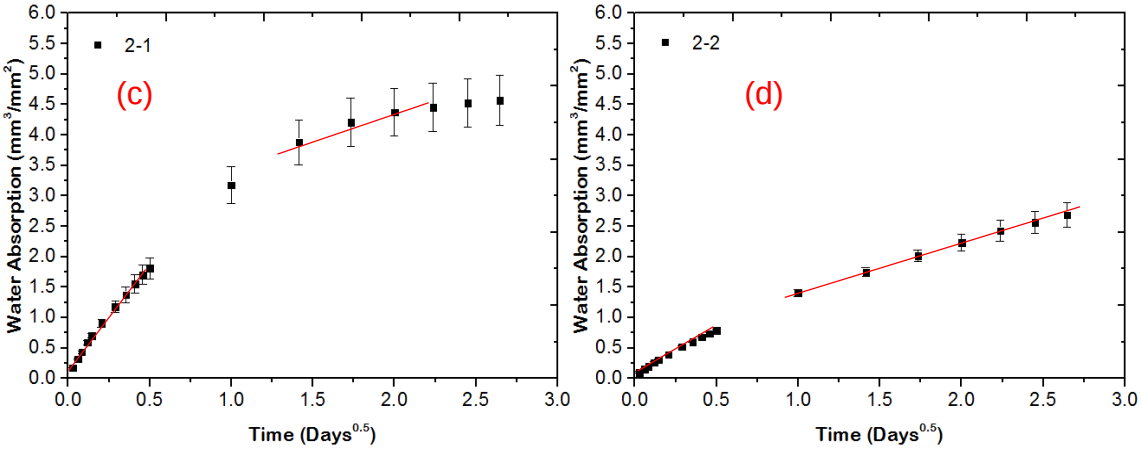

Figure 3-14b: Effect of w/c, and Conditioning on Water absorption. (c) Mixture No.2 (50%RH), (d) Mixture No.2 (75%RH).

Figure 3-14 shows that as RH increases, water absorption decreases. This is consistent with expectations based on previous studies by Castro et al. (2011) [34]. Further, samples conditioned at a lower RH show a total absorption that is greater than that of similar samples conditioned at a higher RH [24]. It should be noted that this also valid for increasing w/c [34].

The initial sorptivity, secondary sorptivity and total absorption for samples conditioned in chambers show a linear trend related to w/c and the RH at which samples were conditioned at [34]. Furthermore, both Table 3-7 and Figure 3-14

show that mixtures with higher w/c exhibit higher initial sorptivity and secondary sorptivity. This observation is valid for both samples conditioned at 50%RH and 75%RH, as shown in Figure 3-14.

TABLE 3-7: The Rate of Fluid Absorption, and Linear Correlations for Figure 3-14

Group	1st sorptivity		correlation coefficient (r)		2nd sorptivity		correlation coefficient (r)
	mm/day$^{0.5}$	*10^{-3} mm/S$^{0.5}$			mm/day$^{0.5}$	*10^{-3} mm/S$^{0.5}$	
1-1	2.578	8.769	0.9927		0.5569	1.895	0.9827
1-2	1.188	4.042	0.9960		0.5395	1.835	0.9997
2-1	4.062	13.82	0.9944		0.8550	2.909	0.9587
2-2	1.479	5.032	0.9986		0.8058	2.741	0.9998

Note: Group 1-1 (Mixture No.1 at 50%RH), Group 1-2 (Mixture No.1 at 75%RH), Group 2-1 (Mixture No.2 at 50%RH), Group 2-2 (Mixture No.2 at 75%RH).

For all four mixtures considered in this study, laboratory results for the effect of w/c, sample conditioning and air content on water absorption characteristics are presented in Figure 3-15. Each point on the graph is the average of three specimen readings per mixture design calculated as the slope of the absorption curve vs. the square root of time during the first 7 days of the absorption test.

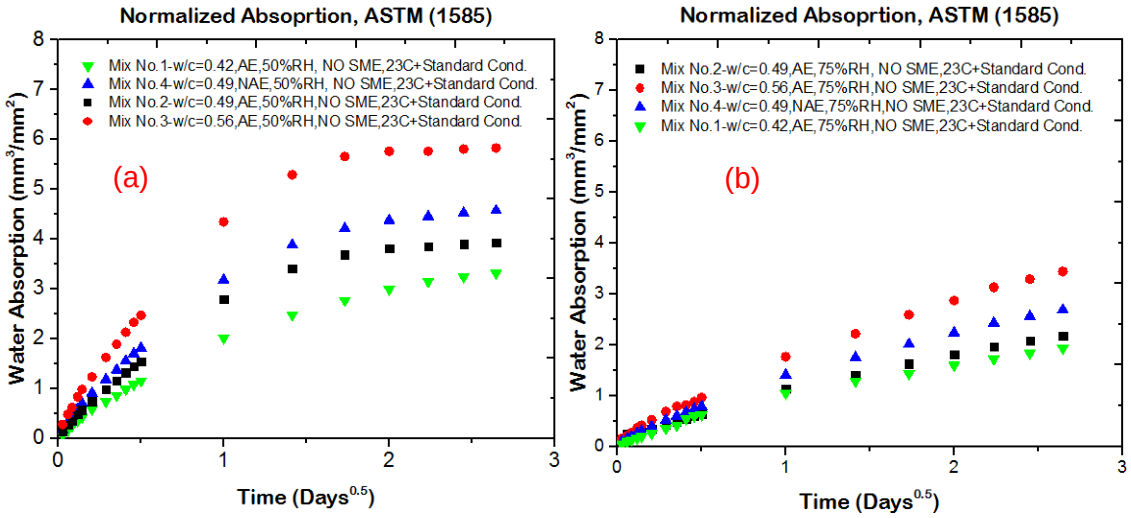

Figure 3-15: Effect of w/c, Conditioning, Air Content on Water absorption. (a) Specimens (Mixture No.1-4) conditioned at 50%RH, (b) Specimens (Mixture No.1-4) conditioned at 75%RH

TABLE 3-8: The Rate of Fluid Absorption, and Linear Correlations for Figure 3-15a

Mixture ID. (w/c-A)	1st sorptivity		correlation coefficient (r)		2nd sorptivity		correlation coefficient (r)
	mm/day$^{0.5}$	*10^{-3} mm/S$^{0.5}$			mm/day$^{0.5}$	*10^{-3} mm/S$^{0.5}$	
No.1 (0.42-6.6%)	2.240	7.623	0.9923		0.5926	2.016	0.9716
No.2 (0.49-7.0%)	2.928	9.961	0.9973		0.6416	2.183	0.9729
No.3 (0.56-6.0%)	4.582	15.60	0.9954		1.081	3.678	0.9962
No.4 (0.49-1.7%)	3.411	11.61	0.9947		0.7969	2.711	0.9782

Note: A = air content (percentage of voids) in the concrete

TABLE 3-9: The Rate of Fluid Absorption, and Linear Correlations for Figure 3-15b

Mixture ID. (w/c-A)	1st sorptivity		correlation coefficient (r)		2nd sorptivity		correlation coefficient (r)
	mm/day$^{0.5}$	*10^{-3} mm/S$^{0.5}$			mm/day$^{0.5}$	*10^{-3} mm/S$^{0.5}$	
No.1 (0.42-6.6%)	0.988	3.360	0.9841		0.5388	1.833	0.9994
No.2 (0.49-7.0%)	1.233	4.195	0.9935		0.6431	2.188	0.9977
No.3 (0.56-6.0%)	1.683	5.725	0.9851		1.036	3.542	0.9953
No.4 (0.49-1.7%)	1.458	4.960	0.9969		0.7874	2.679	0.9978

Note: A = air content (percentage of voids) in the concrete

The results presented in Figure 3-14 are also in reasonable agreement with Figure 3-15 and previous studies that the rate of water absorption increases as the w/c increases and RH decreases [34]. As can be seen, the linear relationship between the absorption vs. the square root of time was obtained in all cases with correlation coefficients generally in excess of 0.97. As seen in Figures 3-15a and 3-15b, the non-air entrained mixture with the w/c ratio of 0.49 achieved the greatest amount of water absorption after 7 days. In contrast, the least amount of water absorption for any sample in Figures 3-15a or 3-15b were specimens fabricated from the mixture with a w/c of 0.42. When air entrainment was considered and compared with similar samples that were not air entrained, corresponding to the mixtures a

w/c of 0.49, it was observed that air entrained samples had slower rates of fluid absorption. This trend is likely attributed to a difference in cement paste content.

3.5.3. Influence of Material Composition on Chloride Penetration, Cs and Dapp

The following Figures 3-16a, 3-16b, 3-17a, 3-17b, and 3-18a, 3-18b display the chloride profiles that were developed from concrete samples fabricated from mixture designs No.1-4, which were obtained after 4 and 9 months of exposure to NaCl, $CaCl_2$ and $MgCl_2$ deicing salts. Note: the naming convention as shown in the charts, for example in Figure 3-16a (a), “18” represents the specimen ID as shown in Figure 3-5 (see section 3.3.4), “Plain” signifies a specimen not treated with SME-PS, “0.49” represents the corresponding w/c, “NaCl” characterizes the corresponding salt exposure condition and “AE” denotes a sample that was air entrained, where “NAE” is defined as non-air entrained sample. Full details of the laboratory test results can be seen in Appendix B.

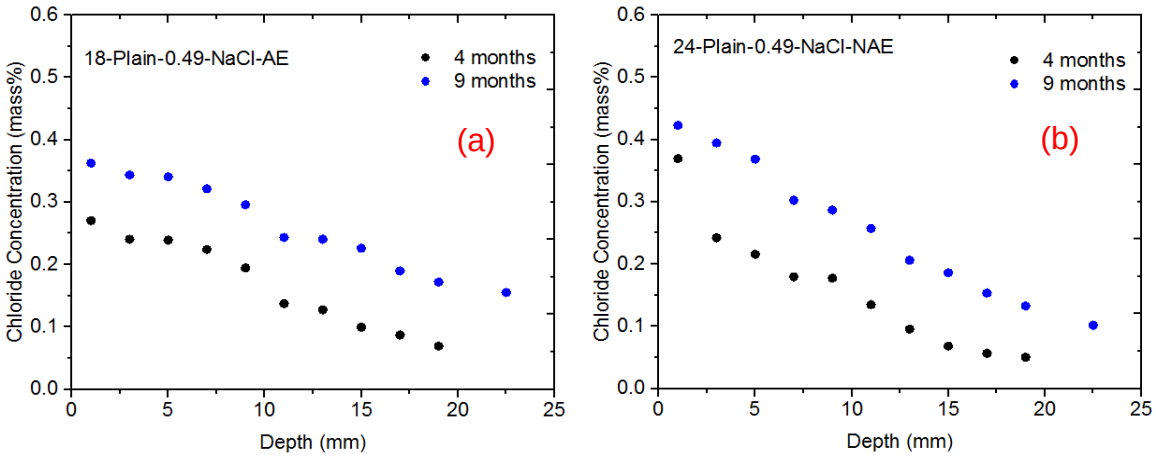

Figure 3-16a: Chloride Profiles with time of exposure to NaCl. (a) Mixture.2, (b) Mixture.4

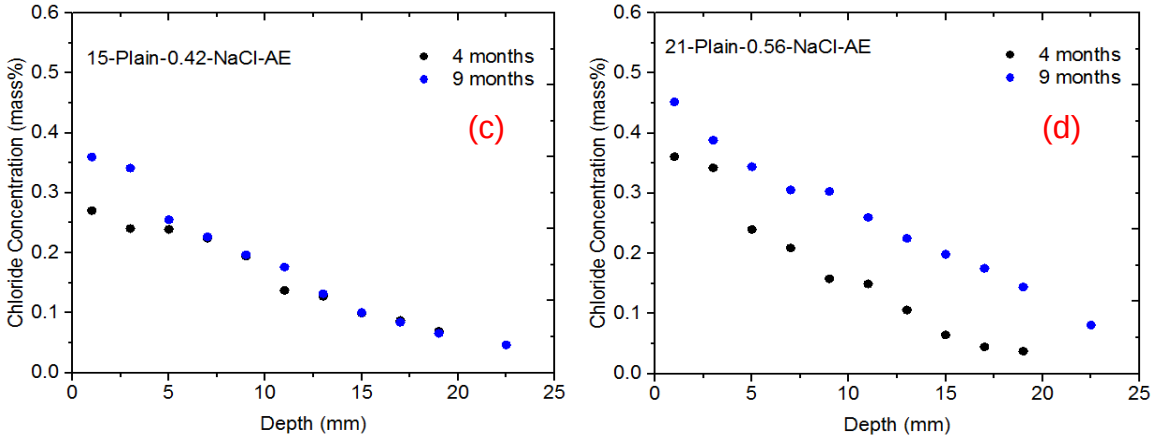

Figure 3-16b: Chloride Profiles with time of exposure to NaCl. (c) Mixture.1, (d) Mixture.3

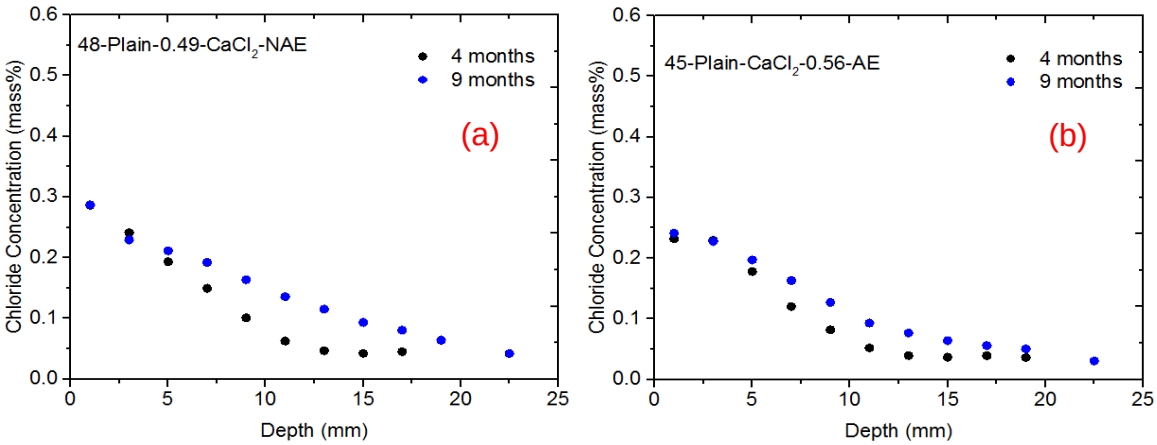

Figure 3-17a: Chloride Profiles with time of exposure to $CaCl_2$. (a) Mixture.4, (b) Mixture.3

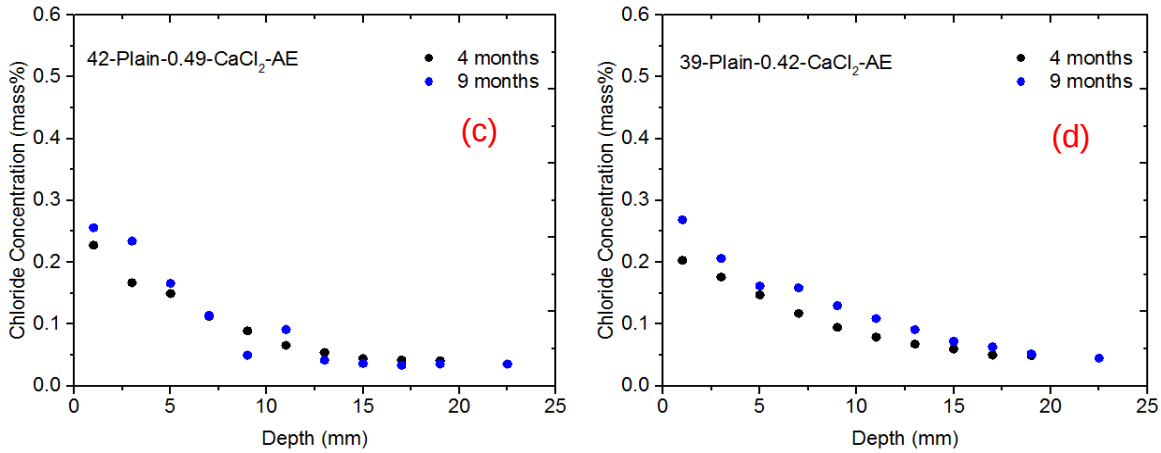

Figure 3-17b: Chloride Profiles with time of exposure to $CaCl_2$. (c) Mixture.2, (d) Mixture.1

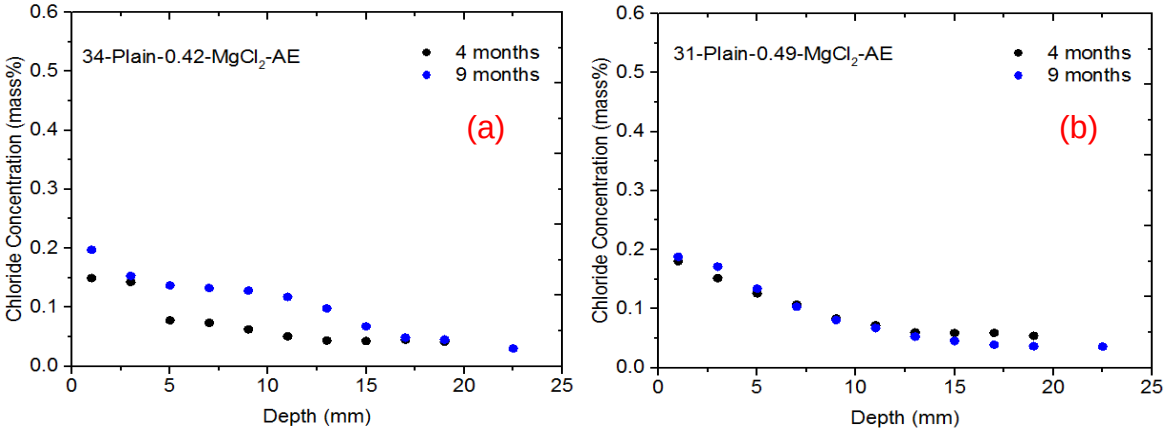

Figure 3-18a: Chloride Profiles with time of exposure to $MgCl_2$. (a) Mixture.1, (b) Mixture.2

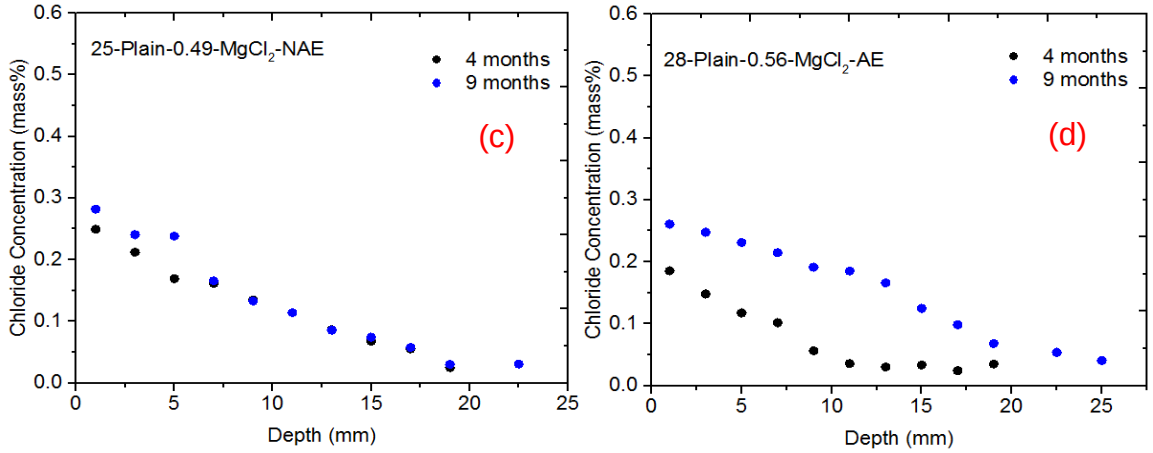

Figure 3-18b: Chloride Profiles with time of exposure to $MgCl_2$. (c) Mixture.4, (d) Mixture.3

The chloride concentration, obtained for the figures above are represented as the chloride content as a function of the % weight of cementitious materials in each sample. The chloride concentration was plotted against the depth into the concrete from the surface that was exposed to deicing salts. The plots show a clear indication that cored specimens from each mixture design yielded different chloride contents for a given depth over time. The chloride profiles of each exposure period were superimposed on the plots to show the chloride content with respect to time.

As shown above, with each exposure period the chloride concentration increased in the layers, which indicates the accumulation of chlorides deposited in the concrete. The diffusivity of the chloride into the cementitious system can be visualized by observing the chloride content that has diffused into the deeper layers. Furthermore, a steeper slope tends to indicate a higher diffusivity, while a more moderate slope typically indicates a lower diffusivity. A typical fitting for a sample is shown in Figure 3-19. It should be noted that typically, mathematical fitting using Fick's second law does not exactly fit data points. Further, mathematical fitting using Fick's second law may not be the best representation of what is actually occurring in the specimens for the reason that the assumptions behind Fick's second law are restrictive and simplistic.

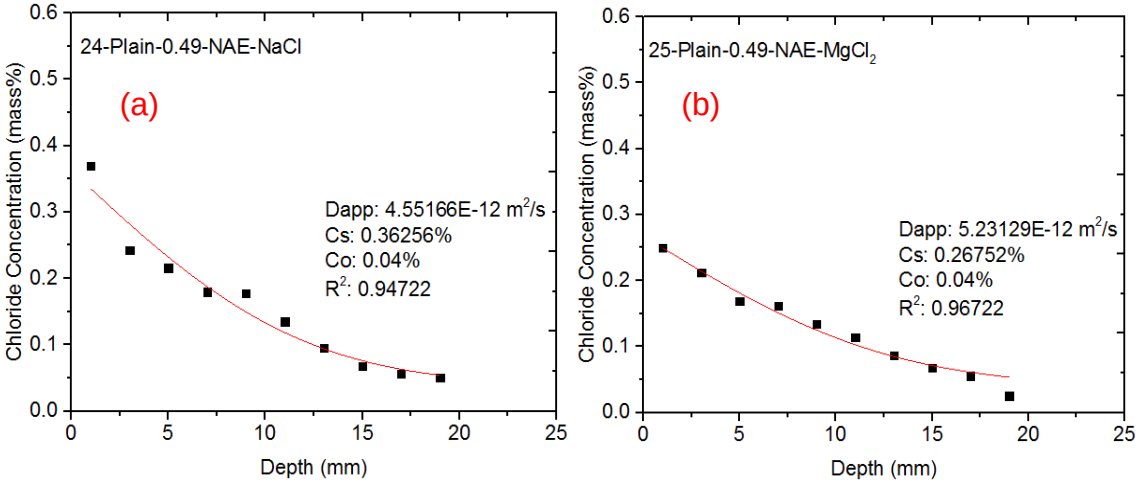

Figure 3-19: Mathematical fitting of the chloride profile for Mixture.4 after 4 months of exposure to NaCl (a), and $MgCl_2$ (b) deicing salt.

Tables 3-10 and 3-11 contain the Dapp and Cs values obtained from the non-linear regression analysis of the chloride concentration profiles for slabs not exposed to SME-PS along with its corresponding maximum depth of chloride penetration

determined by the visible chloride depth of penetration test as outlined in section 3.4.4. The correlation factors (R^2) determined by OriginPro non-linear regression software are also given. The non-linear relationship between the chloride concentration (by % mass of concrete) vs. the depth from the surface of the concrete (mm) was obtained in all cases with correlation coefficients generally in excess of 0.90. Based upon the high R^2 values, Fick's second law can provide a close approximation of how the chloride concentration changes over depth in the specimens. Graphical representation of the data presented in Tables 3-10 and 3-11 can be found in Appendix E.

Table 3-10: Apparent diffusion coefficient (Dapp), surface chloride content (Cs), and correlation factors for untreated specimens extracted from the CAI site Apr. 2015

Exposure Condition	Air Content (%)	w/c	Dapp* ($x10^{-12}$ m^2/s)	Cs* (mass%)	R^2	**Approx. depth of Cl^- Penetration (mm)
NaCl	6.6	0.42	2.75	0.2963	0.9513	8.9
	7.0	0.49	9.43	0.3005	0.9473	10.2
	6.0	0.56	4.35	0.4088	0.9742	15.9
	1.7	0.49	4.55	0.3626	0.9472	15.8
$MgCl_2$	6.6	0.42	1.90	0.1736	0.9423	7.3
	7.0	0.49	4.27	0.1909	0.9851	7.9
	6.0	0.56	3.63	0.1943	0.9646	8.6
	1.7	0.49	5.23	0.2675	0.9672	7.3
$CaCl_2$	6.6	0.42	4.17	0.2208	0.9983	9.8
	7.0	0.49	2.15	0.3058	0.946	10.3
	6.0	0.56	2.90	0.2836	0.9609	11.3
	1.7	0.49	2.69	0.3294	0.9856	12.0

Note: *Based on a C_o = 0.04 (mass %). ** Silver Nitrate Spray Test

Table 3-11: Apparent diffusion coefficient (Dapp), surface chloride content (Cs), and correlation factors for untreated specimens extracted from the CAI site Sept. 2015

Exposure Condition	Air Content	w/c	Dapp* ($x10^{-12}$ m^2/s)	Cs* (mass%)	R^2	**Approx. depth of Cl^- Penetration (mm)
NaCl	6.6	0.42	2.80	0.3940	0.9860	18.6
	7.0	0.49	1.13	0.3885	0.9712	20.6
	6.0	0.56	5.82	0.4595	0.9793	22.5
	1.7	0.49	5.52	0.4554	0.9917	17.6
$MgCl_2$	6.6	0.42	3.07	0.2010	0.9131	12.0
	7.0	0.49	1.28	0.2149	0.9892	13.9
	6.0	0.56	4.86	0.2787	0.9484	14.8
	1.7	0.49	1.99	0.3162	0.9717	11.9
$CaCl_2$	6.6	0.42	4.59	0.1971	0.9341	14.5
	7.0	0.49	1.17	0.2451	0.9911	14.5
	6.0	0.56	2.38	0.2752	0.9861	15.9
	1.7	0.49	3.14	0.2965	0.9869	14.3

Note: *Based on a C_o = 0.04 (mass %). ** Silver Nitrate Spray Test

As shown in the charts above, it was observed that the approximate depth of chloride penetration after 4 and 9 months of exposure obtained from the silver nitrate spray tests increased with increasing w/c for both exposure periods. However, the relationship between the apparent diffusivity (Dapp) results tabulated in Tables 3-10 and 3-11 and the w/c for the mixtures were inconclusive in determining which samples exhibited higher or lower apparent diffusivities. Therefore, the apparent diffusion results could not be used to characterize the concrete mixture designs in this experimental investigation. Furthermore, it is believed that more representative samples may need to be cored in order to duly evaluate apparent diffusivity characteristics of the concrete mixture designs used in this experiment. However, it should be known that w/c plays a critical role in influencing diffusion characteristics in concrete. Typically, the rate of diffusion into concrete increases with increasing w/c. However, Previous studies have shown that the values of Dapp can vary over an order of magnitude for the same concrete, and it is often observed that very poor correlations exist between w/c and diffusion coefficients [35].

Tables 3-10 and 3-11 show across all exposure conditions samples that had the highest surface chloride concentrations were mostly observed in slabs fabricated from the mixture with a w/c of 0.56. The maximum amount of chlorides for these slabs after 4 months of exposure to NaCl, $MgCl_2$ and $CaCl_2$ had surface concentrations of 0.408%, 0.194% and 0.284 % by mass of concrete respectively. Conversely, specimens that displayed the least amount of chlorides present at the surface across all exposure conditions for air entrained samples were observed in specimens fabricated from the mixture with a w/c of 0.42. This is expected as the w/c decreases, the lower the Cs will be [36]. The results for the air entrained mixtures after 9 months of exposure showed similar results. Where, the lowest amount of chloride at the surface overall was seen in samples fabricated from the mixture with a w/c of 0.42. Conversely, the uppermost amount of chloride at the surface was seen from samples fabricated from the mixture with a w/c of 0.56. It is interesting to note that the highest amount of chlorides that were present at the surface for both air entrained and non-air entrained specimens were observed in slabs fabricated from the non-air entrained mixture with a w/c of 0.49. The maximum amount of chlorides for these slabs after 4 months of exposure to NaCl, $MgCl_2$, and $CaCl_2$ had surface concentrations of 0.363%, 0.268% and 0.329 % by mass concrete respectively. The results for the non-air-entrained mixture after 9 months of exposure also presented similar results. This is likely in part attributed to the non-air entrained samples having higher paste contents. Table 3-12, displays the amount of chlorides that penetrated into the first layer of concrete and the observed difference in the amount of chlorides contained at the surface and the first layer into the concrete. The difference between the amount of chlorides that each specimen was able to mitigate can assist in understanding how well each mixture is able to impede chloride ingress. Ideally, optimal results would resemble conventional concrete that can stop the ingress of chlorides the most.

TABLE 3-12: Chloride concentrations at the surface and first layers of the concr for untreated specimens extracted from the CAI site Apr. and Sept. 2015

Exposure Duration:	4 months		9 months	
Sample ID (w/c-A-E)	Cs (% mass)	$[Cl^-]$ (% mass) 1st Layer	Cs (% mass)	$[Cl^-]$ (% mass) 1st Layer
0.42-6.6%-NaCl	0.2963	0.2406	0.3940	0.3598
0.49-7.0%-NaCl	0.3005	0.2706	0.3885	0.3625
0.56-6.0%-NaCl	0.4088	0.3609	0.4595	0.4519
0.49-1.7%-NaCl	0.3626	0.3603	0.4554	0.4229
0.42-6.6%-$MgCl_2$	0.1736	0.1495	0.2001	0.1753
0.49-7.0%- $MgCl_2$	0.1909	0.1805	0.2149	0.1880
0.56-6.0%- $MgCl_2$	0.1943	0.1854	0.2787	0.2478
0.49-1.7%- $MgCl_2$	0.2675	0.2493	0.3162	0.2820
0.42-6.6%- $CaCl_2$	0.2208	0.2031	0.1971	0.1686
0.49-7.0%- $CaCl_2$	0.3058	0.2560	0.2451	0.2278
0.56-6.0%- $CaCl_2$	0.2836	0.2521	0.2752	0.2414
0.49-1.7%- $CaCl_2$	0.3294	0.2865	0.2965	0.2868

Note: A = air content (percentage of voids) in the concrete. E = salt exposure condition

The results tabulated in Table 3-12, show that the w/c can influence the transport of chloride ions through a cementitious system. Based on the results tabulated in Table 3-12, for all air entrained mixtures the concrete with the highest % of chlorides contained at surface layer (Cs) after 4 and 9 months of exposure to NaCl, $MgCl_2$ and $CaCl_2$ were specimens fabricated from the mixture with a w/c of 0.42. After 4 and 9 months of salt exposure, the chloride in the first layer was 13.6% and 11.8% less respectively than at the surface. For all mixtures considered in this study, the lowest % of chlorides contained at surface was seen in samples that were fabricated from the non-air entrained mixture with a w/c of 0.49. After 4 and 9 months of salt exposure, the chloride in the first layer was 6.8% and 7.1% less respectively than at the surface. It was also observed, that the air entrained mixture with a w/c of 0.49 had a higher % of chlorides contained at surface for both exposure periods, than the non-air entrained mixture with a w/c of 0.49. For the concrete specimens fabricated from the air entrained mixtures with a w/c of 0.49 and w/c of 0.56, the chloride in the first layer was 10.6% less after 4 months of

exposure, 8.8% less after 9 months of exposure (i.e., w/c =0.49), and 9.1% less after 4 months of exposure, and 8.3% less after 9 months of exposure (i.e., w/c =0.56) to chloride respectively than at the surface.

3.5.4. Influence of Material Composition on Salt Water Ponding Tests

The following charts shown in Figures 3-20a and 3-20b display the chloride profiles that were achieved from concrete samples prepared to the four mixture designs given in Table 3-2, that were ponded in 10% by mass NaCl solution. The chloride profiles were measured after 136 days of exposure to NaCl solution and fit using Fick's second law of diffusion to determine Cs and Dapp. Note: the naming convention shown in the charts below follows the same naming convention as outlined in section 3.4.3. The non-linear relationship between the chloride concentration vs. the depth from the surface of the concrete was obtained in all cases with correlation coefficients generally in excess of 0.96.

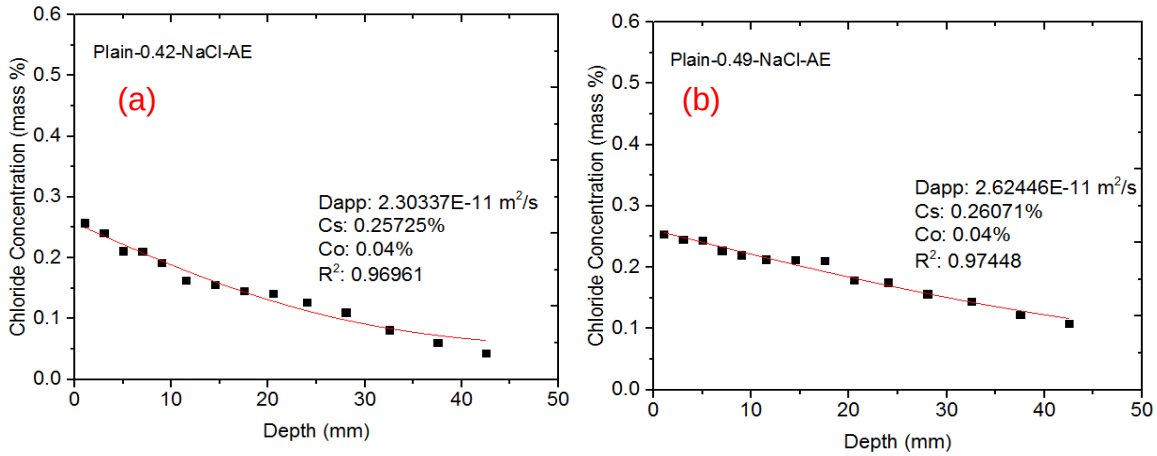

Figure 3-20a: Ponding Cl Profiles with time of exposure to NaCl. (a) Mixture.1, (b) Mixture.2

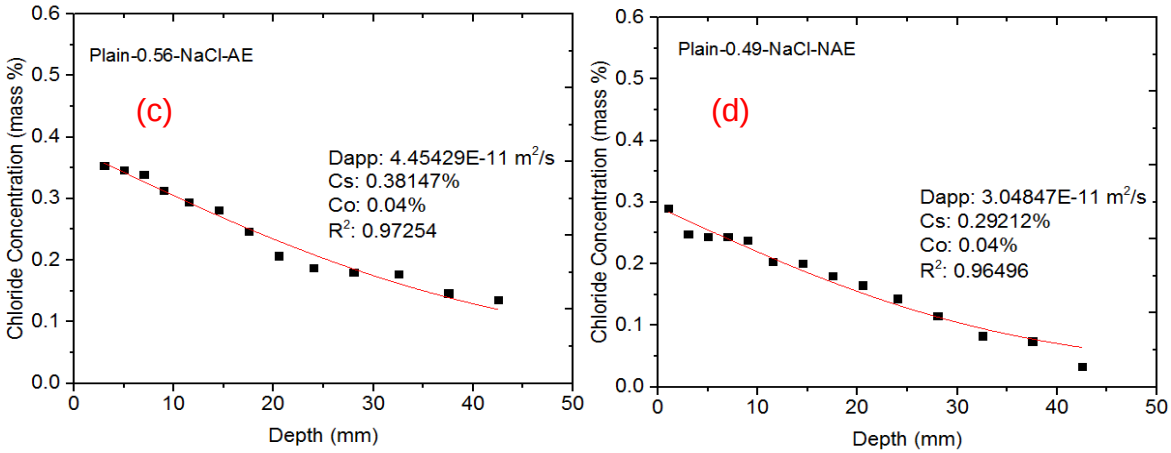

Figure 3-20b: Ponding Cl Profiles with time of exposure to NaCl. (c) Mixture.3, (d) Mixture.4

The results shown in Figures 3-20a and 3-20b suggest that a linear relationship can be found between the w/c and the diffusion coefficient. In Figures 3-20a and 3-20b, it clearly appears, that an increase in w/c leads to an increase in Dapp. For instance, the concrete with a w/c of 0.42 increased from 2.30E-11 m^2/s to 2.62E-11 m^2/s and to 4.45E-11 m^2/s increasing the w/c from 0.42 to 0.49 and to 0.56 respectively. Conversely, as it can be observed in Tables 3-10 and 3-11, and in Figures 3-20a and 3-20b, specimens that displayed the least amount of chlorides present at the surface across were observed in specimens fabricated from the mixture with a w/c of 0.42. It was also observed that for the concrete mixture designs with w/c of 0.49, the non-air entrained specimens had a higher average surface chloride concentration. These results are in reasonable agreement with those presented in Figures 3-16a through 3-18b.

3.6. Summary and Conclusions

This chapter reports results from a laboratory investigation involving the characterization of concrete materials using three different experiments (i.e., water absorption, chloride ion penetration, and salt water ponding tests) to evaluate the effect of material composition and sample conditioning on the performance of concrete samples exposed to fluid and chloride ingress. The experiments were carried out on samples prepared to four different concrete mixture designs, with water to cementitious materials ratios (w/c) of 0.42, 0.49 and 0.56. An analysis of the data and the main theoretical issues that influence fluid transport in concrete is presented. The following observations can be made regarding the influence of material composition and sample conditioning on fluid and chloride absorption into concrete.

- First, for the chloride diffusion test, with little exception, fitting Fick's 2nd law of diffusion to chloride concentration profiles developed from each concrete mixture after exposure to various salts, show that samples with a higher water to cement binder ratio (i.e., capillary pore volume) and a more open pore network (i.e., lower tortuosity coefficient) exhibit higher surface chloride concentrations (Cs) and diffusion coefficients (Dapp), at the same material age.
- Secondly, the measurements in this study show that continual exposure to salt ingress overtime results in an increase in Cs and Dapp regardless of water to cement binder ratio or salt type.
- Third, for the fluid absorption test, the data shows fluid absorption in concrete is influenced by the drying environment used to conditioned samples. Furthermore, the absorption measurements in this study show that samples stored at a lower relative humidity absorb more fluid.
- Fourth, fluid absorption increases as a function of increasing paste content for samples normalized by the surface in contact with water.

- Finally, the resistivity test method was used to identify the formation factor of each concrete mixture. The results show that resistivity increases with a decrease w/c (i.e., decreased pore volume and a reduction in the connectivity of the pore network). This indicates materials that exhibit a higher resistivity are indicative of materials that are more resistance to corrosion and salt penetration.

CHAPTER 4. THE USE OF SOY METHYL ESTER AS A TOPICAL SEALANT: AN ANALYSIS OF THE EFFECTS OF SME-PS ON CONCRETE DURABILITY

4.1. Introduction

Two recent projects in Indiana, one located south of Lafayette, Indiana on US 231 and another located in Fishers, Indiana evaluated the long-term performance of SME-PS in the field. The purpose of the projects was to quantify the service life of SME-PS from cored specimens extracted from the field after 3 to 4 years of environmental exposure [9]. From laboratory measurements, it was found that the SME-PS treated samples although with some exception, reduced chloride penetration when compared to control samples [9]. However, there was a 20% increase in chlorides after 3 to 4 years of exposure in some samples that were treated with SME [9]. The use of pore blockers, water repelling agents and topical concrete sealers enables improvements in the service life of concrete structures. SME-PS, which has been studied as a surface applied concrete sealant, has demonstrated the ability to extend the service life of concrete [3, 4, 9]. The goal of using SME-PS is to provide a suitable economical and biodegradable replacement for conventional sealers that achieve similar performance. However, there is not enough information available to accurately quantify the long term performance of SME-PS used in the field to determine when reapplication is necessary or how to model concrete durability using SME-PS blends. The purpose of this chapter is to characterize the long and short term performance of the concrete specimens highlighted in Chapter 3 treated with SME-PS. The results herein highlight a continuation of the understanding and quantifying of the short and long term performance of SME-PS and its effect on concrete durability.

4.2. SME-PS Research Overview

The concrete pavements installed at the CAI site each consisted of five rows of three 5 ft. x 6 ft. by 6-inch-thick slabs, that were cast in wooden concrete forms (Figures: 4-1 and 4-2).

Figure 4-1: Pavement Form Installation for Mixture #1 at The Center for Aging Infrastructure Exposure Site (August 2014)

Figure 4-2: Center for Aging Infrastructure: Sidewalk Slab Exposure Site (November 2014)

As described in chapter 3, deicing salt was applied to slab surfaces both with and without treatment of SME-PS. This was done to later compare the effectiveness of using SME-PS to mitigate chloride ingress and surface scaling with samples that

did and did not have SME-PS. It should be noted, that research is ongoing in order to further quantify how SME-PS degrades in the field over time. Therefore, slab specimens at the CAI site will continue to undergo salt exposure as of September 2015. Unless otherwise noted in this chapter all field specimens utilized the four concrete mixtures that were characterized in Chapter 3. The experiment was divided into several different sections as described in Table 4-1. Specimens with SME-PS were characterized using fluid absorption tests and chloride ion penetration tests to understand how SME-PS changes fluid absorption and chloride ingress in concrete overtime. Surface scaling test, by method of visual examination was performed on field specimens with and without SME-PS to determine how SME-PS changes damage in concrete overtime.

TABLE 4-1: SME-PS Experimental Program

Property	Test Method	Description
SME-PS Long Term Study		
Chloride Penetration	Titration	Field Samples
	Visual Penetration	Field Samples
Surface Scaling	ASTM 672	Field Samples
SME-PS Short Term Study		
Water Absorption	ASTM C1585	Lab Samples
SME Depth of Penetration	Visual Penetration	Field Samples
Salt Water Ponding	ASTM C1543-10a	Lab Samples

4.3. Soy Methyl Ester Polystyrene Application

The primary goal of the CAI site is to start to characterize how long SME-PS remains effective at preventing chlorides and fluid penetration before re application is needed. As outlined in section 3.3.4 in Chapter 3 of this thesis, 24 of the 36 slab sections at CAI site were used for two different SME-PS coating application rates: 1) one dosage of SME with 2%PS, and 2) two dosages of SME with 2%PS. Three slab sections fabricated from each concrete pavement mixture design for each salt exposure condition (i.e., $MgCl_2$, $CaCl_2$ and $NaCl_2$) were coated with one and two

applications of SME-PS (Figure 4-3). The remaining 12 sections (i.e., 3 sections for each mixture design) were left uncoated.

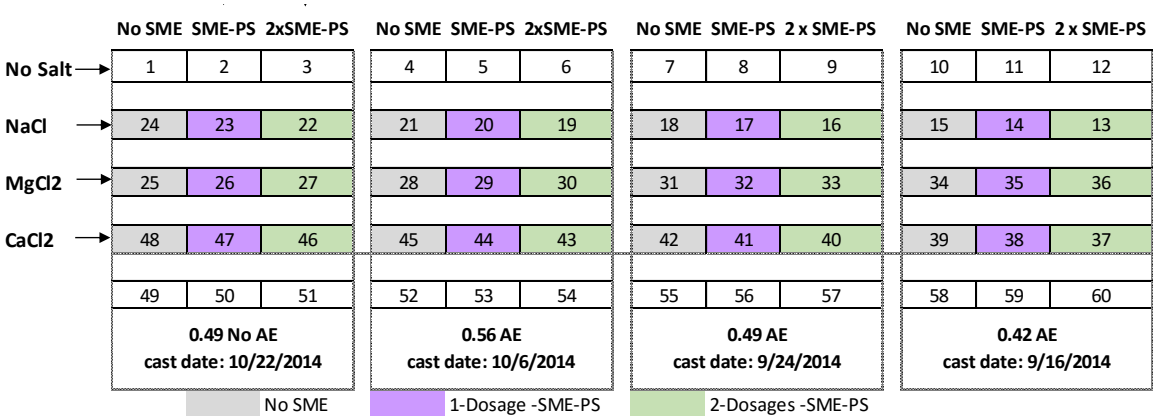

Figure 4-3: General Site Layout of the Exposure Site at CAI (2)

After a minimum time of 28 days was allowed for curing, the SME-PS was applied to the concrete field specimens at an average rate of 12.3 ml of SME-PS/ft^2 using a backpack sprayer. The average approximate application rate was calculated by determining the volume (ml) per surface area (ft^2) using the surface area of 15.75-in x 10.25-in pan, mass (grams) applied, and the interpolated specific gravity for an SME blend for 2%PS reported in Figure 4-5 by Coates [3]. Using a backpack sprayer as shown in Figure 4.4 to apply SME/SME-PS is suggested for sealing pavements.

Figure 4-4: RL Pro Backpack Sprayer used in field application of SME-PS.

The procedure for sealing the sidewalk pavements at the CAI site, is analogous to the procedure used to salt the sidewalk pavements as discussed in section 3.3.4.1 of Chapter 3. The method for treating a pavement slab with SME-PS is to start at the beginning of each slab pavement and make side to side or up and down passes with the wand and sprayer nozzle while moving forward to cover all the unexposed regions of the pavement with SME-PS. With full spraying pressure, one should be able to complete the following procedure at a walking pace using about 1 gallon of SME-PS for every 300 sq. ft. of pavement surface. However, it should be noted that an increase in PS content results in an increased specific gravity and density of the blend, which can change the approximate volume rate of SME-PS used in the field [3].

SME Blend	% PS Content	Density (g/ml)	Specific Gravity, (SG)
Soy Methyl Ester	0	0.8565	0.8825
SME-1%PS	1	0.8591	0.885
SME-5%PS	5	0.8619	0.888
SME-10%PS	10	0.8705	0.8969
SME-20%PS	20	0.8827	0.9094
SME-40%PS	40	0.902	0.9293

Figure 4-5: Table of SME-PS Blend Specific Gravities [9].

Therefore, adjustments to specific spraying conditions such as the types of nozzles used, spray pressure, walking pace and the PS content of the SME used, needs to be taken into consideration when calculating the amount of SME-PS needed for field application. As outlined in Chapter 3, an elevation between 3-6 inches was maintained between the spraying wand and the concrete surface for proper coating. All field pavement specimens where topically treated in one phase on November 23, 2014. The temperature conditions during the application of the SME-PS sealant was monitored to make sure the SME-PS did not reach the cloud point temperature. The minimum temperature was 46.9ºF (8.3ºC), the maximum 55.0ºF (12.8ºC) and the mean temperature was 51.0ºF (10.6ºC).

4.4. Laboratory Testing

The laboratory testing investigations primarily focused on evaluating the short term performance of the concrete mixtures characterized in Chapter 3 treated with SME-PS. The laboratory testing plan also focused on evaluating the long term performance of SME-PS in the field and the effects SME-PS has on limiting the ingress of water and aqueous solutions containing chlorides. Tests to evaluate these properties include: 1) Water Absorption Tests, 2) Chloride Ion Penetration Tests, and 3) Salt Water Ponding Tests. The laboratory investigations included standard test methods to evaluate fluid transport properties of the concrete in regard to the performance and behavior of the constituent materials and sealant under various testing conditions.

4.4.1 Water Absorption into Topically Treated Concrete

Concrete specimens were evaluated using ASTM C1585-13, to determine the rate of absorption of water by hydraulic cement concrete topically treated with SME-PS. The procedure for testing samples for water absorption follows the methodology outlined in chapter 3. For specimens that required the application of SME-PS, the SME was applied to the specimens shortly after the conditioning of

the samples concluded. Topically treating the concrete specimens consisted of applying SME with 2% polystyrene (PS) at laboratory room temperatures. SME-PS was applied to one side of an exposed un-epoxied surface with a paint brush. After samples were coated with SME-PS, the specimens were sealed in plastic storage containers and placed back into their respective environmental humidity chambers to allow the specimens to absorb the SME-PS for several days before being recoated with SME-PS. The purpose of storing the samples in relative humidity chambers, after coating the samples with SME-PS is to prevent or reduce the amount of drying the specimen may experience before testing. After samples were recoated with SME-PS, the specimens were placed back into the environmental humidity chambers for several more days before testing began.

4.4.2 Chloride Ion Penetration into Topically Treated Concrete

As previously mentioned in section 4.2, the four concrete mixtures characterized in Chapter 3 of this experimental investigation were used to evaluate the impact of using SME-PS to mitigate chloride ingress under different testing parameters (i.e., air content and water to binder ratio). As mentioned in Chapter 3, the depth of chloride ion penetration can be determined experimentally with titration methods. The results analyzed in this phase of the experimental investigation used data from cores specimens extracted from SME-PS treated concrete slabs. The first batch of SME-PS treated specimens were extracted from the CAI April 2015 and the second batch September 2015. The procedure for evaluating and analyzing SME-PS treated specimen data followed the same titration procedural method as outlined in Chapter 3 (refer to section 3.4.4 for reference).

4.4.3 Salt Water Ponding on Topically Treated Concrete

The procedure for evaluating SME-PS treated specimens using ASTM C1543-10a herein used the same procedural method as outlined in Chapter 3 (refer to section 3.4.5 for reference). The chloride concentration profiles obtained from specimens fabricated from the mixtures characterized in section 3.4.3 and topically treated

specimens can be found in Appendix B. The y-axis on the chloride concentration profiles denoted “chloride concentration” is the total chloride content given in % by mass of the concrete sample. It should be noted that total chloride concentration is equal to the free and bound chloride in the cementitious system.

4.4.4 Soy Methyl Ester Polystyrene Depth of Penetration Test

The method for determining the depth of SME-PS penetration into concrete used a visible depth of penetration test to determine how far the SME-PS was absorbed into each specimen. This was accomplished by observing large particle agglomeration between SME-PS and dry constituent materials after mixing blends containing SME-PS with an aqueous solution. As previously highlighted by Coates [3] when SME-PS blended solutions, which contain hydrophobic agents come into contact with dry constituent materials before being added to an aqueous solution, the particles tend to coat the SME-PS and agglomerate throughout the mixing process. The procedure for approximating the average depth of SME-PS penetration into concrete used ground concrete powder extracted from slab sections at the CAI site that were used for titration tests. As previously stated in section 3.4.4.1 of chapter 3, the cored specimens from the CAI site were ground in incremental depths of 2mm from the top most depth of the specimen that was exposed to deicing salts to the outermost maximum depth of chloride penetration. 3.0000 ± 0.0005 g of ground concrete powder from each incremental depth of 2mm was added to a 250 ml beaker, mixed with preheated deionized (DI) water and then stirred using a glass stirring rod. The depth of penetration of SME-PS was then visibly determined by observing the large particle agglomeration between the deionized water, SME-PS and dry constituent materials as shown in Figures 4-6 and 4-7. Figure 4-7 shows topically treated (left) and untreated (right) samples from the same mixture that had been ground into a powder and mixed with deionized water.

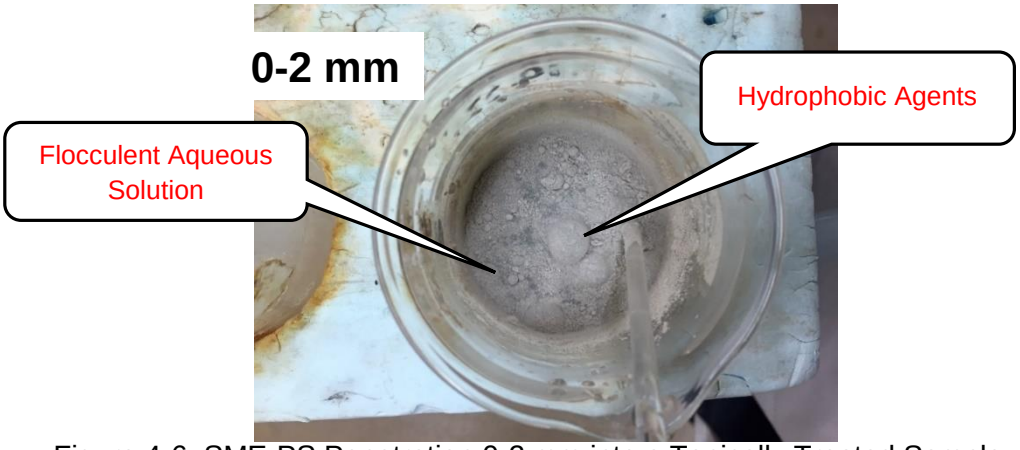

Figure 4-6: SME-PS Penetration 0-2 mm into a Topically Treated Sample

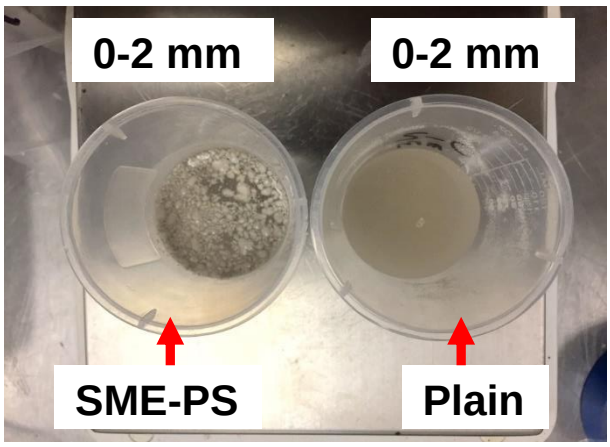

Figure 4-7: Sample containing SME (Left) vs. Plain Sample (Right)

4.5. Field Testing

Specimens that were extracted from the Center for Aging Infrastructure site April 2015 and September 2015 were analyzed to determine the chloride depth of penetration, Dapp and Cs using titration in this study. As previously stated, the same SME-PS treatment that was applied to pavement slab specimens in the field was also applied to specimens in the laboratory. As indicated previously in Chapter 3, due to the time associated with taking cores, only one sample per treatment area (slab) and one control sample were extracted from the CAI site.

4.5.1 Scaling Resistance

The field investigation phase of this study included monitoring the concrete pavements form each mixture design that was cast for this investigation for surface scaling. The surface scaling resistance of the field specimens fabricated from the concrete mixtures considered in this investigation was monitored between December 2014-January 2016. The visible deterioration of the concrete field specimens at the CAI site used a deterioration rating scale presented by Krauss (2009) that rates the effect of surface scaling from 0 to 5 (Table 4-2) [40].

Figure 4-8: Center for Aging Infrastructure: Sidewalk Slab Exposure Site (January 2015)

TABLE 4-2: Concrete Deterioration Rating Scale, Krauss (2009) [40].

Scale	Title	Characteristics
0	No scaling	No evidence of deterioration
1	Light scaling	Loss of cement paste around larger of fine aggregate particles or minor fine cracking of the coating. No delamination or loss of coating and no course aggregate particles exposed. Only minor loss of cement paste or coating around edges of sample or at surface voids.
2	Moderate scaling.	Loss of mortar with coarse aggregate particles exposed or clearly visible. Cracking, local delamination or loss of coating integrity in local areas. Loss of mortar or coating around edges of sample or surface voids may be present.
3	Heavy scaling	Loss of mortar around coarse aggregate particles which protrude above adjacent mortar remaining. Loss of bond and loss of coating material exposing areas of the concrete.
4	Severe scaling	Loss of concrete (loss of coarse aggregate particles) and cracking of concrete. Includes cracking and disintegration of coarse and fine aggregate particles. Major cracking or loss of coating integrity.
5	Failure	Fracture or disintegration of specimen into two or more pieces.

4.5.2 Damage Development in Cementitious Materials Exposed to Salt

Research has shown that damage in concrete can occur during the hot summer temperatures between deicing salts and concrete [5]. Therefore, field specimens at the CAI site were monitored for damage during hot summer temperatures. At room temperature (i.e., 23°C) and calcium chloride salt concentrations at or above 12% by mass in the solution can result in the formation of calcium oxychloride [5, 41, 42]. As reported by Farnam (2015), at salt concentrations greater than 15% the damage caused by the formation of calcium oxychloride is considerable which can result in blocked pores and decreased fluid ingress [5].

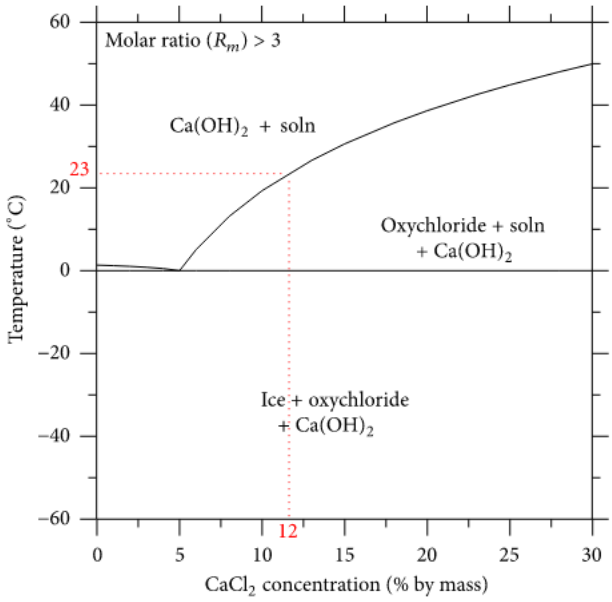

Figure 4-9: $CaCl_2$-$Ca(OH)_2$-H_2O phase diagram for different $Ca(OH)_2/CaCl_2$ molar ratios (R_m) developed from [5].

4.6. Results and Discussions

4.6.1 Influence of SME-PS on Water Absorption

Figure 4-10, presents normalized water absorption data, the effects of w/c, air content, sample conditioning and topical sealer treatment on the water absorption characteristics of the four concrete mixtures characterized in chapter 3. Table 4-3 summarizes the average % reduction in water absorption achieved for samples treated with 2 applications of SME-PS. It should be noted that untreated samples were tested at the same time as topically treated concrete samples.

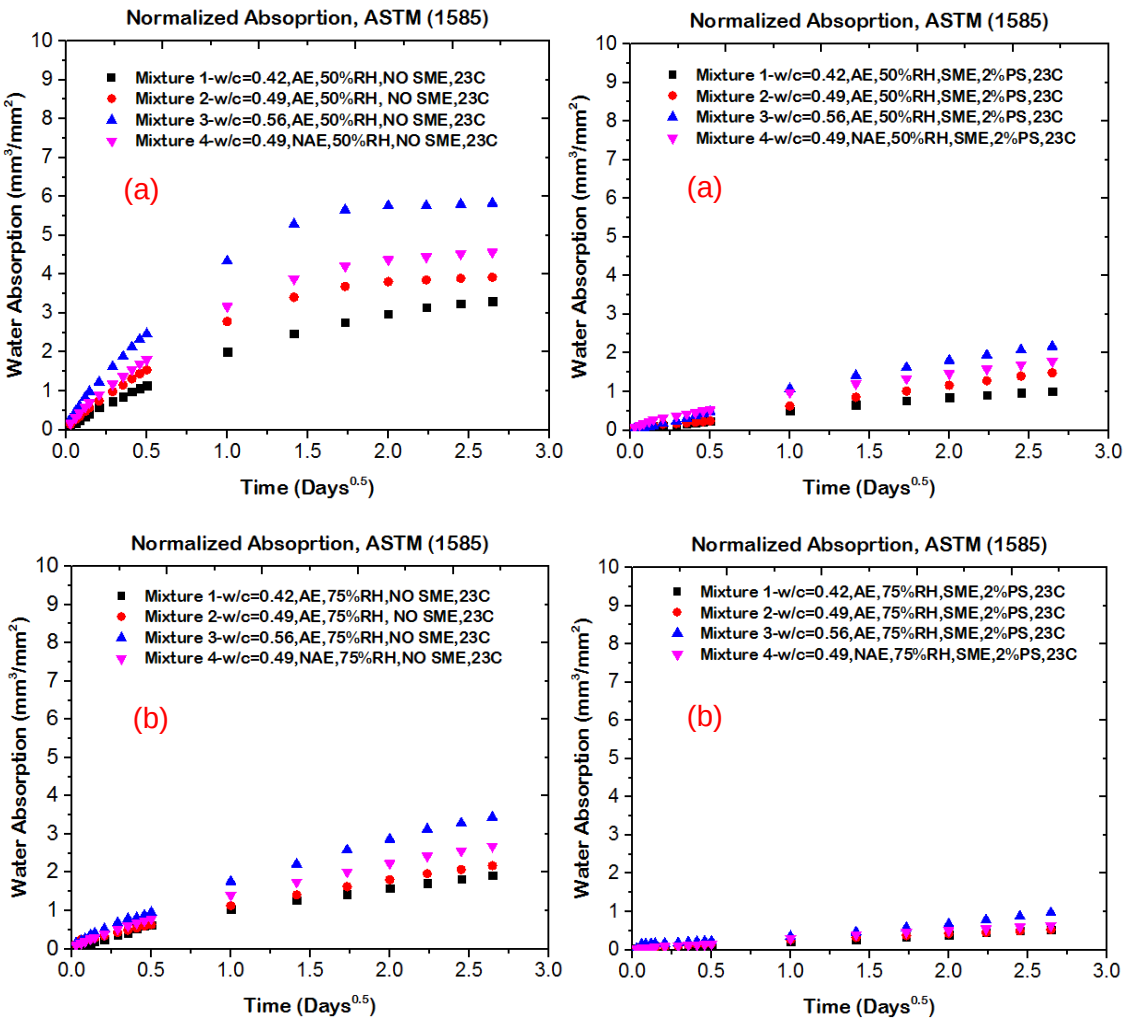

Figure 4-10: Effect effects of water to cement (w/c), air content, sample conditioning, and sealant treatment on water absorption. Specimens conditioned at: (a) 50%RH, (b) at 75%RH

TABLE 4-3: Average % Reduction in Water Absorption After 7 Days

SME-PS Blend	Sample ID: w/c,A,SAM No-%RH	% Reduction	Standard Deviation of % Reduction	Max % Reduction
SME-2%PS	0.42,6.6%,0.14-50%	73.7%	6.4%	80.5
SME-2%PS	0.49,7.0%,0.23-50%	74.8%	7.2%	84.3
SME-2%PS	0.56,6.0%,0.20-50%	78.8%	9.0%	89.1
SME-2%PS	0.49,1.7%,0.55-50%	64.6%	5.6%	70.8
SME-2%PS	0.42,6.6%,0.14-75%	72.9%	6.8%	80.1
SME-2%PS	0.49,7.0%,0.23-75%	76.2%	2.3%	82.7
SME-2%PS	0.56,6.0%,0.20-75%	76.5%	3.7%	80.7
SME-2%PS	0.49,1.7%,0.55-75%	67.0%	16.0%	80.4

Note: A = *air content* (percentage of voids) in the concrete. RH = relative humidity

As seen in Table 4-3, when the SME-PS was applied topically, the water absorption results for samples conditioned at 50% and 75% RH showed an average % reduction in water absorption for all mixtures between 65%-79% and 67%-77% respectively. This confirms that SME-PS blends can reduce the volume of water absorbed per unit area considerably as reported by Golias [4] and Coates [3]. For samples conditioned at 50%RH, the mixture with a w/c of 0.56 achieved the highest average % reduction in water absorption after 7 days, with a reduction of 78.8%. In contrast the worst performance was seen by samples with a w/c of 0.42, which reduced water absorption by an average of 73.7%. The maximum reduction for any sample was 89.1%, was also achieved by a sample with a w/c of 0.56. For samples conditioned at 75%RH, the best performance was also seen in samples fabricated from the mixture with a w/c of 0.56, which achieved the highest average % reduction in water absorption after 7 days, with a 76.5% reduction. In contrast, the worst performance was also seen by samples fabricated from mixture with a w/c of 0.42, which reduced water absorption by an average of 72.9%. A higher % reduction in water absorption was achieved by specimens fabricated from the air entrained mixture with a w/c of 0.49 and air content of 7.0%, than specimens fabricated from the non-air entrained samples with the same w/c and air content of 1.7%

4.6.2 Influence of SME-PS on Chloride Penetration, Cs and Dapp

In total 36 chloride concentration profiles were obtained for each batch of cores extracted April 2015 and September 2015. For reference, it should be noted that the average background/initial chloride concentration that was measured from plain control specimens that were characterized in Chapter 3, had a Co value of 0.04% by mass of concrete. This value was used to fit data using Fick's second law of diffusion. The total chloride concentration profiles for all specimens exposed to NaCl in this study as a function of w/c and sealant coating application rate can be seen in Figures 4-11 through 4-13. Full details of the laboratory test results can be seen in Appendix B. According to the results, the SME-PS reduced the chloride

penetration and concentration of all the specimens. As the volume of air decreased (i.e., increased paste content) for the mixture with a w/c of 0.49, the concentration of chlorides observed in the sample was higher, especially at a shallower depth. However, the concentration and penetration of chlorides on average decreased at deeper depths compared to the entrained air mixture of the same w/c. This is likely attributed to an increase in paste volume and tortuosity. Table 3-2, illustrates that the non-air entrained mixture contained a higher volume of cement paste than the air entrained mixture. Castro et al. (2011) verified the relationship that mixtures containing higher volumes of cement paste absorb more fluid [19]. This explains the higher concentration of chlorides observed in non-air entrained samples when compared to air entrained samples. The performance of the SME-PS at reducing chloride concentration does not appear to be significantly influenced by w/c. However, no matter the salt exposure condition, a specimen that was topically treated with SME-PS which had a lower w/c also had a lower chloride concentration overtime. Conversely, an increase in w/c typically resulted in an increase in chloride concentration. This is expected for the reason that samples with higher w/c exhibit higher rates of chloride diffusion than samples with lower w/c.

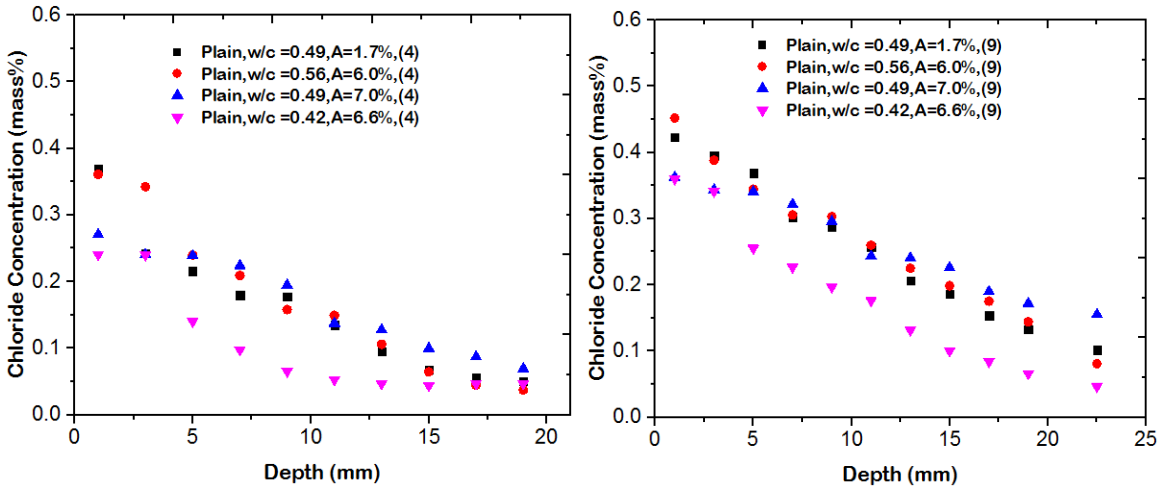

Figure 4-11: Chloride Concentration Profiles with Time of Exposure to NaCl for Plain Specimens. Note: (4) Indicates 4 Months of Exposure to NaCl. (9) Indicates 9 Months of Exposure to NaCl.

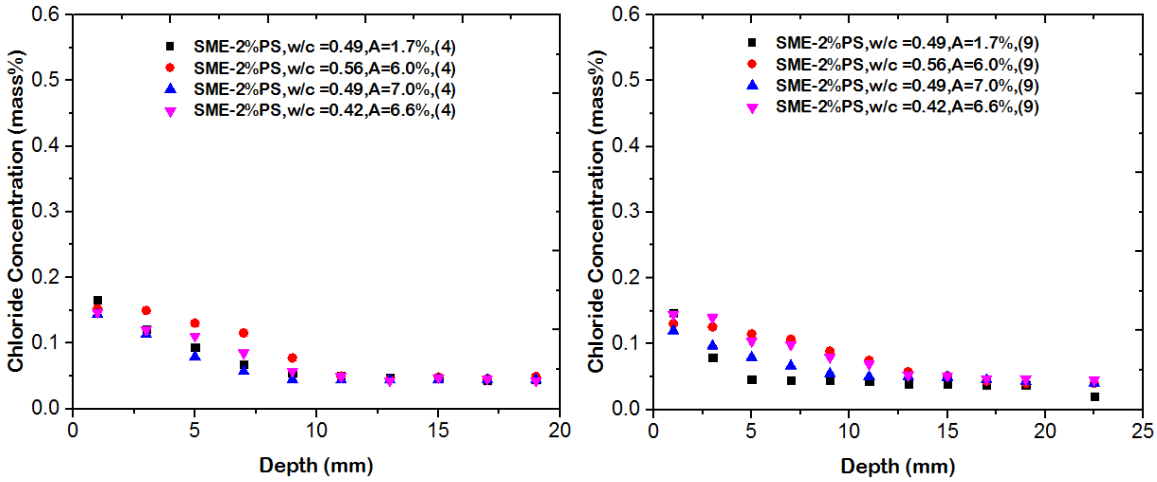

Figure 4-12: Chloride Profiles with Time of Exposure to NaCl for Specimens Treated with One Dosage of SME-2%PS. Note: (4) Indicates 4 Months of Exposure to NaCl. (9) Indicates 9 Months of Exposure to NaCl.

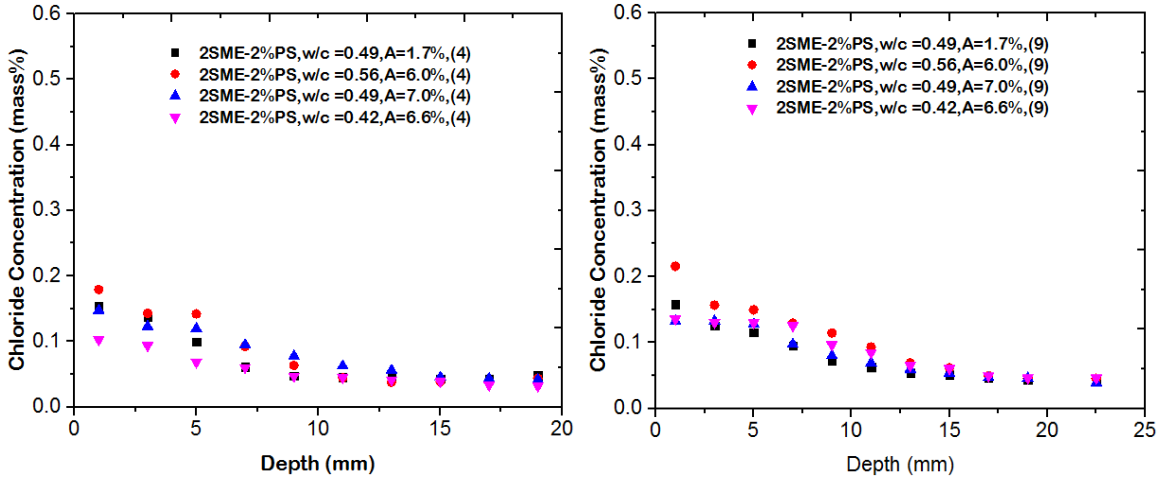

Figure 4-13: Chloride Concentration Profiles with Time of Exposure to NaCl for Specimens Treated with Two Dosages of SME-2%PS. Note: (4) Indicates 4 Months of Exposure to NaCl. (9) Indicates 9 Months of Exposure to NaCl.

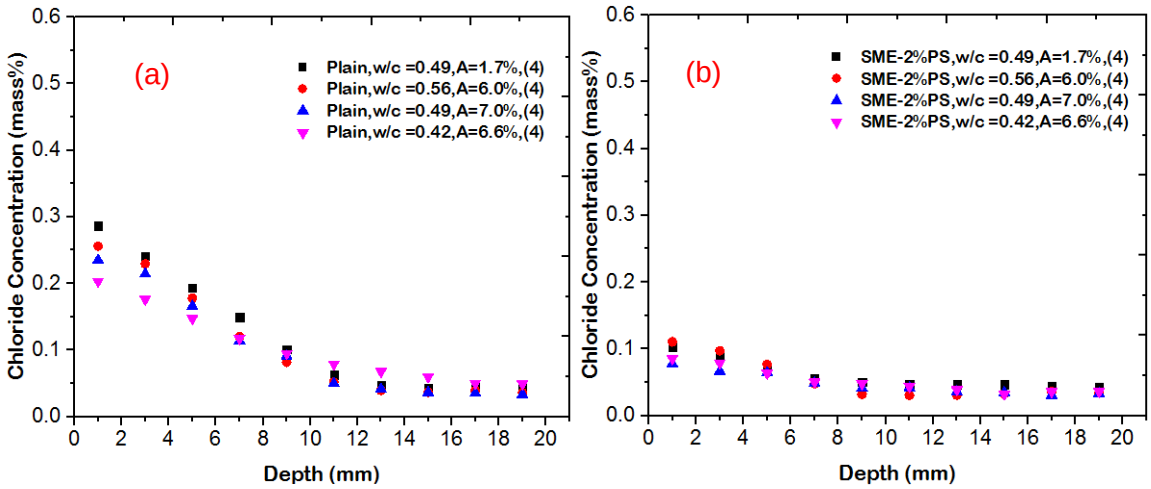

Figure 4-14: Chloride Concentration Profiles with Time of Exposure to $CaCl_2$ for Plain Specimens (a). Figure 4-15: Chloride Profiles with Time of Exposure to NaCl for Specimens Treated with One Dosage of SME-2%PS (b). Note: (4) Indicates 4 Months of Exposure to $CaCl_2$.

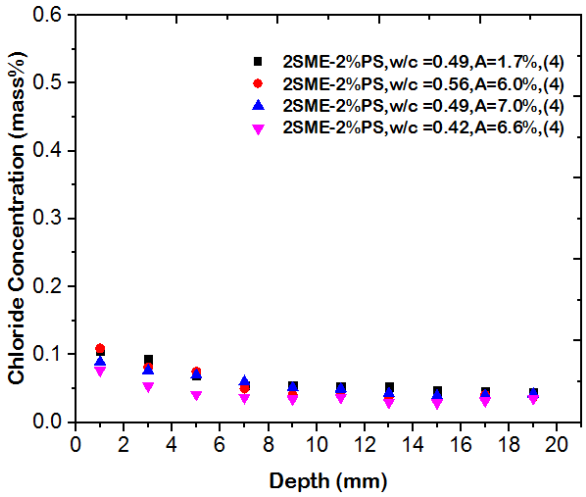

Figure 4-16: Chloride Concentration Profiles with Time of Exposure to $CaCl_2$ for Specimens Treated with Two Dosages of SME-2%PS (c). Note: (4) Indicates 4 Months of Exposure to $CaCl_2$.

Tables 4-4 through 4-7 contain Dapp and Cs resulting from the non-linear regression analysis of the chloride concentration profiles for slabs exposed to SME. The correlation factors (R^2) determined by OriginPro non-linear regression software are also given. The non-linear relationship between the chloride concentration (by % mass of concrete) vs. the depth from the surface of the

concrete in millimeters was obtained in all cases with correlation coefficients generally in excess of 0.90. The % reduction in surface chloride concentrations for topically treated samples exposed to NaCl, $MgCl_2$ and $CaCl_2$ are presented in Figures 4-17 through 4-23.

Table 4-4: Dapp, surface chloride content, and correlation factors for topically treated specimens extracted from the CAI site Apr. 2015 (One dosage of SME-2%PS).

Exposure Condition	Air Content (%)	w/c	Sample ID (Fig.3-5)	Dapp (x10-12 m^2/s)	Cs (mass%)	R^2
NaCl	6.6	0.42	14	2.56	0.1638	0.9731
	7.0	0.49	17	1.24	0.1668	0.9884
	6.0	0.56	20	3.66	0.1811	0.9216
	1.7	0.49	23	1.59	0.1839	0.9912
$MgCl_2$	6.6	0.42	35	2.65	0.0750	0.9919
	7.0	0.49	32	7.25	0.0932	0.9225
	6.0	0.56	29	4.25	0.0950	0.9676
	1.7	0.49	26	2.36	0.1441	0.9467
$CaCl_2$	6.6	0.42	38	3.66	0.0833	0.9692
	7.0	0.49	41	3.53	0.0922	0.9733
	6.0	0.56	44	1.62	0.1312	0.9529
	1.7	0.49	47	2.28	0.1105	0.9731

Table 4-5: Dapp, surface chloride content, and correlation factors for untreated specimens extracted from the CAI site Apr. 2015 (Two dosages of SME-2%PS).

Exposure Condition	Air Content	w/c	Sample ID (Fig. 3-5)	Dapp (x10-12 m^2/s)	Cs (mass%)	R^2
NaCl	6.6	0.42	13	3.24	0.1120	0.9797
	7.0	0.49	16	3.99	0.1609	0.9815
	6.0	0.56	19	2.32	0.2058	0.9498
	1.7	0.49	22	1.53	0.1837	0.9595
$MgCl_2$	6.6	0.42	36	3.84	0.0865	0.9520
	7.0	0.49	33	6.05	0.0905	0.9748
	6.0	0.56	30	2.31	0.0935	0.9593
	1.7	0.49	27	1.22	0.1132	0.9341
$CaCl_2$	6.6	0.42	37	8.80	0.0860	0.9425
	7.0	0.49	40	2.82	0.0954	0.9884
	6.0	0.56	43	1.24	0.1227	0.9650
	1.7	0.49	46	2.62	0.1119	0.9217

Table 4-6: Dapp, surface chloride content, and correlation factors for topically treated specimens extracted from the CAI site Sept. 2015 (One dosage of SME-2%PS).

Exposure Condition	Air Content (%)	w/c	Sample ID (Fig. 3-5)	Dapp (x10-12 m^2/s)	Cs (mass%)	R^2
NaCl	6.6	0.42	14	1.81	0.1273	0.9786
	7.0	0.49	17	1.07	0.1495	0.9820
	6.0	0.56	20	2.38	0.1607	0.9542
	1.7	0.49	23	1.50	0.1923	0.9562
$MgCl_2$	6.6	0.42	35	2.42	0.0741	0.9778
	7.0	0.49	32	2.36	0.0856	0.9530
	6.0	0.56	29	1.19	0.0866	0.9304
	1.7	0.49	26	3.98	0.1271	0.9458
$CaCl_2$	6.6	0.42	38	1.03	0.0699	0.9707
	7.0	0.49	41	1.20	0.0806	0.9568
	6.0	0.56	44	2.06	0.0989	0.9803
	1.7	0.49	47	4.51	0.1064	0.9766

Table 4-7: Dapp, surface chloride content, and correlation factors for untreated specimens extracted from the CAI site Sept. 2015 (Two dosages of SME-2%PS).

Exposure Condition	Air Content	w/c	Sample ID (Fig. 3-5)	Dapp (x10-12 m^2/s)	Cs (mass%)	R^2
NaCl	6.6	0.42	13	4.07	0.1546	0.9344
	7.0	0.49	16	2.20	0.1557	0.9554
	6.0	0.56	19	2.11	0.2193	0.9742
	1.7	0.49	22	1.43	0.1688	0.9919
$MgCl_2$	6.6	0.42	36	1.58	0.0754	0.9381
	7.0	0.49	33	2.26	0.0873	0.9679
	6.0	0.56	30	7.13	0.0912	0.9139
	1.7	0.49	27	2.43	0.1604	0.9575
$CaCl_2$	6.6	0.42	37	1.08	0.0720	0.9625
	7.0	0.49	40	1.88	0.0760	0.9812
	6.0	0.56	43	7.54	0.1016	0.9866
	1.7	0.49	46	2.49	0.0962	0.9914

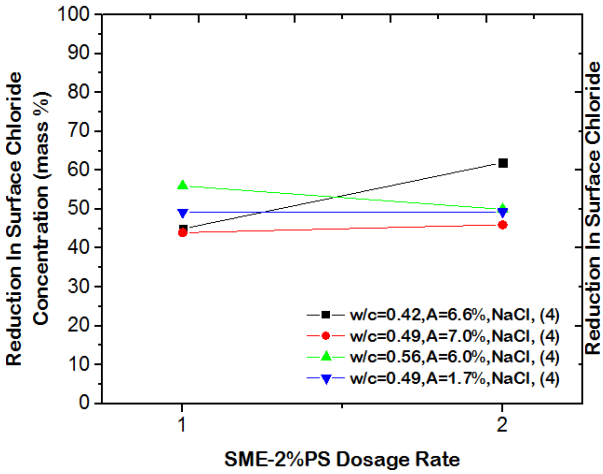

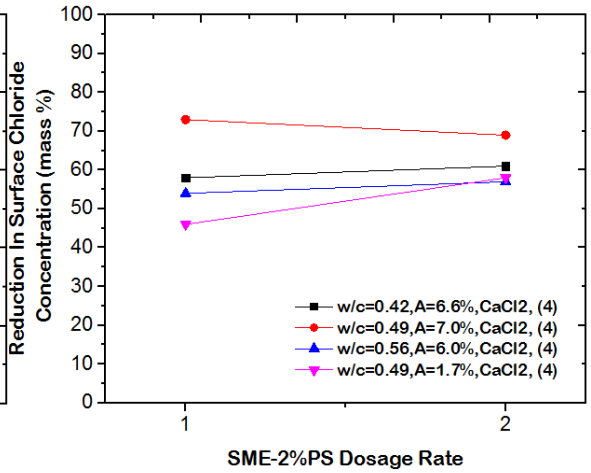

Figure 4-17: % Reduction in Surface Chloride Concentration for topically treated samples exposed to NaCl (a). Figure 4-18: % Reduction in Surface Chloride Concentration for topically treated samples exposed to $CaCl_2$(b). Note: (4) Indicates 4 Months of Exposure to Salt.

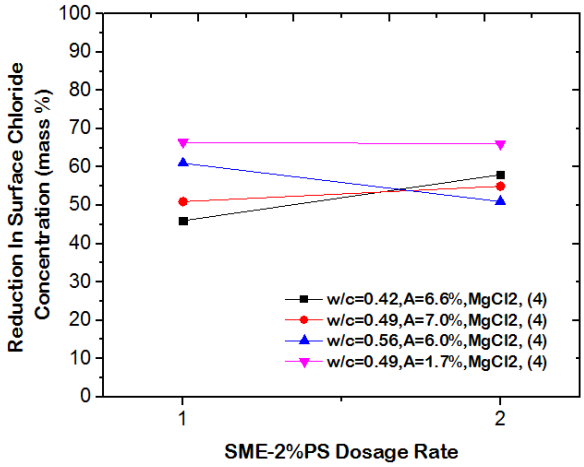

Figure 4-19: % Reduction in Surface Chloride Concentration for topically treated samples exposed to $MgCl_2$(c). Note: (4) Indicates 4 Months of Exposure to Salt.

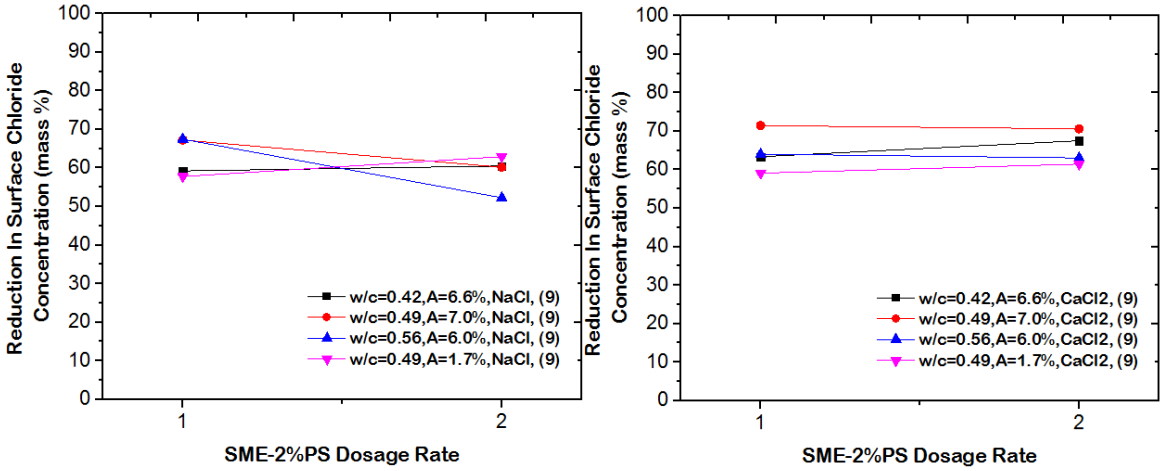

Figure 4-20: % Reduction in Surface Chloride Concentration for topically treated samples exposed to NaCl (a). Figure 4-21: % Reduction in Surface Chloride Concentration for topically treated samples exposed to $CaCl_2$(b). Note: (9) Indicates 9 Months of Exposure to Salt.

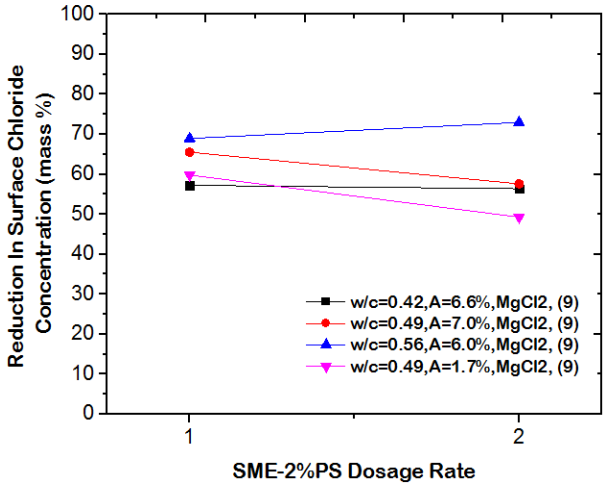

Figure 4-22: % Reduction in Surface Chloride Concentration for topically treated samples exposed to $MgCl_2$(c). Note: (9) Indicates 9 Months of Exposure to Salt

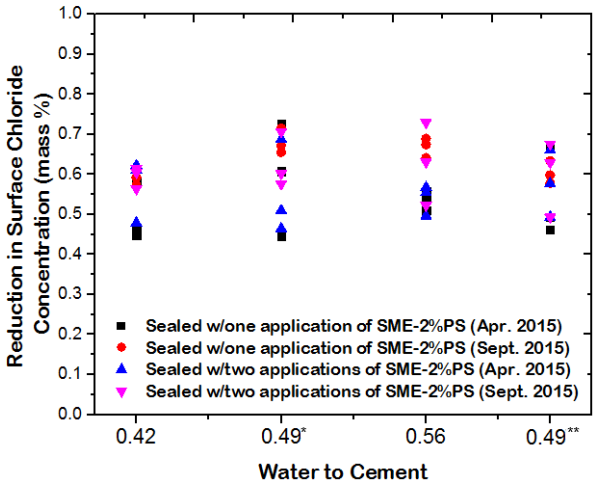

Figure 4-23: Influence of w/c on the % Reduction in Surface Chloride Concentration for topically treated samples exposed to Salt Ingress from December 2014 through September 2015. Note: 0.49*, and 0.49** indicates a mixture with an air content of 7.0%, and 1.7% respectively.

The effect of w/c on Cs for topically treated specimens is illustrated in Tables 4-4 through Table 4-7. Profiles with higher w/c had higher Cs values. This is expected for the reason that samples with higher w/c exhibit higher rates of chloride diffusion than samples with lower w/c. However, with some exception, the effect of w/c on the total chloride content reported in Table 4-8 and 4-9 is not as apparent. This is likely attributed to the fact that not enough representative samples were evaluated in this study. However as previously stated, Cs is not a measured value of the chloride concentration at the surface, but a value that was obtained from nonlinear regression analysis. Samples that were treated with SME-PS decreased Cs by as much as 45-70%, regardless of the type of salt used. The effect of the SME-PS application rate does not appear to significantly influence the performance of the applied SME-PS at further reducing Cs. The 2nd dosage of SME-PS reduced Cs by only an additional 1-6%. The results presented in Figures 4-17 through 4-22, indicate approximately the same level of reduction of the amount of chlorides at the surface for both one and two applications of SME-PS. Hence, at this time point, the second coating of SME-PS did not show significant benefit in significantly reducing Cs.

TABLE 4-8: Chloride concentrations at the surface, 5mm, and 10 mm into the concrete for topically treated specimens extracted from the CAI site Apr. and Sept. 2015.

Exposure Duration:	4 months*			9 months*		
Sample ID (w/c-A-E)	Cs (% mass)	[Cl-] (% mass) 5 mm depth	[Cl^-] (% mass) 10 mm depth	Cs (% mass)	[Cl-] (% mass) 5mm depth	[Cl^-] (% mass) 10 mm depth
0.42-6.6%-NaCl	0.1638	0.1107	0.0572	0.1273	0.1037	0.0794
0.49-7.0%-NaCl	0.1668	0.0791	0.0447	0.1495	0.0797	0.0546
0.56-6.0%-NaCl	0.1811	0.1306	0.0774	0.1607	0.1149	0.0890
0.49-1.7%-NaCl	0.1839	0.0943	0.0549	0.1923	0.0463	0.0444
0.42-6.6%-$MgCl_2$	0.0750	0.0679	0.0516	0.0741	0.0689	0.0531
0.49-7.0%- $MgCl_2$	0.0932	0.0563	0.0502	0.0856	0.0647	0.0476
0.56-6.0%- $MgCl_2$	0.0950	0.0671	0.0480	0.0866	0.0412	0.0379
0.49-1.7%- $MgCl_2$	0.1441	0.088	0.0495	0.1271	0.0605	0.0478
0.42-6.6%- $CaCl_2$	0.0833	0.0633	0.0479	0.0699	0.0512	0.0390
0.49-7.0%- $CaCl_2$	0.0922	0.0643	0.0413	0.0806	0.0472	0.0409
0.56-6.0%- $CaCl_2$	0.1312	0.0768	0.0320	0.0989	0.0472	0.0410
0.49-1.7%- $CaCl_2$	0.1105	0.0723	0.0509	0.1064	0.0844	0.0571

Note: A = air content (percentage of voids) in the concrete. E = salt exposure condition. Based on one application of SME-2%PS*

TABLE 4-9: Chloride concentrations at the surface, 5mm, and 10 mm into the concrete for topically treated specimens extracted from the CAI site Apr. and Sept. 2015.

Exposure Duration:	4 months*			9 months*		
Sample ID (w/c-A-E)	Cs (% mass)	[Cl-] (% mass) 5 mm depth	[Cl^-] (% mass) 10 mm depth	Cs (% mass)	[Cl-] (% mass) 5mm depth	[Cl^-] (% mass) 10 mm depth
0.42-6.6%-NaCl	0.1120	0.0685	0.0471	0.1546	0.1301	0.0965
0.49-7.0%-NaCl	0.1609	0.1197	0.0780	0.1557	0.1279	0.0801
0.56-6.0%-NaCl	0.2058	0.1422	0.0635	0.2193	0.1497	0.1145
0.49-1.7%-NaCl	0.1837	0.0994	0.0474	0.1688	0.1151	0.0725
0.42-6.6%-$MgCl_2$	0.0865	0.0668	0.0478	0.0754	0.0507	0.0371
0.49-7.0%- $MgCl_2$	0.0905	0.0766	0.0635	0.0873	0.0752	0.0611
0.56-6.0%- $MgCl_2$	0.0935	0.0549	0.0336	0.0912	0.0625	0.0577
0.49-1.7%- $MgCl_2$	0.1132	0.0607	0.0416	0.1604	0.1063	0.0860
0.42-6.6%- $CaCl_2$	0.0860	0.0413	0.0345	0.0720	0.0614	0.0440
0.49-7.0%- $CaCl_2$	0.0954	0.0700	0.0513	0.0760	0.0426	0.0412
0.56-6.0%- $CaCl_2$	0.1227	0.0750	0.0401	0.1016	0.0644	0.0469
0.49-1.7%- $CaCl_2$	0.1119	0.0698	0.0541	0.0962	0.0742	0.0581

Note: A = air content (percentage of voids) in the concrete. E = salt exposure condition. Based on two applications of SME-2%PS*

The magnitude of deviation for the % reduction in Cs appears to be the lowest in concretes with a w/c of 0.42. Whereas, the magnitude of deviation for the % reduction in Cs for concrete with a w/c of 0.56 appears to be slightly lower than concretes with a w/c of 0.49*. Figure 4-23, shows specimens that were non-air entrained pertaining to the mixture with a w/c of 0.49 and air content of 1.7% resulted in a smaller magnitude of deviation in the % reduction in Cs than air entrained specimens pertaining to the mixture of the same w/c and air content of 7.0%. Furthermore, while the data presented in Figures 4-17 through 4-22 shows that range in the % reduction in Cs is similar regardless of the type of salt that was used. Furthermore, Figure 4-23 appears to show the % reduction in Cs slightly increases with increasing w/c.

The visible chloride depths of penetration for samples taken from the CAI site 4 months after the initial application of deicing salt in April 2015 illustrated in Table 4-10 were compared to samples that were taken 9 months after the initial application of deicing salt in September 2015 (Table 4-11).

TABLE 4-10: Visible Chloride Depth of Penetration (mm) for Samples Taken Apr. 2015

Specimen ID: (%Salt Conc., SME Dosage Rate)	w/c =0.42, A=6.6%	w/c =0.49, A=7.0%	w/c =0.56, A=6.0%	w/c =0.49, A=1.7%
10% NaCl-No SME	8.9	10.2	15.9	15.8
10% NaCl- SME-2%PS	5.0	7.7	9.1	6.0
10% NaCl-2XSME-2%PS	2.3	3.8	4.8	4.7
10% $MgCl_2$ -No SME	7.3	7.9	8.6	7.3
10% $MgCl_2$ -SME-2%PS	3.7	4.5	6.0	6.5
10% $MgCl_2$ -2XSME-2%PS	1.9	2.5	5.1	5.7
10% $CaCl_2$ -No SME	9.8	10.3	11.3	12.0
10% $CaCl_2$ -SME-2%PS	9.2	4.4	7.8	1.2
10% $CaCl_2$ -2XSME-2%PS	6.3	4.7	7.8	2.0

TABLE 4-11: Visible Chloride Depth of Penetration (mm) for Samples Taken Sept.2015

Specimen ID: (%Salt Conc., SME Dosage Rate)	w/c =0.42, A=6.6%	w/c =0.49, A=7.0%	w/c =0.56, A=6.0%	w/c =0.49, A=1.7%
10% NaCl-No SME	18.6	20.6	22.5	17.6
10% NaCl- SME-2%PS	13.2	8.3	10.1	11.1
10% NaCl-2XSME-2%PS	7.9	7.9	9.1	9.2
10% $MgCl_2$ -No SME	12.0	13.9	14.8	11.9
10% $MgCl_2$ -SME-2%PS	5.0	4.5	6.2	5.1
10% $MgCl_2$ -2XSME-2%PS	3.2	2.9	4.5	3.2
10% $CaCl_2$ -No SME	14.5	14.5	15.9	14.3
10% $CaCl_2$ -SME-2%PS	5.3	4.8	7.6	10.8
10% $CaCl_2$ -2XSME-2%PS	3.4	2.9	3.7	4.6

The results in Tables 4-10 and 4-11 show that the 2nd application of SME-PS does appear to further decrease the depth of chloride penetration. Furthermore, the samples that were treated with a 2nd application of SME-PS resulted in an average reduction in chloride depth of about 16% and 24% greater than that of the smaller dosage, for 4 and 9 months of salt exposure respectively. After 4 months of salt exposure, the chloride penetration depth was reduced by 45%, 34%, and 46% for the NaCl, $MgCl_2$ and $CaCl_2$ for a single dosage of SME-PS respectively. Equally, for the same period of exposure, the chloride penetration depth was reduced by 69%, 51% and 51% for the NaCl, $MgCl_2$ and $CaCl_2$ for specimens that were coated with a 2nd application of SME-PS respectively. Overall, the depth of chloride penetration for all tropically treated specimens that were coated with a single application of SME-PS was reduced by an average of 42% compared with untreated control samples. Further, specimens that were coated with a 2nd application of SME-PS reduced the visible depth of chloride penetration by an average of 58% for specimens treated with for 10% by mass NaCl, $MgCl_2$ and $CaCl_2$. It should be noted that 10% by mass NaCl, $MgCl_2$ and $CaCl_2$ is the concentration of salt that was applied to the pavements and not the salt concentration in the pavement. After 9 months of salt exposure, the chloride penetration depth was reduced by 38%, 43% and 52% for the NaCl, $MgCl_2$ and

$CaCl_2$ for a single dosage of SME-PS respectively. Furthermore, for the same period of exposure, the chloride penetration depth was reduced by 57%, 74% and 75% for the NaCl, $MgCl_2$ and $CaCl_2$ for specimens that were coated with a 2^{nd} application of SME-PS respectively. Generally, after 9 months of salting exposure using a single dosage rate of SME-PS, the visible depth of chloride penetration for all tropically treated specimens was reduced by an average of 44% compared with untreated samples for the same exposure time. While specimens that were coated with a 2^{nd} application of SME-PS reduced the visible depth of chloride penetration by an average of 69%. Tables 4-10 and 4-11 highlight the variability encountered while measuring the visual depth of chloride penetration for specimens of the same w/c but different air contents. With some exception, specimens tested in April and September fabricated from the mixture design with a w/c of 0.49 and air content of 1.7%, Table 4-10 shows an increase in the chloride depth of penetration as air content decreases (i.e., paste volume decreases), which is expected in this case. This is for the reason that the paste content for the non-air entrained specimens is higher. As previously mentioned above, mixtures that have higher paste contents have been reported to exhibit higher rates of fluid absorption [19]. The water absorption results reported in chapter 3 and 4 confirm this.

4.6.2.1. Modeling Chloride Diffusion into Concrete with SME-PS

To analyze the effect of SME-PS on chloride diffusion into concrete, statistical analysis was employed using Fick's second law of diffusion to refit chloride concentration profiles obtained from SME-PS treated specimens (see Figures 4-24 and 4-25) with 50% to 60% of the Cs values obtained from plain control samples. The estimated values of 50-60% were chosen for Cs based on experimental results from slabs containing SME-PS. The experimental results indicate Dapp does not change significantly in the presence of SME-PS, which indicates SME-PS blends may change chloride binding. This impacts the total chloride concentration in cementitious systems. Since, Cs changes significantly and Dapp does not widely change in the presence of SME-PS, this specifies the

chloride in the pore solution is not drastically effected. Furthermore, the results show that the diffusion of chloride ions into concrete treated with SME-PS can be modeled by taking a fraction of Cs in Fick 2nd Law. This is critically important from a design and cost prospective, since tests do not need to be conducted with SME-PS to determine the benefits of surface treatment. Details of similar chloride profiles refit using a fraction of Cs in Fick's 2nd law can be seen in Appendix D.

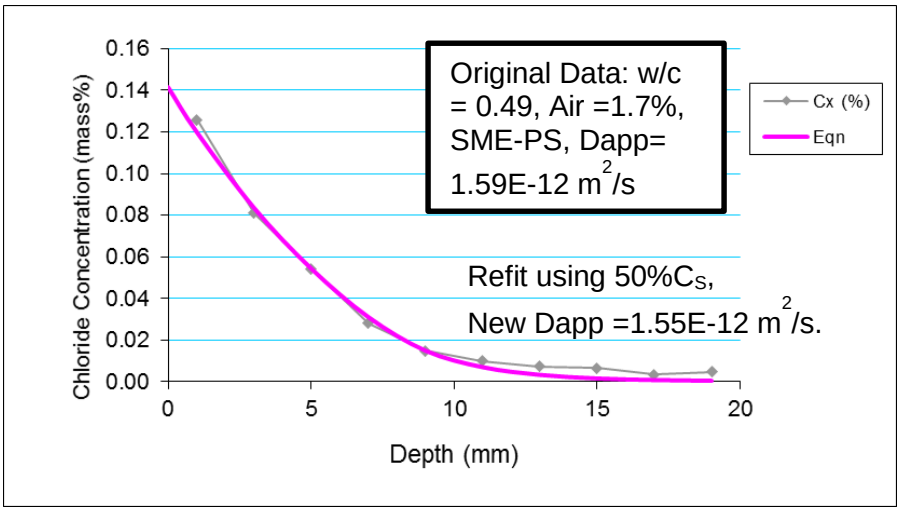

Figure 4-24: Chloride profile- w/c =0.49, air content = 1.7%, refit for Dapp using 50% of Cs from a similar plain sample. Note: samples were exposed to $CaCl_2$ for 4 months

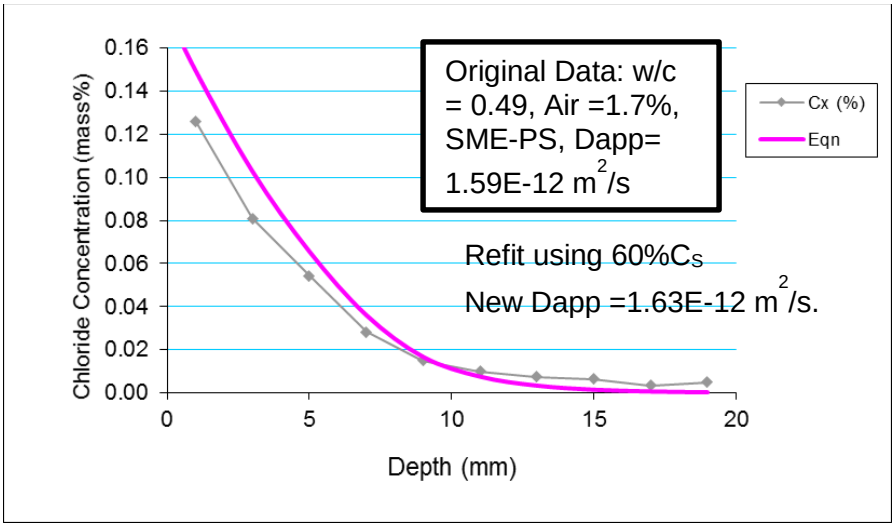

Figure 4-25: Chloride profile- w/c =0.49, air content = 1.7%, refit for Dapp using 60% of Cs from a similar plain sample. Note: samples were exposed to $CaCl_2$ for 4 months

4.6.3 Influence of SME-PS on Salt Water Ponding Tests

In total, 24 chloride concentration profiles were obtained from the four mixtures studied in this investigation that were ponded in 10% by mass reagent grade NaCl solution. The total chloride concentration profiles for all specimens exposed to NaCl in this study, as a function of w/c and sealant coating application rate, can be seen in Figures 4-24 through 4-25. As previously mentioned in section 3.4.4, each point on the chloride ponding concentration profile below is the average of several test specimen readings per mixture design. However, it should be noted only two specimen readings per mixture design were used to construct the graph below.

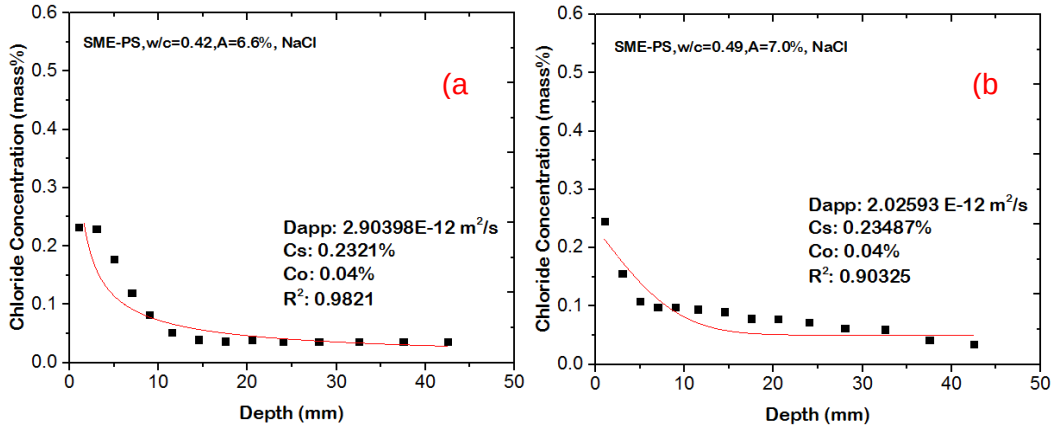

Figure 4-26: Chloride Concentration Profiles for Specimens Ponded in 10% by mass NaCl that were Treated with Two Dosages of SME-2%PS. (a) Mixture No 1, (b) Mixture No 2.

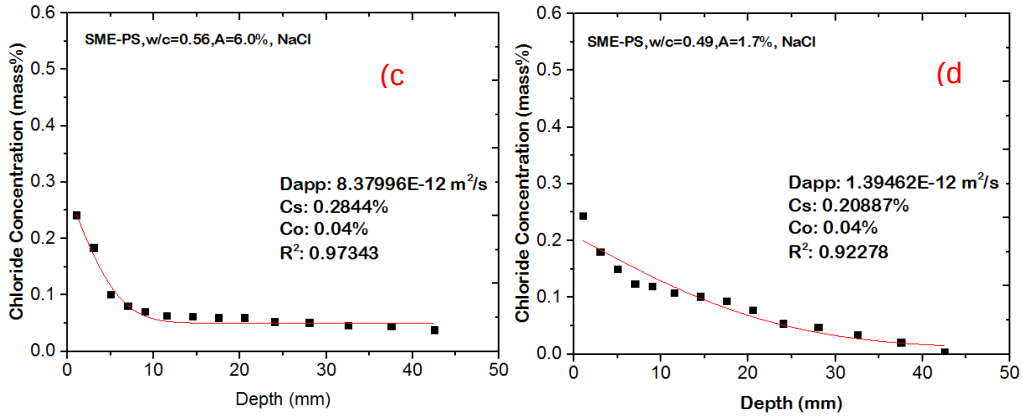

Figure 4-27: Chloride Concentration Profiles for Specimens Ponded in 10% by mass NaCl that were Treated with Two Dosages of SME-2%PS. (c) Mixture No 3, (d) Mixture No 4.

The SME-PS was most effective at reducing the surface chloride concentration for specimens fabricated from the mixture design with a w/c of 0.49 and air content of 1.7%, after 136 days of ponding. The results highlighted in Figures 4-24 through 4-25 indicate that SME-PS sealant is slightly more effective at mitigating chloride ingress with increasing w/c. These results are in good agreement with the results highlighted in Figure 4-23. The SME-PS decreased the surface chloride concentration by about 9.8%, 9.9%, 25.4% and 28.5% for the mixtures 1, 2, 3, and 4 respectively.

4.6.4 Influence of Concrete Mixture on SME-PS Penetration

The results displayed in Tables 4-12 and 4-13 illustrate the depth of SME-PS penetration that was visibly determined by observing particle agglomeration between deionized water, SME-PS and dry constituent materials. In total 468 measurements (i.e., 13 measurements per sample) were made on 36 different cored specimens (i.e., 24-topically treated specimens and 12-plain/untreated reference specimens). Full details of the laboratory test results can be seen in Appendix C.

TABLE 4-12: Depth of SME-PS Penetration Summary for Mixtures No: 1, 2, 3, and 4

W/C, Porosity Mixture No:	0.49, 13.8% Mixture No.4		0.56, 22.3%, Mixture No.3		0.49, 21.5%, Mixture No.2		0.42, 18.5%, Mixture No.1	
Sealer Dosage Rate[1]	1	2	1	2	1	2	1	2
Approximate Mean Sealer Depth of Penetration (mm)	2.0	2.7	6.0	6.7	3.3	4.0	2.7	3.3
Max:	2.0	4.0	6.0	8.0	4.0	4.0	4.0	6.0
Min:	2.0	2.0	6.0	6.0	2.0	4.0	2.0	2.0

Note: 1-One Dosage of SME-2%PS, 2-2 Dosages of SME-2%PS[1].

The approximate experimental values suggest that the concrete water to cement ratio influences the penetration of the sealant. In this test, the average from 2 samples shows clear increase in penetration depth with higher water to cement ratios. Furthermore, the results demonstrate that a higher penetration depth of

SME-PS in general is associated with mixtures that exhibit faster rates of fluid absorption (i.e., higher paste contents).

4.6.5 Influence of SME-PS on Scaling Resistance

The 36 pavement sections that were considered in this study, located at the CAI site, were assessed by visual examination for scaling damage. The pavements were given a rating based on the concrete deterioration rating scale presented in section 4.5.1 [40]. The results presented in Tables 4-14 through 4-16, were measured at the end of the first winter season following the initial application of deicing salt exposure, which extended from December 21, 2014 to March 20, 2015, and once again during the 2015-2016 winter season. The ratings reported in Tables 4-14 through 4-16, for the first winter cycle are based on the visual examination of pavement specimens examined on March 20, 2015, the last day of the 2014-2015 winter season. Ratings reported during the second winter cycle of field exposure are based on the visual examination of slab specimens examined on March 2, 2016. The rating scale was explained in Table 4-2 in section 4.5.1 with “5” being the most severe scaling damage and “0” meaning no scaling damage. Figures 4-27a through 4-27b show the visual difference between a deterioration rating from 0 to 2. Figures 4-28a through Figure 4-31 highlight topically treated and untreated specimens that were exposed to salt ingress from December 2014 to March 2, 2016.

Figure 4-28: Center for Aging Infrastructure: Sidewalk Slab Exposure Site (February 2016)

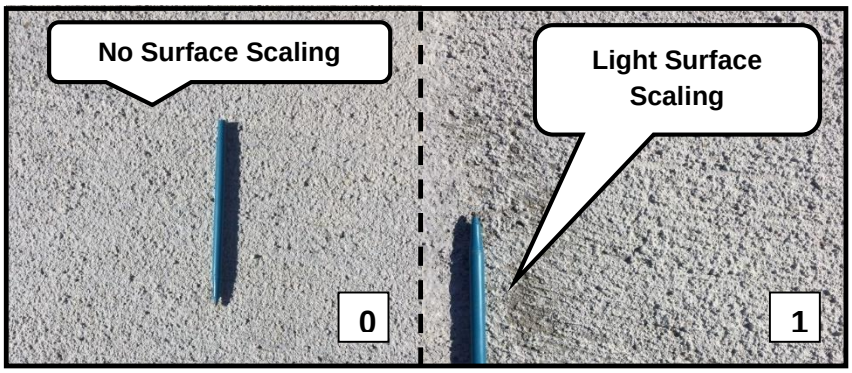

Figure 4-29a: Scaling rating from 0 to 1.

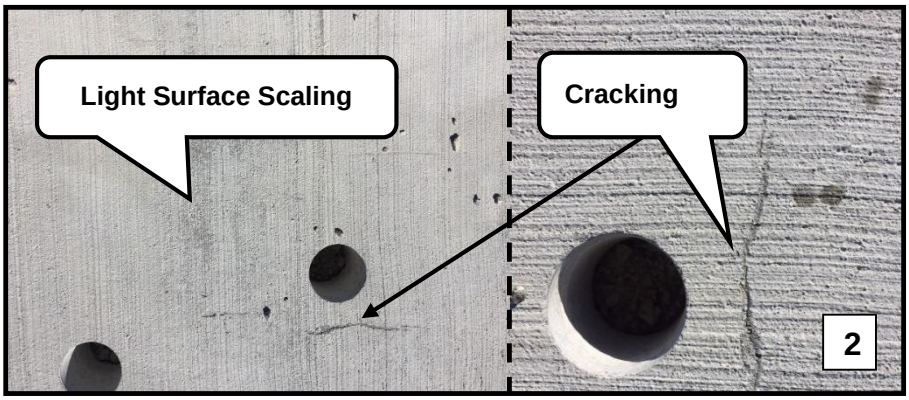

Figure 4-29b: Scaling rating from 0 to 1.

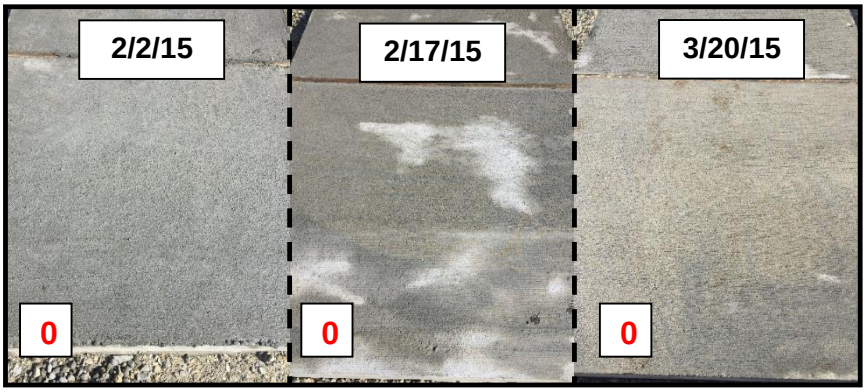

Figure 4-30a: Visual Examination of an Untreated Non-Air Entrained Pavement Fabricated from a Mixture with a w/c=0.49, Air Volume=1.7%, and SAM=0.55 That Has Been Exposed to 10%$CaCl_2$

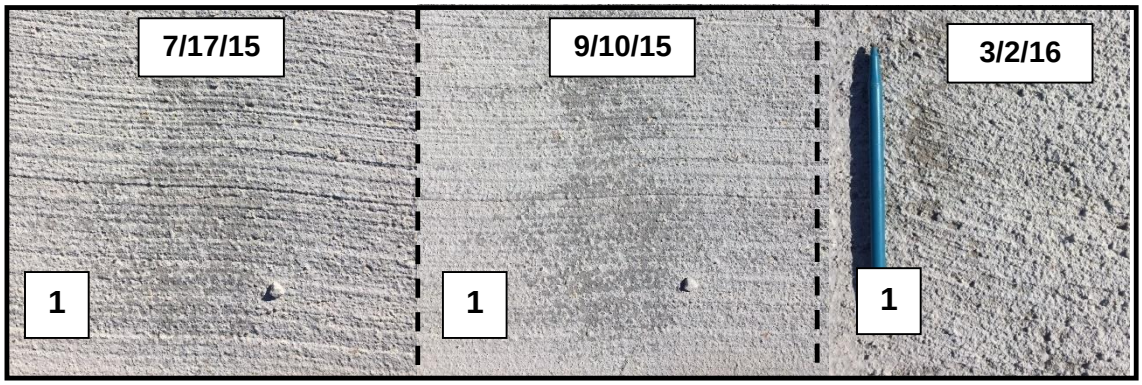

Figure 4-30b: Visual Examination of an Untreated Non-Air Entrained Pavement Fabricated from a Mixture with a w/c=0.49, Air Volume=1.7%, and SAM=0.55 That Has Been Exposed to 10%$CaCl_2$

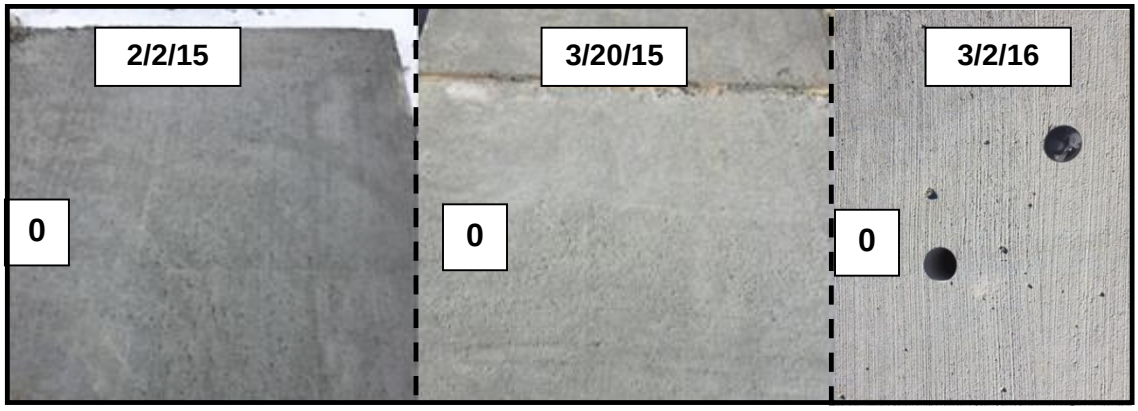

Figure 4-31: Visual Examination of a Topically Treated Non-Air Entrained Pavement Fabricated from a Mixture with a w/c=0.49, Air Volume=1.7%, and SAM=0.55 That Has Been Exposed to 10%$CaCl_2$

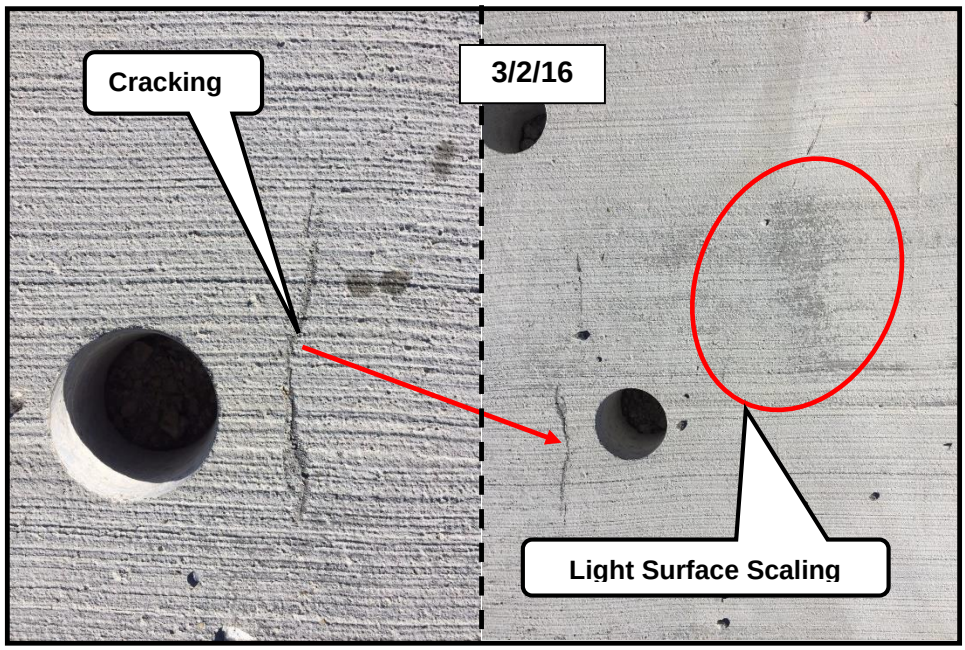

Figure 4-32: Visual Examination of an Untreated Pavement Fabricated from a Mixture with a w/c=0.56, Air Volume=6.0%, and SAM=0.20 That Has Been Exposed to 10%$CaCl_2$

Figure 4-33: Visual Examination of a Topically Treated Pavement Fabricated from a Mixture with a w/c=0.56, Air Volume=6.0%, and SAM=0.20 That Has Been Exposed to 10%$CaCl_2$

TABLE 4-13: Scaling Rating for Field Exposure to Calcium Chloride		20-Mar-15	2-Mar-16
Sample ID (w/c, A, SAM No-Salt Conc.)	SME Dosage Rate[3]	Visual Rating[1]	Visual Rating[2]
0.49,1.7%,0.55 -10%$CaCl_2$	0	1	1
0.49,1.7%,0.55 -10%$CaCl_2$	1	0	0
0.49,1.7%,0.55 -10%$CaCl_2$	2	0	0
0.56,6.0%,0.20 -10%$CaCl_2$	0	1	2
0.56,6.0%,0.20 -10%$CaCl_2$	1	0	0
0.56,6.0%,0.20 -10%$CaCl_2$	2	0	0
0.49,7.0%,0.23 -10%$CaCl_2$	0	0	0
0.49,7.0%,0.23 -10%$CaCl_2$	1	0	0
0.49,7.0%,0.23 -10%$CaCl_2$	2	0	0
0.42,6.6%,0.14 -10%$CaCl_2$	0	0	0
0.42,6.6%,0.14 -10%$CaCl_2$	1	0	0
0.42,6.6%,0.14 -10%$CaCl_2$	2	0	0

Note: Rating is based on visual examination of slab specimens examined on March 20, 2015[1], and March 2, 2016[2]. 0-No SME, 1-One Dosage of SME-2%PS, 2-2 Dosages of SME-2%PS[3].

TABLE 4-14: Scaling Rating for Field Exposure to Magnesium Chloride		20-Mar-15	2-Mar-16
Sample ID (w/c, A, SAM No-Salt Conc.)	SME Dosage Rate[3]	Visual Rating[1]	Visual Rating[2]
0.49,1.7%,0.55 -10%$MgCl_2$	2	0	0
0.49,1.7%,0.55 -10%$MgCl_2$	1	0	0
0.49,1.7%,0.55 -10%$MgCl_2$	0	1	1
0.56,6.0%,0.20 -10%$MgCl_2$	2	0	0
0.56,6.0%,0.20 -10%$MgCl_2$	1	0	0
0.56,6.0%,0.20 -10%$MgCl_2$	0	0	1
0.49,7.0%,0.23 -10%$MgCl_2$	2	0	0
0.49,7.0%,0.23 -10%$MgCl_2$	1	0	0
0.49,7.0%,0.23 -10%$MgCl_2$	0	0	0
0.42,6.6%,0.14 -10%$MgCl_2$	2	0	0
0.42,6.6%,0.14 -10%$MgCl_2$	1	0	0
0.42,6.6%,0.14 -10%$MgCl_2$	0	0	0

Note: Rating is based on visual examination of slab specimens examined on March 20, 2015[1], and March 2, 2016[2]. 0-No SME, 1-One Dosage of SME-2%PS, 2-2 Dosages of SME-2%PS[3].

TABLE 4-15: Scaling Rating for Field Exposure to Sodium Chloride		20-Mar-15	2-Mar-16
Sample ID (w/c, A, SAM No-Salt Conc.)	SME Dosage Rate[3]	Visual Rating[1]	Visual Rating[2]
0.49,1.7%,0.55 -10%$NaCl_2$	0	0	1
0.49,1.7%,0.55 -10%$NaCl_2$	1	1	1
0.49,1.7%,0.55 -10%$NaCl_2$	2	0	0
0.56,6.0%,0.20 -10%$NaCl_2$	0	0	0
0.56,6.0%,0.20 -10%$NaCl_2$	1	0	0
0.56,6.0%,0.20 -10%$NaCl_2$	2	0	0
0.49,7.0%,0.23 -10%$NaCl_2$	0	0	0
0.49,7.0%,0.23 -10%$NaCl_2$	1	0	0
0.49,7.0%,0.23 -10%$NaCl_2$	2	0	0
0.42,6.6%,0.14 -10%$NaCl_2$	0	0	0
0.42,6.6%,0.14 -10%$NaCl_2$	1	0	0
0.42,6.6%,0.14 -10%$NaCl_2$	2	0	0

Note: Rating is based on visual examination of slab specimens examined on March 20, 2015[1], and March 2, 2016[2]. 0-No SME, 1-One Dosage of SME-2%PS, 2-2 Dosages of SME-2%PS[3].

Specimens that were topically treated with either one or two applications of SME-PS exhibited no signs of surface scaling after the first or second winter season under field exposure conditions. This is expected since SME-PS blends reduce the penetration of fluids and salts which can initiate mechanisms known to cause scaling damage. However, as seen in Tables 4-14 through 4-16, the majority of the slabs at the Center for Aging Infrastructure site had no visible surface scaling damage after two winter seasons. One possible reason why no surface scaling has been seen on slabs that have no SME-PS could stem from the fact that the chloride concentration in the slabs was not great enough to cause any damage. Therefore, at this point, scaling damage is negligible for these pavements. For the majority of the untreated pavement sections exposed to 10% by mass NaCl, $CaCl_2$ and $MgCl_2$, no noticeable surface scaling damage had occurred on air or non-air entrained slabs for the first winter cycle. Normally, concrete specimens that are non-air entrained experience surface scaling and freeze thaw damage at a greater rate than concretes that are air entrained. This could explain why after 15 months of salt exposure that 60% of untreated specimens fabricated from the non-air entrained mixture with a w/c of 0.49 and air volume of 1.7% were the majority of

the specimens that were observed to have surface scaling damage, no matter the type of salt that was used. On the other hand, specimens fabricated from the mixture with a w/c of 0.56 and air volume of 6.0% accounted for the remaining 40% of samples that showed surface scaling damage after 15 months of salt exposure. This is likely in part attributed to the fact that specimens with higher w/c have inadequate strength compared to specimens with lower w/c and therefore have weaker surfaces because they are more porous. Therefore, under the influence of salt ingress and freezing and thawing cycles, the paste on top of a specimen with a higher w/c is likely to deteriorate quicker than a specimen with a lower w/c. Tables 4-14 through 4-16 illustrate that after 15 months of salt exposure specimens that were fabricated from the mixture design with a w/c of 0.56 only showed surface scaling damage on specimens that were exposed to $MgCl_2$ and $CaCl_2$. Furthermore, while it is noted that many of the specimens had no visible surface scaling damage, it appears that the $MgCl_2$ did the least amount of damage to specimens that did show signs of surface scaling damage. $CaCl_2$ caused more damage to the concrete than $MgCl_2$ as is shown in Figure 4-30. As previously mentioned, aqueous solutions containing $CaCl_2$ and $MgCl_2$ can cause the formation of calcium oxychloride and magnesium oxychloride which is known to cause damage in concrete. Furthermore, the formation of calcium oxychloride or magnesium oxychloride can likely be a contributing factor as to why signs of damage were only exhibited by specimens exposed to $CaCl_2$ and $MgCl_2$. However, it should be noted that no noticeable change in deterioration was observed in specimens during periods of higher temperatures, where calcium chloride salt concentrations at or above 12% are known to form calcium oxychloride [5, 41, 42].

4.7. Summary and Conclusions

Fluid transport tests were used to investigate how SME-PS changes fluid absorption and chloride ingress into concrete. The experimental results highlighted in this study and previous studies [3, 4] show that soy methyl ester (SME), a

derivative of soy bean oil, along with the incorporation of polystyrene (PS) is very successful at reducing fluid absorption and chloride penetration into different concrete mixtures. The following observations can be made regarding the influence of material composition and sample conditioning on fluid absorption and chloride diffusion into concrete topically treated with SME-PS.

- First, samples that were conditioned in 50% and 75% relative humidity chambers and then treated with SME-PS, reduced water absorption with an average expected reduction of between 65-80%, irrespective of the amount of air entrainment or water to cement binder ratio.
- Second, for the fluid absorption tests, the experimental results show that the reduction in water absorption is not significantly influenced by increasing w/c. Increasing the w/c from 0.42 to 0.56 reduced water absorption by only an additional 1-5%.
- Third, for the chloride diffusion tests, the specimens with lower w/c that were topically treated with SME-PS showed lower chloride concentrations overtime compared to specimens with higher w/c.
- Fourth, SME-PS decreased Cs by 45-70%, after 9 months of salt exposure, regardless of the type of salt used. Furthermore, no correlation was observed between $CaCl_2$, $MgCl_2$ or NaCl and how much SME-PS decreased Cs.
- Fifth, the application rate of the SME-PS did not appear to significantly influence the performance of the applied SME-PS at further reducing Cs. The 2nd dosage of SME-PS reduced Cs by only an additional 1-6%.
- Sixth, for the SME-PS depth of penetration test, the experiment results show that the penetration depth of SME-PS is dependent on the porosity of the structure. The results indicate the penetration depth of SME-PS into concrete increases with increasing porosity (i.e., capillary porosity). However, samples that were topically treated with a 2nd application of SME-PS resulted in only a small increase in the penetration depth of

SME-PS. It should be noted that maximum depth of SME-PS penetration into concrete, for any sample was observed to be 6mm.

- Irrespective of the mixture design, an analysis of the effect of SME-PS on the rate of chloride diffusion into concrete using Fick's 2nd Law shows that the apparent diffusion coefficient (Dapp) does not change widely in the presence of SME-PS. This indicates the diffusivity properties of the concrete is not drastically effected by the presence of SME-PS.
- Finally, the results in this study show that the diffusion of chloride ions into concrete treated with SME-PS can be modeled by a fraction of the surface chloride concentration (Cs) in Fick 2nd Law of diffusion with all other variables, including the apparent diffusion coefficient (Dapp) remaining the same as untreated concrete

CHAPTER 5. CONCLUSIONS AND RECOMMENDATIONS

This chapter provides a summary of the thesis. Recommendations for future research on the topic of SME-PS blends are also provided.

5.1. Summary of Work

While, concrete sealants and topical surface treatments can be used to extend to durability of concrete structures, it is difficult to predict the durability of concrete structures sealed with a sealant or topical surface treatment. This is due to a lack of necessary model inputs that can be used to address the durability of concrete structures treated with these materials. This thesis specifically looked at the use of SME-PS blends, to enhance concrete durability and investigated an approach to modeling concrete durability in the presence of SME-PS. The first part of this study discussed in Chapter 3, characterized the constituent materials used in this investigation by using fluid absorption and chloride diffusion models to determine the performance of different concrete materials. It was shown that transport can be heavily influenced by the volume of pores, connectivity of pores and sample conditioning. The second part of this study, outlined in Chapter 4 of this thesis, used fluid transport tests to investigate how SME-PS changes fluid absorption and chloride ingress in cementitious systems and investigated how to predict the service life of concrete materials that have been treated with SME-PS. In general, the use of SME-PS as a topical concrete treatment was successful. In all cases, samples that were topically treated with SME-PS had less chloride ingress than samples that were not treated with SME-PS. Furthermore, a sound theoretical framework was proposed for modeling the durability of concrete materials topically treated with SME-PS. The results show that the diffusion of chloride ions into

concrete treated with SME-PS can be modeled by using a fractional amount (in this case 60% is recommended) of the value of Cs that is used for conventional concrete when Fick 2nd Law is used. This is critically important from a design and cost prospective, since tests do not need to be conducted with SME-PS to determine the benefits of surface treatment.

5.2. Recommendation for Future Research

As for the future work, there is a need for more field work to study the long-term performance of SME-PS blends to determine when re-application is needed. Secondly, chloride binding isotherms using SME-PS blends should be studied to further assess how SME-PS blends change chloride binding and damage in concrete structures. Lastly, chloride profiles should be developed from SME-PS treated samples extracted from the field during later periods and refit using a fraction of Cs (i.e., between 45-70%) in Fick's 2nd Law from similar plain samples to study how modeling chloride diffusion into concrete with SME-PS changes over longer durations.

REFERENCES

REFERENCES

[1] T.C. Powers, T.L. Brownyard, Studies of the physical properties of hardened Portland cement paste, Bull. 22, Res. Lab. of Portland Cement Association, Skokie, IL, U.S., 1948.

[2] Wiese, A. “Assessing The Performance of Sustainable and Luminescent Concrete Sealers”. Master’s thesis, Purdue University, West Lafayette,2015.

[3] Coates, K.C. “Evaluation of Soy Methyl Ester Polystyrene Blends for Use in Concrete Master’s thesis, Purdue University, West Lafayette, 2008.

[4] Golias, M. “The Use of Soy Methyl Ester-Polystyrene Sealants and Internal Curing to Enhance Concrete Durability”. Master’s thesis, Purdue University, West Lafayette, Indiana, 2010.

[5] Y. Farnam, S. Dick, A. Wiese, J. Davis, D. Bentz, and J. Weiss. “The Influence of Calcium Chloride Deicing Salt on Phase Changes and Damage Development in Cementitious Materials”. Journal of Cement and Concrete Composite, Elsevier, Vol. 64, pp. 1-15, 2015.

[6] Yaghoob, F., Washington, T., and Weiss, J. “The Influence of Calcium Chloride Salt Solution on the Transport Properties of Cementitious Materials,” Advances in Civil Engineering, vol. 2015, Article ID 929864, 13 pages, 2015.

[7] Jones, W. “Examining The Freezing and Thawing Behavior of Concretes with Improved Performance Through Internal Curing and Other Methods”. Master’s thesis, Purdue University, West Lafayette, 2015.

[8] Nielsen, J, "Investigation of Concrete Sealer Products to Extend Concrete Pavement Life". *Boise State University, 2011.*

[9] Wiese, A. “Assessing The Performance of Sustainable and Luminescent Concrete Sealers”. Master’s thesis, Purdue University, West Lafayette, 2015.

[10] U.S. Department of Agriculture. SoyStats. American Soybean Association, (2013 ed.).

[11] Coates, K.C., Mohtar, S., Tao, B, Weiss, J., “Can Soy Methyl Esters Reduce Fluid Transport and Improve Durability of Concrete?”. Transportation Research Record: J. of the Transportation Research Board, No 2113, pp. 22-30, 2009.

[12] Liston, L.C. “Using mixtures of fatty acid methyl esters as phase change materials for concrete”. Master’s thesis, Purdue University, West Lafayette, 2014.

[13] Todak, H. “Durability Assessments of Concrete Using Electrical Properties and Acoustic Emission Testing”. Master’s thesis, Purdue University, West Lafayette, 2015.

[14] T.C. Powers, T.L. Brownyard, Studies of the physical properties of hardened Portland cement paste, Bull. 22, Res. Lab. of Portland Cement Association, Skokie, IL, U.S., 1948.

[15] Ahmad. S., Azad, K., and Loughlin, K.F. “A Study of Permeability and Tortuosity of Concrete”. Singapore Concrete Institute, 2005.

[16] Peters, E. “Advanced Petrophysics: Volume 1: Geology, Porosity, Absolute Permeability, Heterogeneity, and Geostatistics”. Pp. 105-106, 2012.

[17] Spragg, R. “The Rapid Assessment of Transport Properties of Cementitious Materials Using Electrical Methods”. Master’s thesis, Purdue University, West Lafayette, 2013.

[18] Snyder, K.A. The relationship between the formation factor and the diffusion coefficient of porous materials saturated with concentrated electrolytes: theoretical and experimental considerations. Concrete Science and Engineering, Vol 3, No.12, pp. 216-224, 2001.

[19] Castro, J., D. Bentz, and J. Weiss. “Effect of sample conditioning on the water absorption of concrete”. Cement and Concrete Composites, Vol. 33, No. 8, Sep. 2011, pp. 805–813.

[20] D. Welchel. “Determining the air void distribution of fresh concrete with the sequential pressure method”. Oklahoma State University, 2014.

[21] T.C. Powers, T.L. Brownyard “The air requirement of frost resistant concrete.” Proceedings of the Highway Research Board No. 29, 184-211, 1949.

[22] Backstrom, J., Burrows, R., Mielenz, R., and Wolkodoff, V. Origin, Evolution, and Effects of the Air Void System in Concrete. Journal of the American Concrete Institute,55, 261-272, 1958.

[23] Lamond, J., and Peilert, J. “Significance of Tests and Properties of Concrete and Concrete-Making Materials”. Issue 169, Part 4, pp. 300-301, 2006.

[24] Rajabipour, F., and Weiss, J. “Electrical conductivity of drying cement paste.” Mater. Struct., 40(10), 1143–1160, 2007.

[25] Weiss, J., Snyder, K., Bullard, J., and Bentz, D. "Using a Saturation Function to Interpret the Electrical Properties of Partially Saturated Concrete." J. Mater. Civ. Eng., 10.1061/(ASCE), 2013.

[26] National Institute of Standards and Technology (NIST). Estimation of Pore Solution Conductivity. Retrieved from http://ciks.cbt.nist.gov/poresolncalc.htm

[27] Lucero, C.L. “Quantifying moisture transport in cementitious materials using neutron radiography”. Master’s thesis, Purdue University, West Lafayette, 2015.

[28] Todak, H. “Durability Assessments of Concrete Using Electrical Properties and Acoustic Emission Testing”. Master’s thesis, Purdue University, West Lafayette, 2015.

[29] Spragg, R., Y. Bu, K. Snyder, D. Bentz, and J. Weiss. “Electrical Testing of Cement-Based Materials: Role of Testing Techniques, Sample Conditioning, and Accelerated Curing”. Publication FHWA/IN/JTRP-2013/28. Joint Transportation Research Program, Indiana Department of Transportation and Purdue University, West Lafayette, Indiana, 2013.

[30] Spragg, R., Castro, J., Nantung, T., Paredes, M., and Weiss, J., "Variability Analysis of the Bulk Resistivity Measured Using Concrete Cylinders". Advances in Civil Engineering Materials, Vol. 1, No. 1, pp. 1-17, 2012.

[31] Spragg, R. “The Rapid Assessment of Transport Properties of Cementitious Materials Using Electrical Methods”. Master’s thesis, Purdue University, West Lafayette, 2013.

[32] W. J. Weiss, T. J. Barrett, C. Qiao, and H. Todak, “Toward a specification for transport properties of concrete based on the formation factor of a sealed specimen,” in Transportation Research Board 95th Annual Meeting, 2016

[33] Parrott, L. Moisture conditioning and transport properties of concrete test specimens. Materials and Structures, 27, 460-468, 1994.

[34] Castro, J., Keiser, L., Golias, M., and Weiss, J. “Absorption and desorption properties of fine lightweight aggregate for application to internally cured concrete mixtures”. Cement and Concrete composites, Volume 33, Issue 10, Pages 1001–1008, 2011.

[35] Bioubakhsh, S. “The penetration of chloride in concrete subject to wetting and drying: measurement and modelling”. Doctoral thesis, UCL (University College London), 2011.

[36] Liu J, Tang K, Pan D, Lei Z, Wang W, Xing F. “Surface Chloride Concentration of Concrete under Shallow Immersion Conditions”. Materials, 2013.

[37] Liu J, Tang K, Pan D, Lei Z, Wang W, Xing F. “Surface Chloride Concentration of Concrete under Shallow Immersion Conditions”. Materials, 2014.

[38] Andrade, C., Mancini, G. “Modelling of Corroding Concrete Structures”. Proceeding of the joint fib-RILEM Workshop held in Madrid, Spain, 2010.

[39] Concrete Terminology, American Concrete Institute CT-13, An ACI Standard, 2013.

[40] Krauss, P. D., Lawler, J., Steiner, K. Proposed Testing Protocols for Surface Applied Concrete Sealers. In NCHRP Project 20-07 Task 235 TRB, Northbrook, Illinois: Wiss, Janney, Elstner Associates, Inc., 2009.

[41] Y. Farnam, S. Dick, A. Wiese, J. Davis, D. Bentz, and J. Weiss. The influence of calcium chloride deicing salt on phase changes and damage development in cementitious materials, Cement and Concrete Composites, Vol. 64, pp. 1-15, 2015.

[42] Y. Farnam, A. Wiese, D. Bentz, J. Davis, and J. Weiss, Damage Development in Cementitious Materials Exposed to Magnesium Chloride Deicing Salt, Journal of Construction and Building Materials, Elsevier, Vol. 93, pp. 384-392, 2015.

[43] Morrow, N.R. and Melrose, J.C. Application of Capillary Pressure Measurements to the Determination of Connate Water Saturation. In Interfacial Phenomena in Petroleum Recovery, 257-287, ed. N.R. Morrow. New York City: Marcel Dekker Inc., 1991.

[44] Hewlett, P. “Lea's Chemistry of Cement and Concrete (Fourth Edition)”. Pp. 547-568, 2004.

[45] Powers, T.C. Copeland, L., Haynes, J.C., and Mann, H.M. “Permeability of Portland Cement Paste”. Proceeding of the Journal of the American Concrete Institute. 3, 285-298, 1954.

[46] David, S. “The Development of a Rapid Test for Determining the Transport Properties of Concrete”. University of New Brunswick, 2007.

[47] Y. Farnam, D. Bentz, A. Sakulich, D. Flynn, and J. Weiss. Measuring Freeze and Thaw Damage in Mortars Containing Deicing Salt Using a Low-Temperature Longitudinal Guarded Comparative Calorimeter and Acoustic Emission, Advances in Civil Engineering Materials (ASTM), Vol. 3, No. 1, 2014, pp. 1–22.

[48] Karam, A. “Chloride Ingress into Submerged Concrete under a Sustained Load”. Master’s thesis, University of Ottawa, 2014.

[49] Shill, S.T. “Chloride penetration into concrete structures exposed to the marine atmosphere”. Master’s thesis, Florida Atlantic University, 2014.

[50] Sumsion, E.S, Spencer, G. “Physical and Chemical Effects of Deicers On Concrete Pavement: Literature Review”. Utah Department of Transportation Research Division, 2013.

[51] Nokken, M.R, and Hooton, D.R. “Electrical Conductivity Testing”. American Concrete International, ACI Committee 236, 2006

APPENDICES

Appendix A- Laboratory Concrete

Table A.1 Concrete Proportions and Volumetric Interpretations

Name	w/c – 0.49	w/c - 0.42	w/c - 0.49	w/c - 0.56
Air, %	1.7%	6.6%	7.0%	6.0%
DOS	87%	63%	67%	70%
DOH	70%	70%	70%	70%
w/c	0.49	0.42	0.49	0.56
Yield	26.84	27.00	26.99	27.03
Cement	573.00	564.00	564.00	550.40
Fine Aggregate Absorption	1.20%	1.20%	1.20%	1.20%
Coarse Aggregate 1 Absorption	1.20%	1.20%	1.20%	1.20%
Coarse Aggregate 2 Absorption	1.20%	1.20%	1.20%	1.20%
Initial Porosity (%)	0.607	0.57	0.606	0.638

Table A.2 Concrete Proportions and Volumetric Interpretations (SSD)

Materials	SG (SSD)	SG (SSD)	SG (SSD)	SG (SSD)
Cement	3.15	3.15	3.15	3.15
Sand	2.65	2.65	2.65	2.65
Coarse Aggregate 1	2.71	2.71	2.71	2.71
Coarse Aggregate 2	2.763	2.763	2.763	2.763
Water	1	1	1	1

Table A.3 Concrete Proportions and Volumetric Interpretations (ft^3)

Materials	Volume, ft3	Volume, ft3	Volume, ft3	Volume, ft3
Cement	2.9	2.9	2.9	2.8
Sand	8.1	7.9	7.7	7.5
Coarse Aggregate 1	10.8	10.6	10.3	10.1
Coarse Aggregate 2	0	0	0	0
Water	4.5	3.8	4.4	4.9
Air	0.5	1.8	1.8	1.8
Σ	26.8	27.0	27.0	27.0

Table A.4 Compressive Strength: Mixture 1, w/c = 0.42, Air =6.6%

Compression test (0.42 AE) -Mixture # 1									
Samples #	Peak load (lb*f)	Peak load (N)	Date of Cast	Type of cracking (ASTM 39)	Diameter of Specimen (mm)	Diameter of Specimen (mm)	Area (mm^2)	f'c (N/mm^2) or MPA	f'c (Mpa)
1	53715	239032	9/16/2014	2	101.6	203.2	8103	29.5	30.5
2	55155	245440	9/16/2014	2	101.6	203.2	8103	30.3	
3	57925	257766	9/16/2014	2	101.6	203.2	8103	31.8	

Table A.5 Compressive Strength: Mixture 2, w/c = 0.49, Air =7.0%

Compression test (0.49 AE) -Mix # 2									
Samples #	Peak load (lb*f)	Peak load (N)	Date of Cast	Type of cracking (ASTM 39)	Diameter of Specimen (mm)	Diameter of Specimen (mm)	Area (mm^2)	f'c (N/mm^2) or MPA	f'c (Mpa)
1	55210	245685	9/24/2014	2	101.6	203.2	8103	30.3	30.4
2	56720	252404	9/24/2014	2	101.6	203.2	8103	31.1	
3	54380	241991	9/24/2014	2	101.6	203.2	8103	29.9	

Table A.6 Compressive Strength: Mixture 3, w/c = 0.56, Air =6.0%

Compression test (0.56 AE) -Mix # 3									
Samples #	Peak load (lb*f)	Peak load (N)	Date of Cast	Type of cracking (ASTM 39)	Diameter of Specimen (mm)	Diameter of Specimen (mm)	Area (mm^2)	f'c (N/mm^2) or MPA	f'c (Mpa)
1	47065	209439	10/6/2014	2	101.6	203.2	8103	25.8	24.9
2	43135	191951	10/6/2014	2	101.6	203.2	8103	23.7	
3	45625	203031	10/6/2014	2	101.6	203.2	8103	25.1	

Table A.7 Compressive Strength: Mixture 4, w/c = 0.49, Air =1.7%

Compression test (0.49 Non AE) -Mix # 4									
Samples #	Peak load (lb*f)	Peak load (N)	Date of Cast	Type of cracking (ASTM 39)	Diameter of Specimen (mm)	Diameter of Specimen (mm)	Area (mm^2)	f'c (N/mm^2) or MPA	f'c (Mpa)
1	76270	339402	10/22/2014	2	101.6	203.2	8103	41.9	41.8
2	74510	331570	10/22/2014	3	101.6	203.2	8103	40.9	
3	77650	345543	10/22/2014	3	101.6	203.2	8103	42.6	

Appendix B-Chloride Concentration Profiles

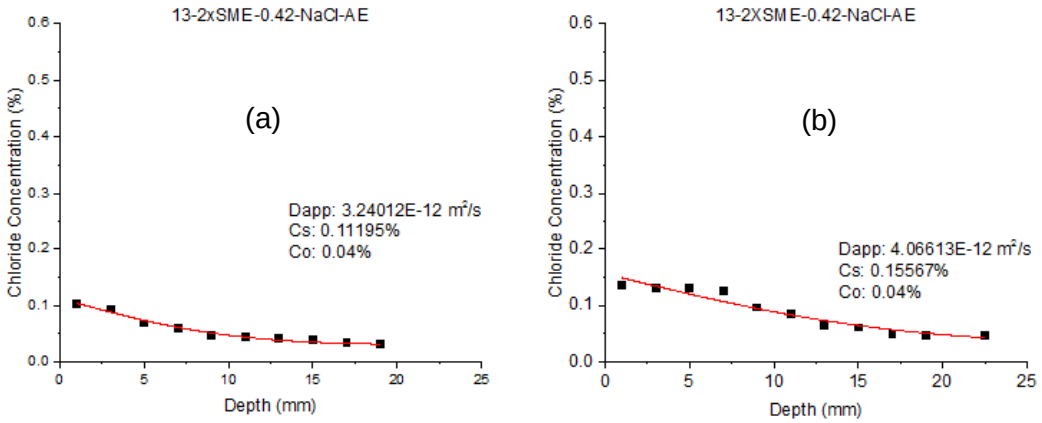

Figure A.1: 2XSME-PS, w/c =0.42, Air = 6.6%. (a) 4, (b) 9 months of exposure to NaCl

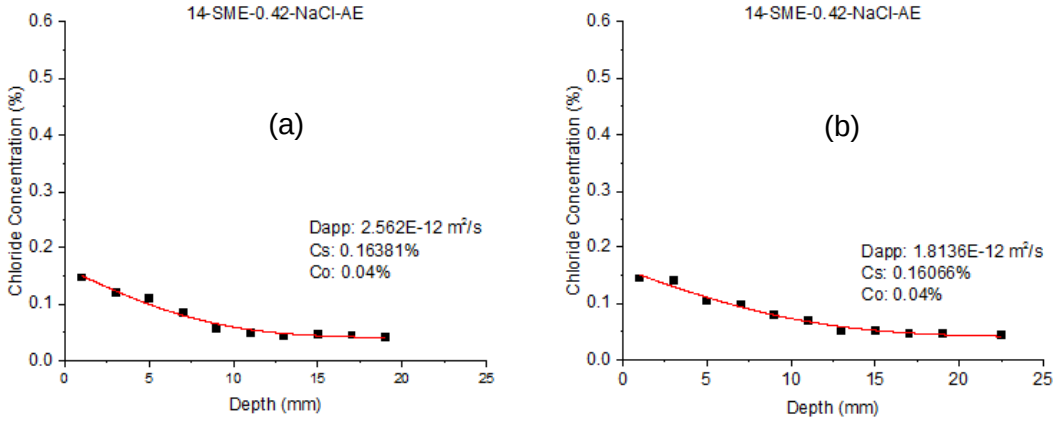

Figure A.2: SME-PS, w/c =0.42, Air = 6.6%. (a) 4, (b) 9 months of exposure to NaCl

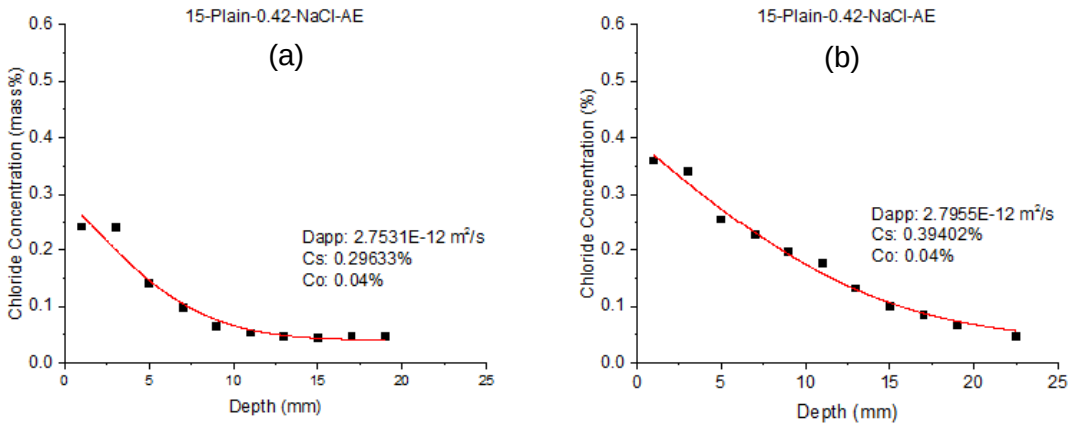

Figure A.3: No SME-PS, w/c =0.42, Air = 6.6%. (a) 4, (b) 9 months of exposure to NaCl

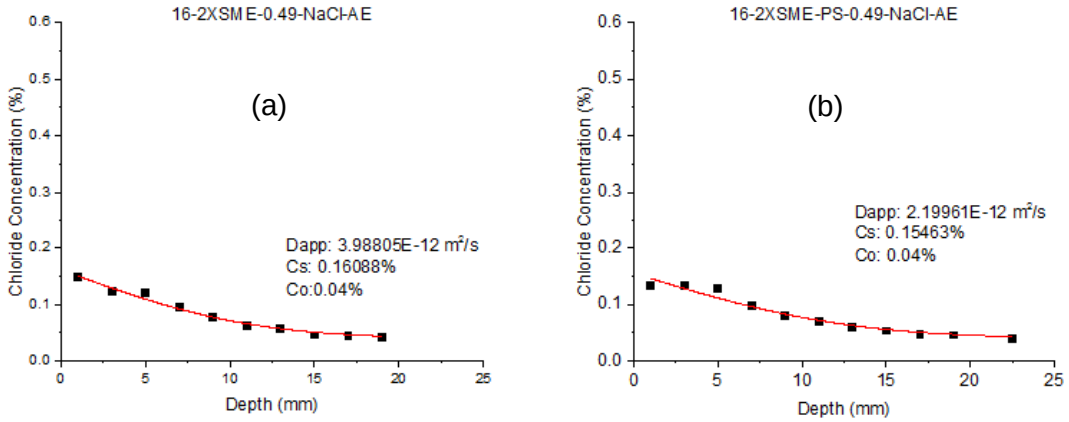

Figure A.4: 2XSME-PS, w/c =0.49, Air = 7.0%. (a) 4, (b) 9 months of exposure to NaCl

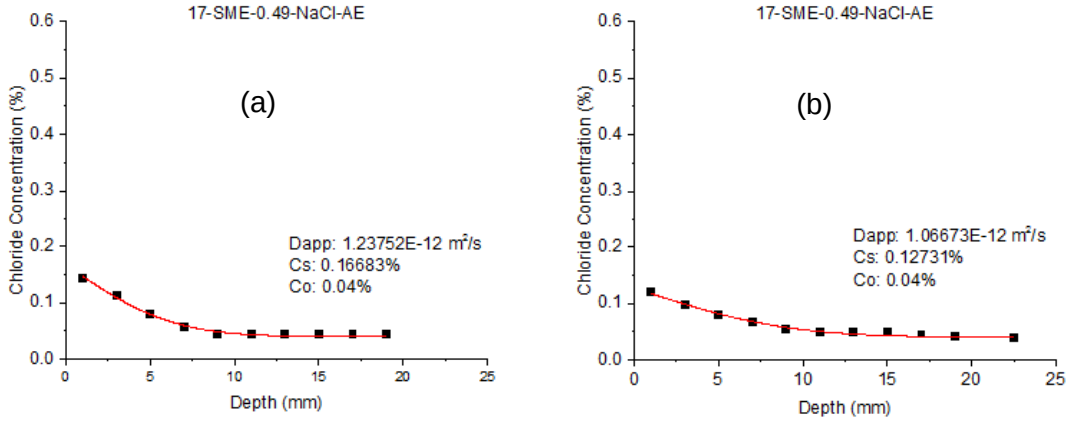

Figure A.5: SME-PS, w/c =0.49, Air = 7.0%. (a) 4, (b) 9 months of exposure to NaCl

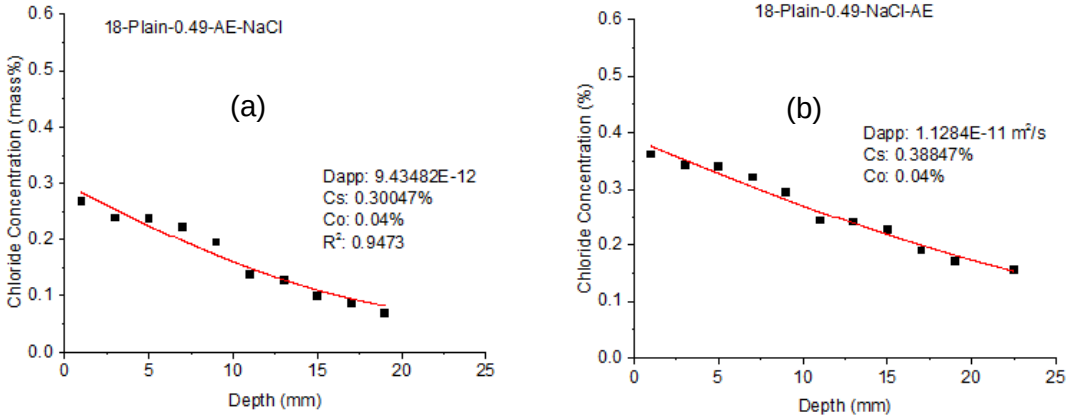

Figure A.6: No SME-PS, w/c =0.49, Air = 7.0%. (a) 4, (b) 9 months of exposure to NaCl

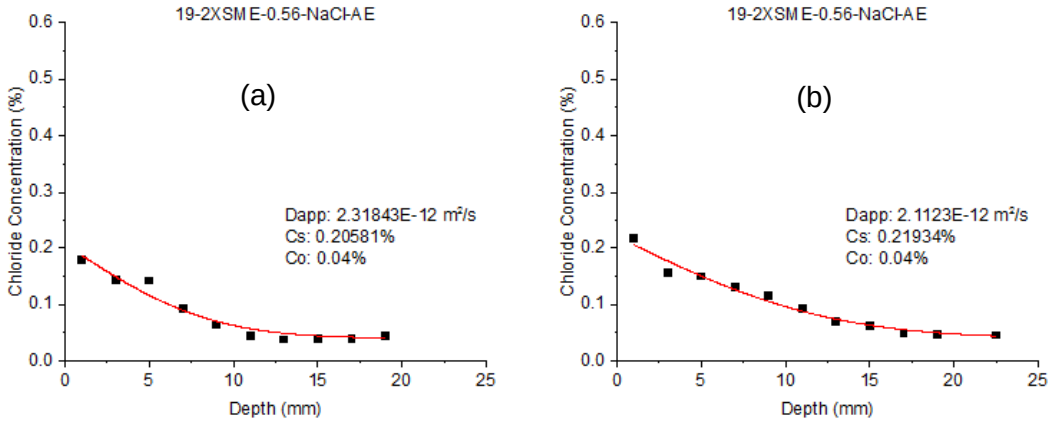

Figure A.7: 2XSME-PS, w/c =0.56, Air = 6.0%. (a) 4, (b) 9 months of exposure to NaCl

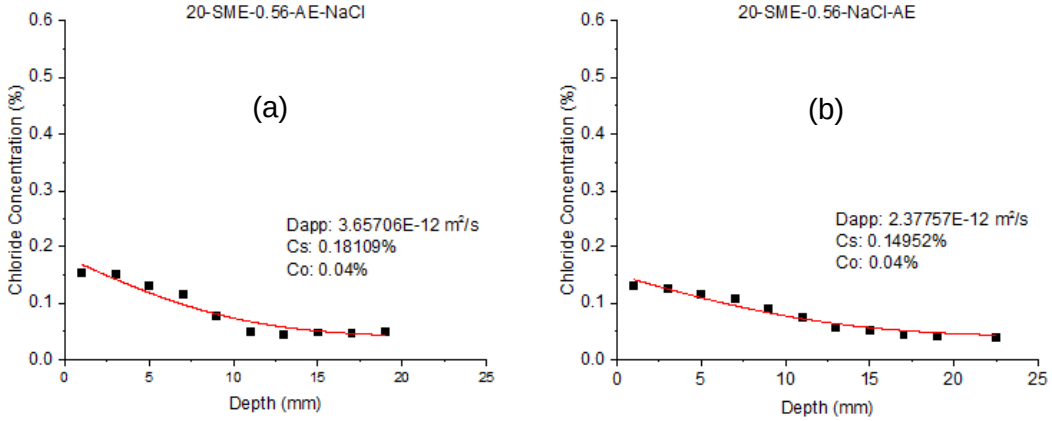

Figure A.8: SME-PS, w/c =0.56, Air = 6.0%. (a) 4, (b) 9 months of exposure to NaCl

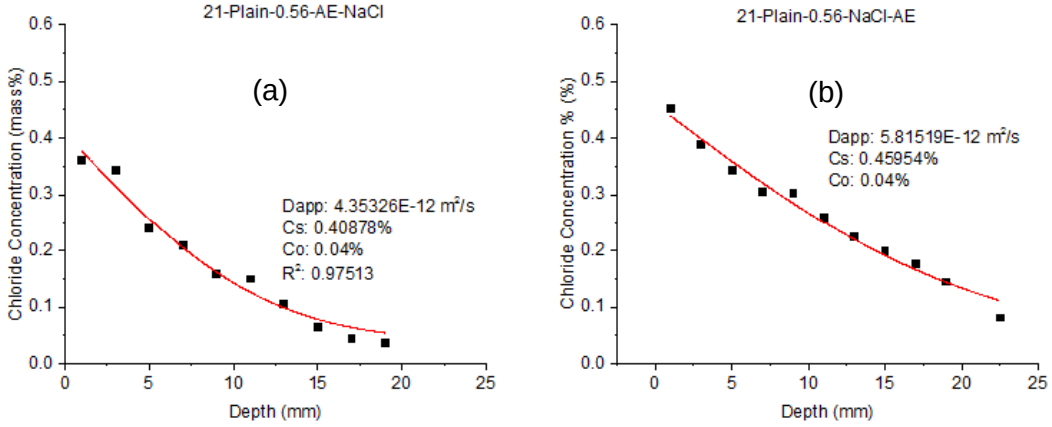

Figure A.9: No SME-PS, w/c =0.56, Air = 6.0%. (a) 4, (b) 9 months of exposure to NaCl

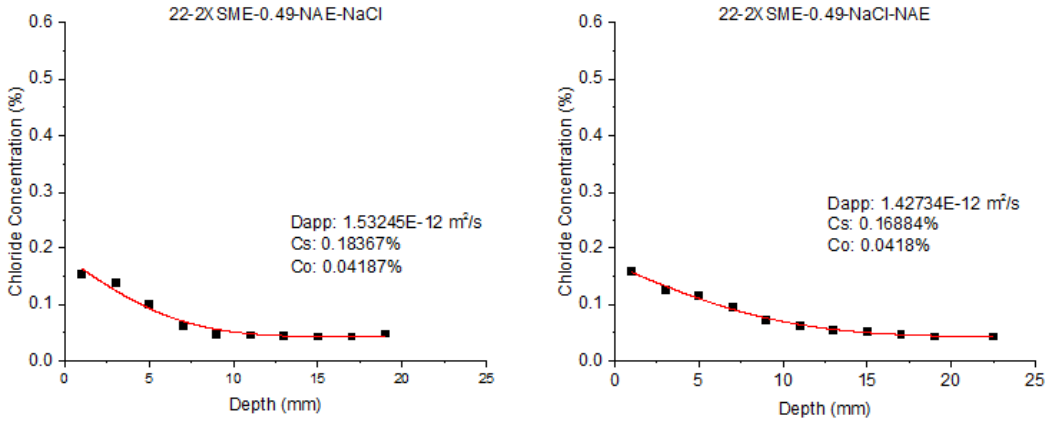

Figure A.10: 2XSME-PS, w/c =0.49, Air = 1.7%. (a) 4, (b) 9 months of exposure to NaCl

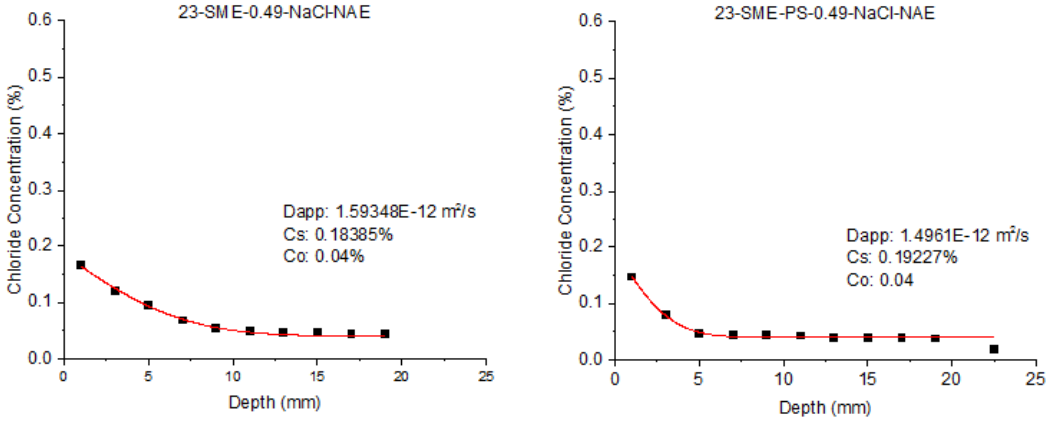

Figure A.11: SME-PS, w/c =0.49, Air = 1.7%. (a) 4, (b) 9 months of exposure to NaCl

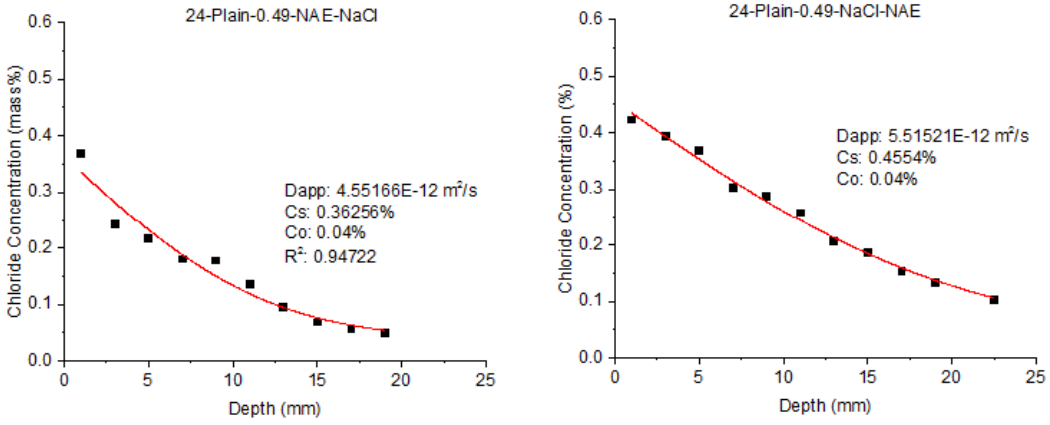

Figure A.12: No SME-PS, w/c =0.49, Air = 1.7%. (a) 4, (b) 9 months of exposure to NaCl

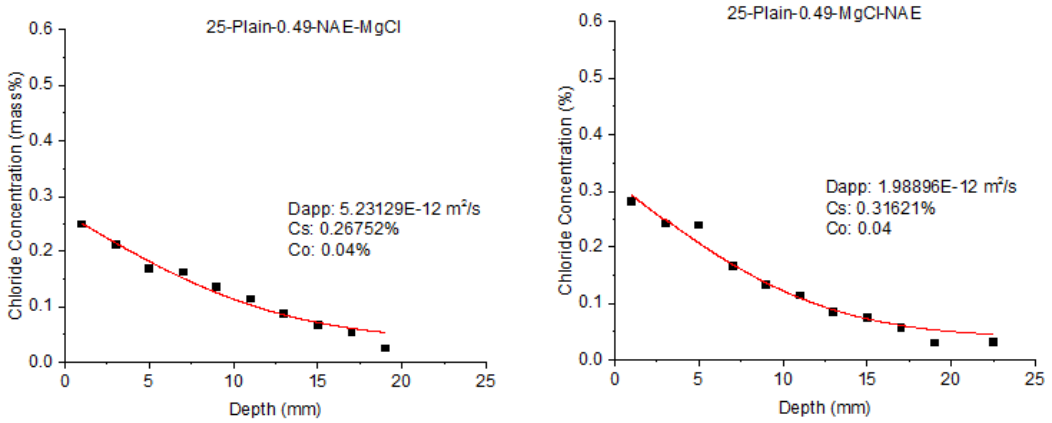

Figure A.13: No SME-PS, w/c =0.49, Air = 1.7%. (a) 4, (b) 9 months of exposure to $MgCl_2$

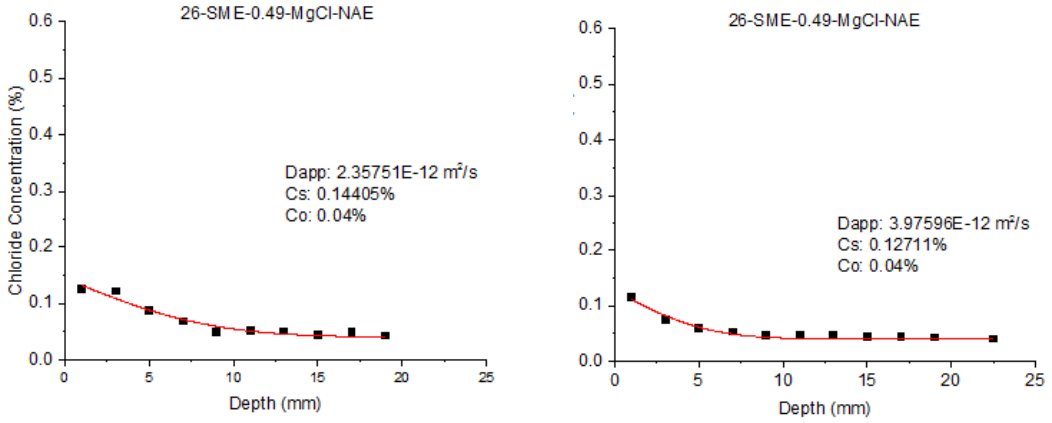

Figure A.14: SME-PS, w/c =0.49, Air = 1.7%. (a) 4, (b) 9 months of exposure to $MgCl_2$

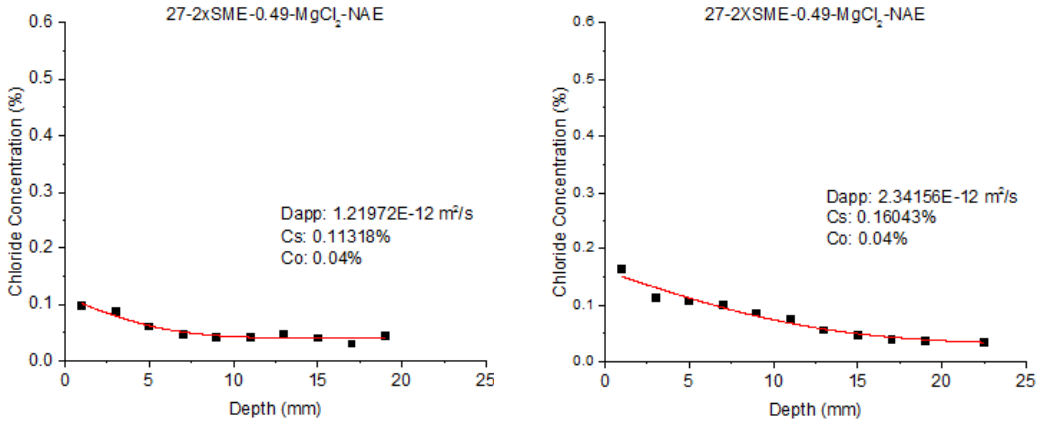

Figure A.15: 2XSME-PS, w/c =0.49, Air = 1.7%. (a) 4, (b) 9 months of exposure to $MgCl_2$

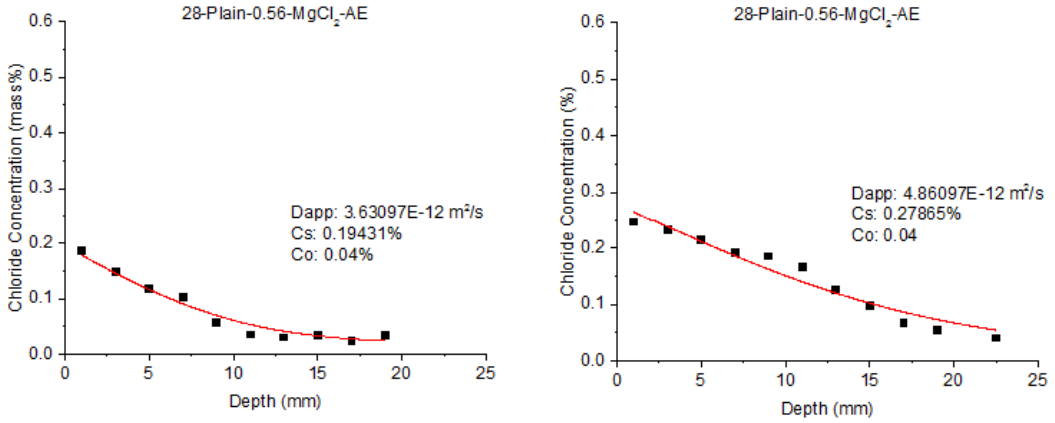

Figure A.16: No SME-PS, w/c =0.56, Air = 6.0%. (a) 4, (b) 9 months of exposure to $MgCl_2$

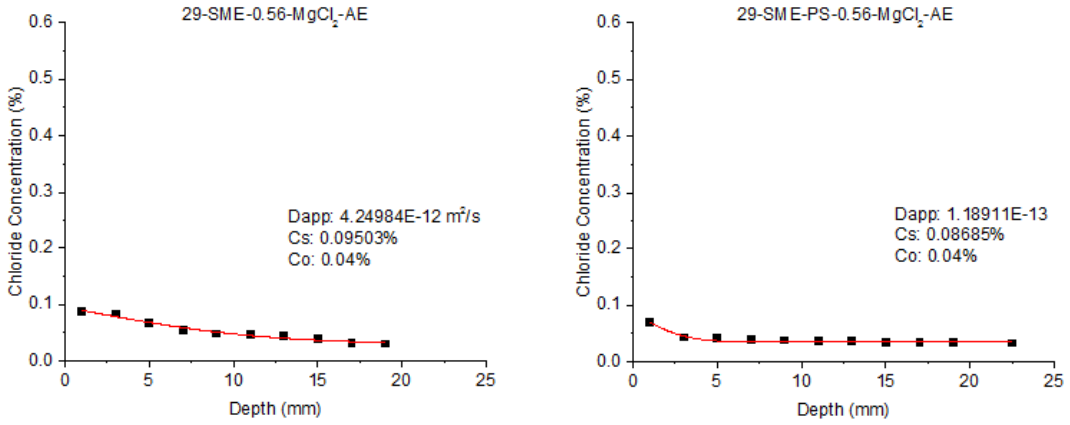

Figure A.17: SME-PS, w/c =0.56, Air = 6.0%. (a) 4, (b) 9 months of exposure to $MgCl_2$

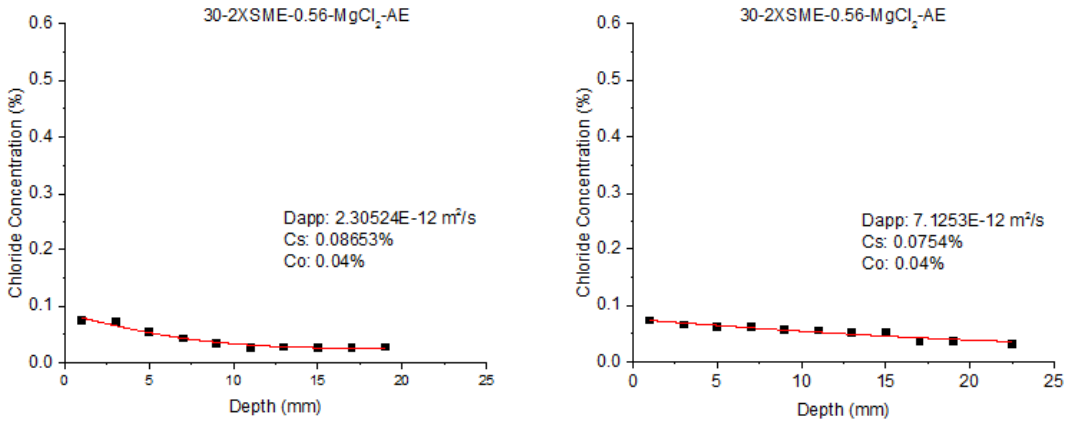

Figure A.18: 2XSME-PS, w/c =0.56, Air = 6.0%. (a) 4, (b) 9 months of exposure to $MgCl_2$

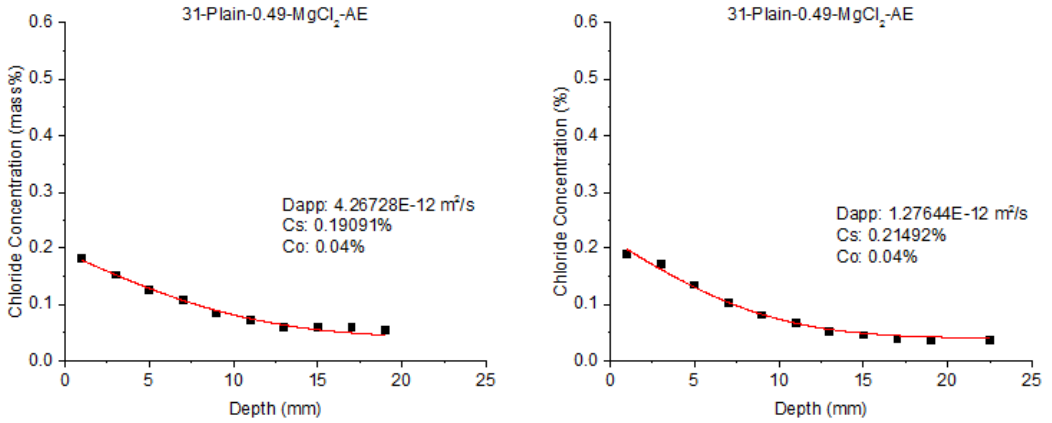

Figure A.19: No SME-PS, w/c =0.49, Air = 7.0%. (a) 4, (b) 9 months of exposure to $MgCl_2$

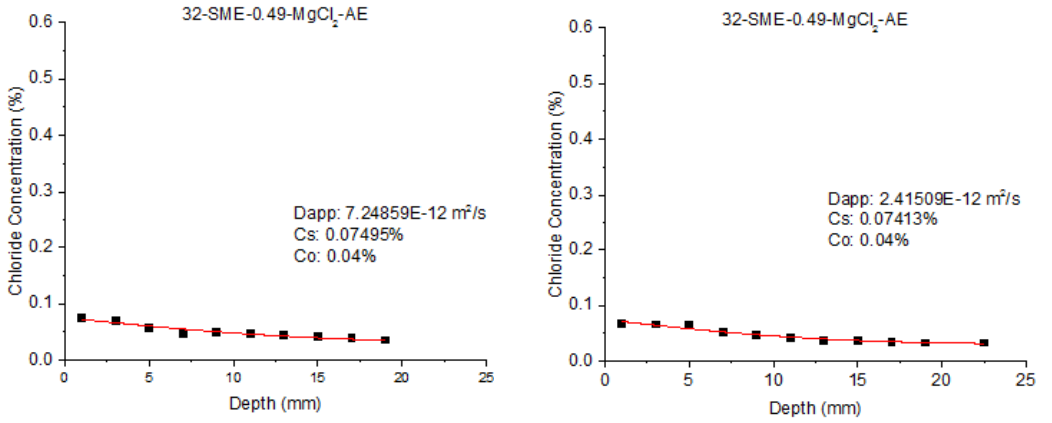

Figure A.20: SME-PS, w/c =0.49, Air = 7.0%. (a) 4, (b) 9 months of exposure to $MgCl_2$

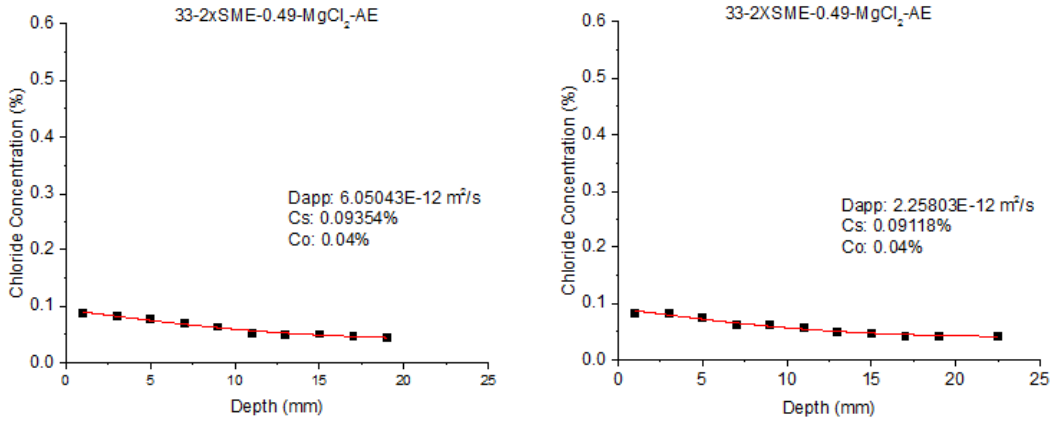

Figure A.21: 2XSME-PS, w/c =0.49, Air = 7.0%. (a) 4, (b) 9 months of exposure to $MgCl_2$

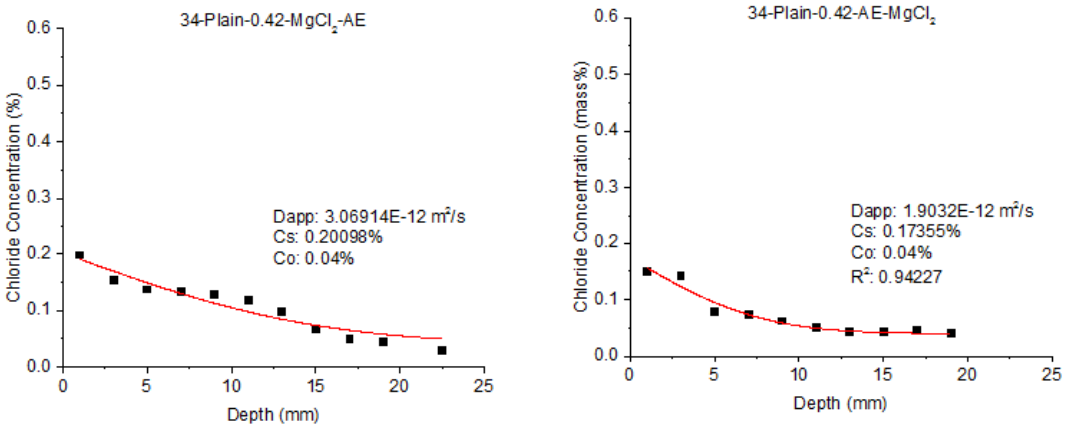

Figure A.22: No SME-PS, w/c =0.42, Air = 6.6%. (a) 4, (b) 9 months of exposure to $MgCl_2$

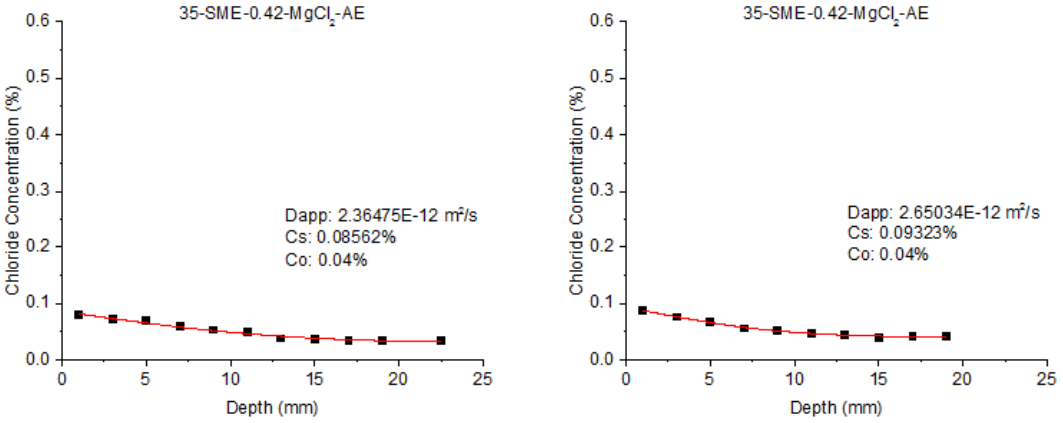

Figure A.23: SME-PS, w/c =0.42, Air = 6.6%. (a) 4, (b) 9 months of exposure to $MgCl_2$

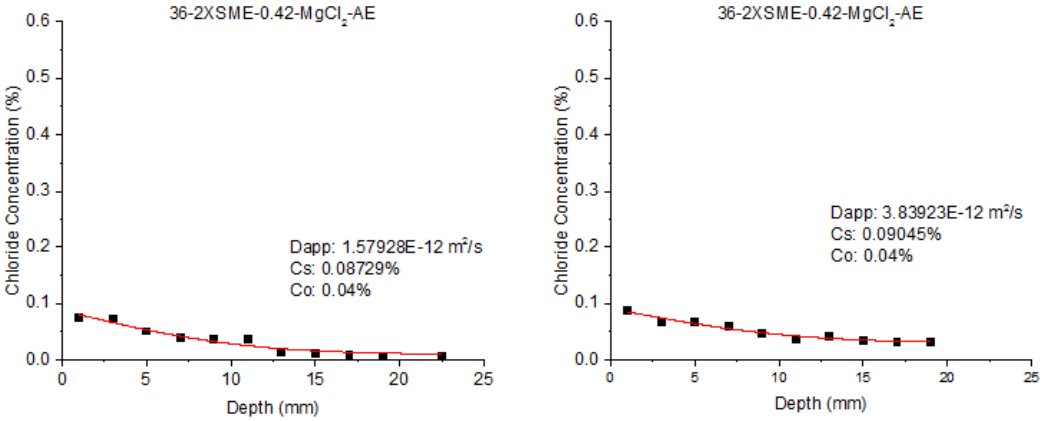

Figure A.24: 2XSME-PS, w/c =0.42, Air = 6.6%. (a) 4, (b) 9 months of exposure to $MgCl_2$

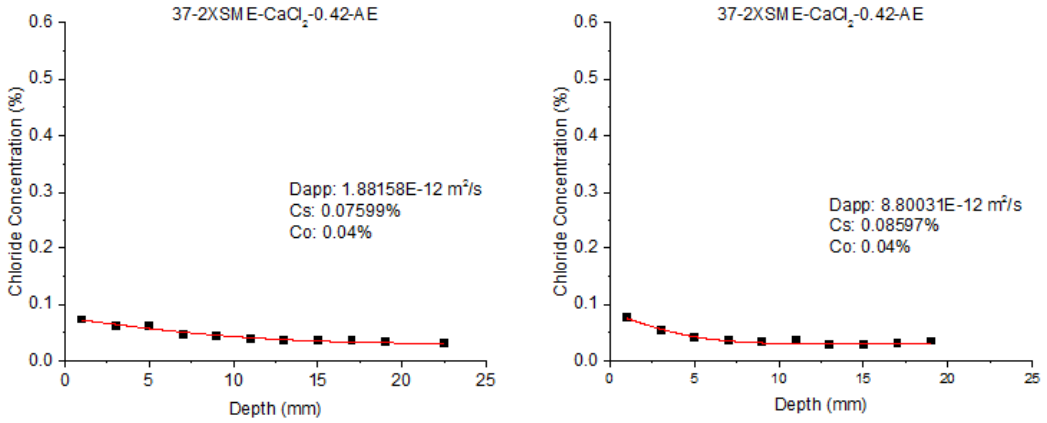

Figure A.25: 2XSME-PS, w/c =0.42, Air = 6.6%. (a) 4, (b) 9 months of exposure to $CaCl_2$

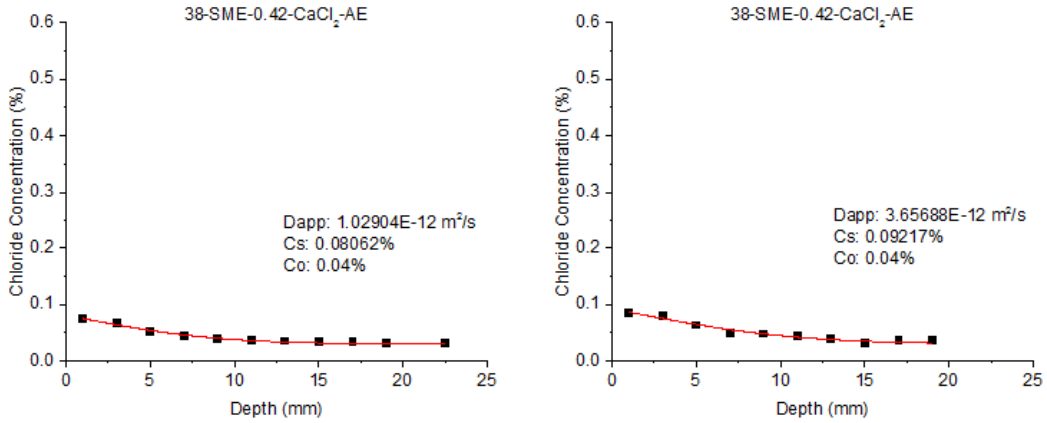

Figure A.26: SME-PS, w/c =0.42, Air = 6.6%. (a) 4, (b) 9 months of exposure to $CaCl_2$

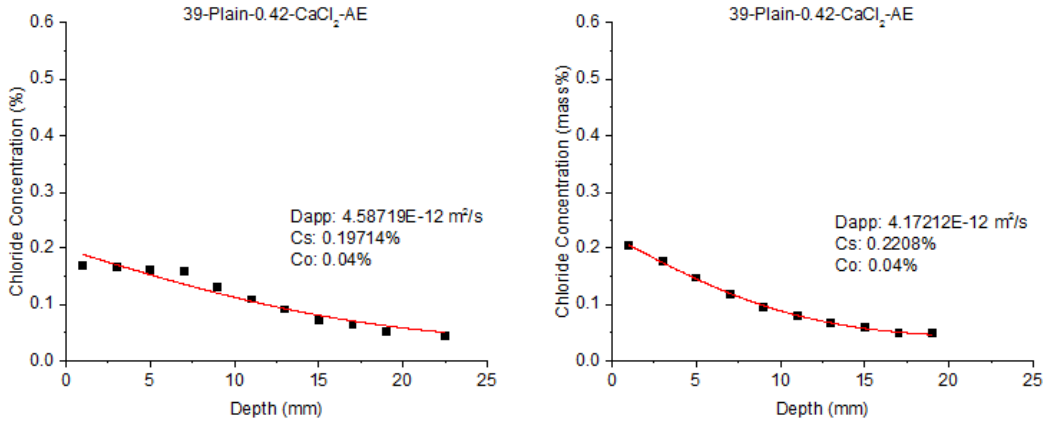

Figure A.27: No SME-PS, w/c =0.42, Air = 6.6%. (a) 4, (b) 9 months of exposure to $CaCl_2$

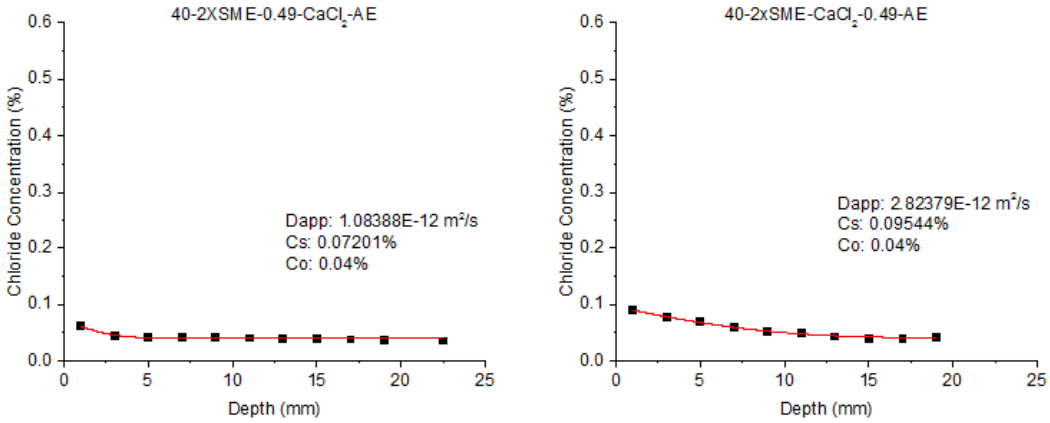

Figure A.28: 2XSME-PS, w/c =0.49, Air = 7.0%. (a) 4, (b) 9 months of exposure to $CaCl_2$

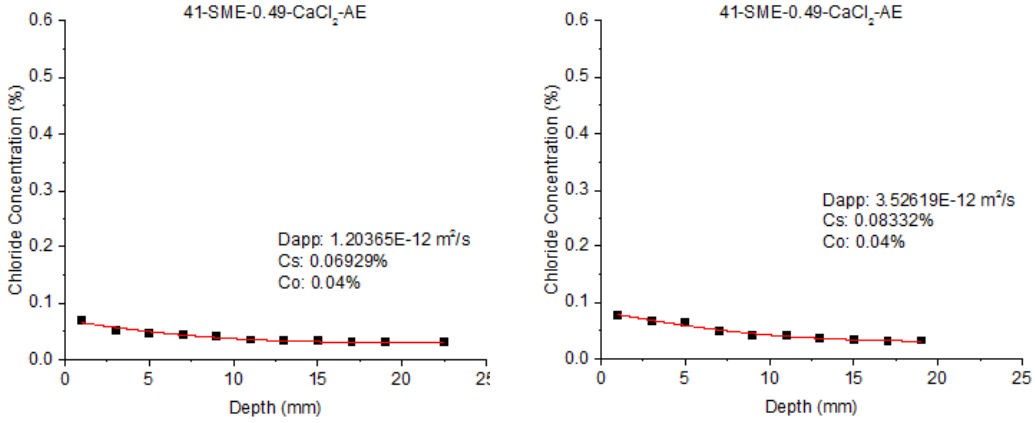

Figure A.29: SME-PS, w/c =0.49, Air = 7.0%. (a) 4, (b) 9 months of exposure to $CaCl_2$

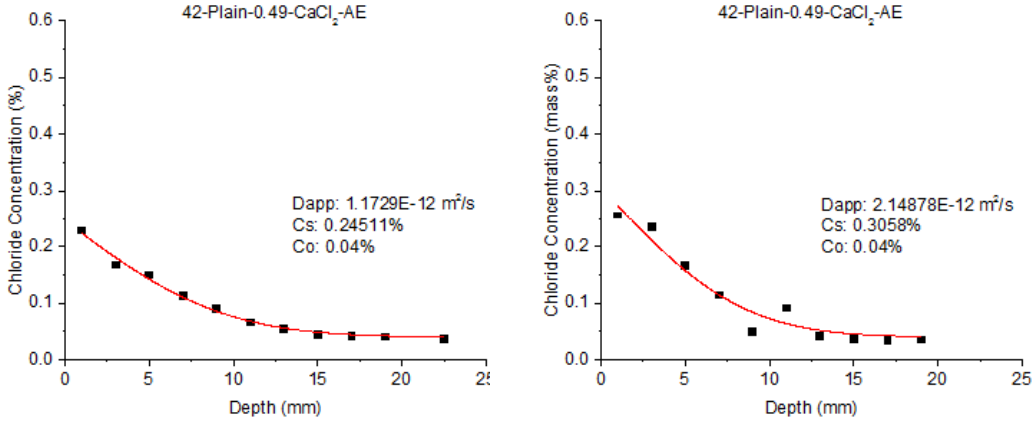

Figure A.30: No SME-PS, w/c =0.49, Air = 7.0%. (a) 4, (b) 9 months of exposure to $CaCl_2$

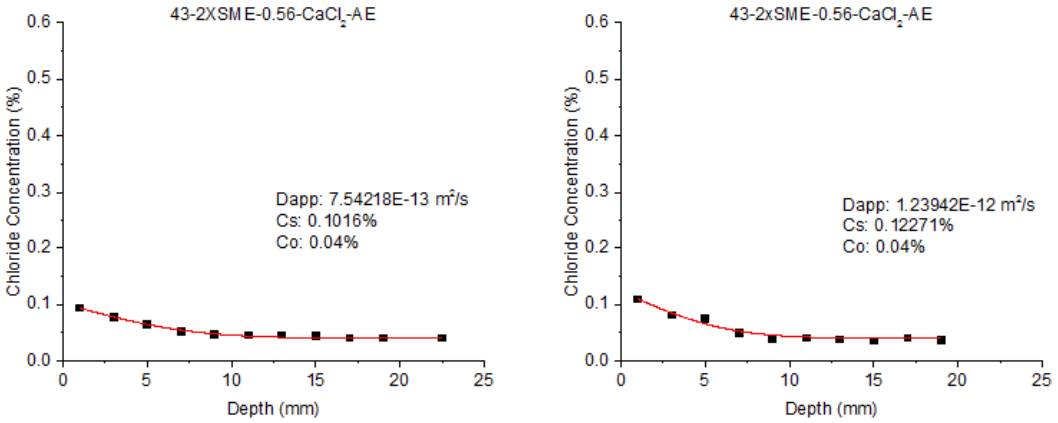

Figure A.31: 2XSME-PS, w/c =0.56, Air = 6.0%. (a) 4, (b) 9 months of exposure to $CaCl_2$

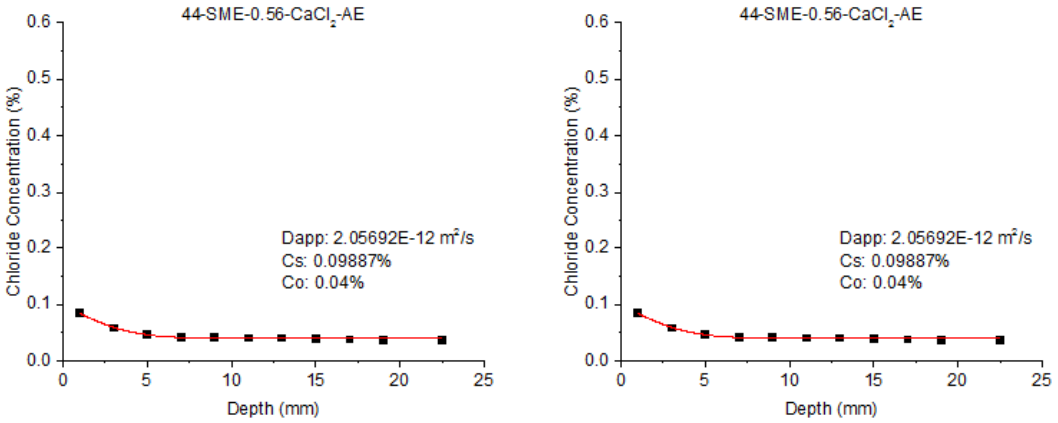

Figure A.32: SME-PS, w/c =0.56, Air = 6.0%. (a) 4, (b) 9 months of exposure to $CaCl_2$

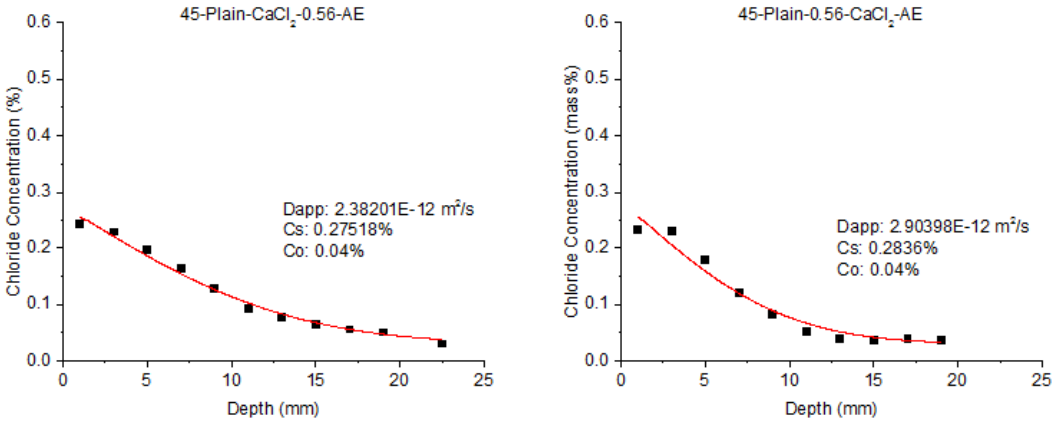

Figure A.33: No SME-PS, w/c =0.56, Air = 6.0%. (a) 4, (b) 9 months of exposure to $CaCl_2$

Appendix C- Sealer Depth of Penetration Information

TABLE A.8: Depth of SME-PS Penetration Summary (All Locations)

Location[1]	Approximate Sealer Depth of Penetration (mm)	W/C, Air Content, SAM No.	Sealer Dosage Rate[2]
13	2	0.42, 6.6%, 0.14	2
14	4	0.42, 6.6%, 0.14	1
16	4	0.49, 7.0%, 0.23	2
17	2	0.49, 7.0%, 0.23	1
19	6	0.56, 6.0%, 0.20	2
20	6	0.56, 6.0%, 0.20	1
22	2	0.49, 1.7%, 0.55	2
23	2	0.49, 1.7%, 0.55	1
26	2	0.49, 1.7%, 0.55	1
27	2	0.49, 1.7%, 0.55	2
29	6	0.56, 6.0%, 0.20	1
30	8	0.56, 6.0%, 0.20	2
32	2	0.49, 7.0%, 0.23	1
33	4	0.49, 7.0%, 0.23	2
35	4	0.42, 6.6%, 0.14	1
36	6	0.42, 6.6%, 0.14	2
37	2	0.42, 6.6%, 0.14	2
38	2	0.42, 6.6%, 0.14	1
40	4	0.49, 7.0%, 0.23	2
41	4	0.49, 7.0%, 0.23	1
43	6	0.56, 6.0%, 0.20	2
44	6	0.56, 6.0%, 0.20	1
46	4	0.49, 1.7%, 0.55	2
47	2	0.49, 1.7%, 0.55	1
Mean:	3.8		
Max:	8.0		
Min:	2.0		

Note: The slab location[1] is based on sample ID numbers specified in Figure 4-3. 0-No SME, 1-One Dosage of SME-2%PS, 2-2 Dosages of SME-2%PS[2]

Appendix D-Refit Chloride Concentration Profiles Using a Fraction of Cs

Chloride profiles developed from SME-PS treated samples extracted from the Center of Aging Infrastructure refit using a fraction of Cs in Fick's 2nd law.

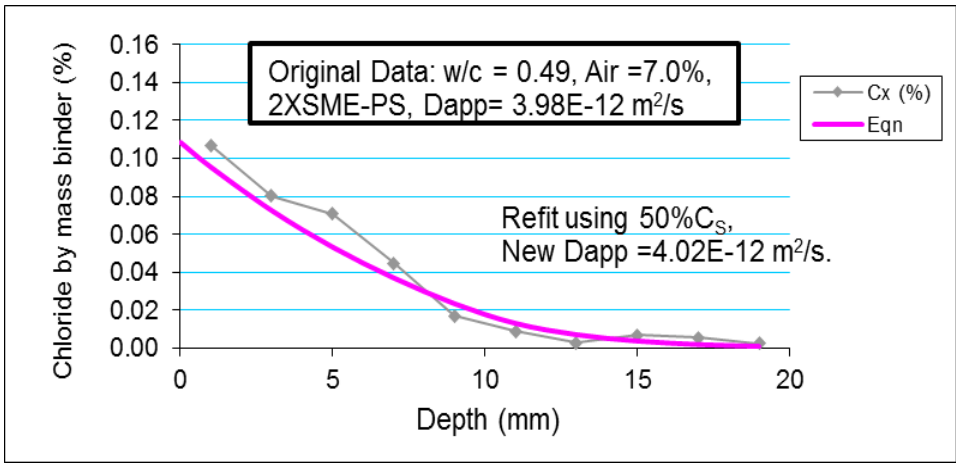

Figure A.34: Chloride profile- w/c =0.49, air content = 7.0%, refit for Dapp using 50% of Cs from a similar plain sample. Note: samples exposed to NaCl for 4 months

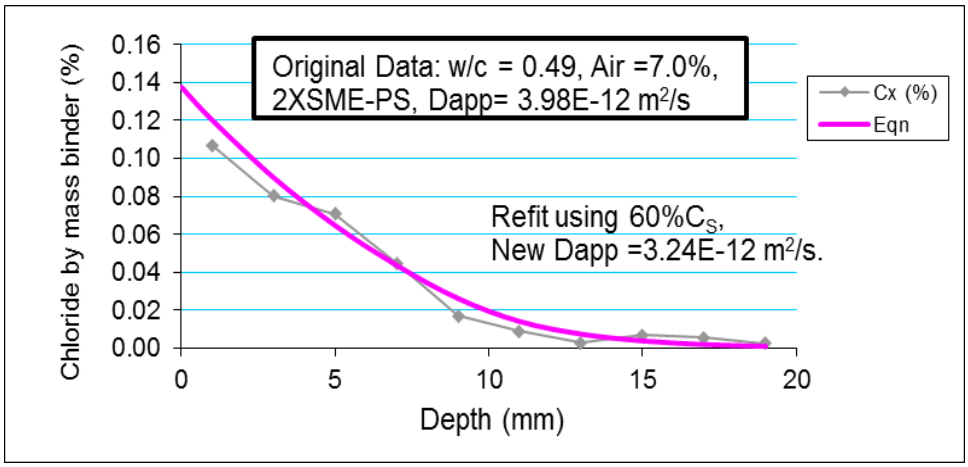

Figure A.35: Chloride profile- w/c =0.49, air content = 7.0%, refit for Dapp using 60% of Cs from a similar plain sample. Note: samples were exposed to NaCl for 4 months

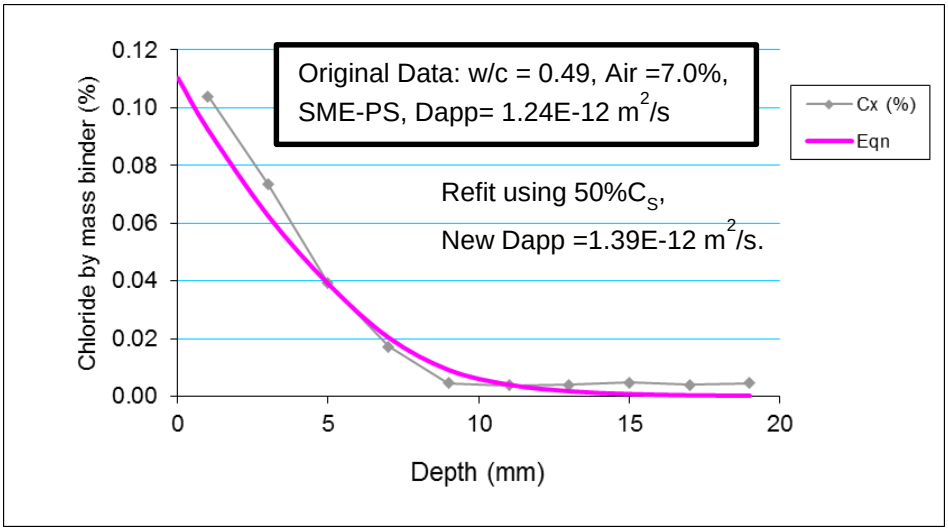

Figure A.36: Chloride profile- w/c =0.49, air content = 7.0%, refit for Dapp using 60% of Cs from a similar plain sample. Note: samples were exposed to NaCl for 4 months

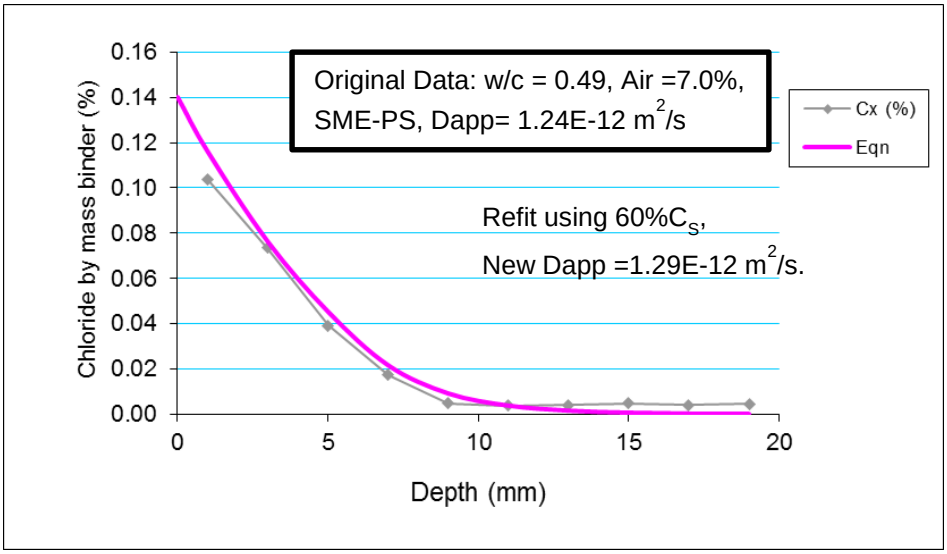

Figure A.37: Chloride profile- w/c =0.49, air content = 7.0%, refit for Dapp using 60% of Cs from a similar plain sample. Note: samples were exposed to NaCl for 4 months

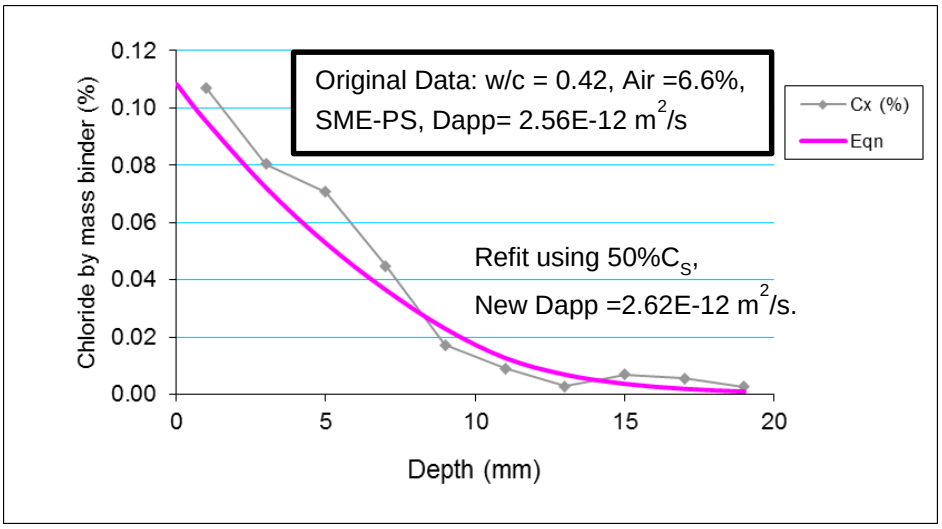

Figure A.38: Chloride profile- w/c =0.42, air content = 6.6%, refit for Dapp using 50% of Cs from a similar plain sample. Note: samples were exposed to NaCl for 4 months

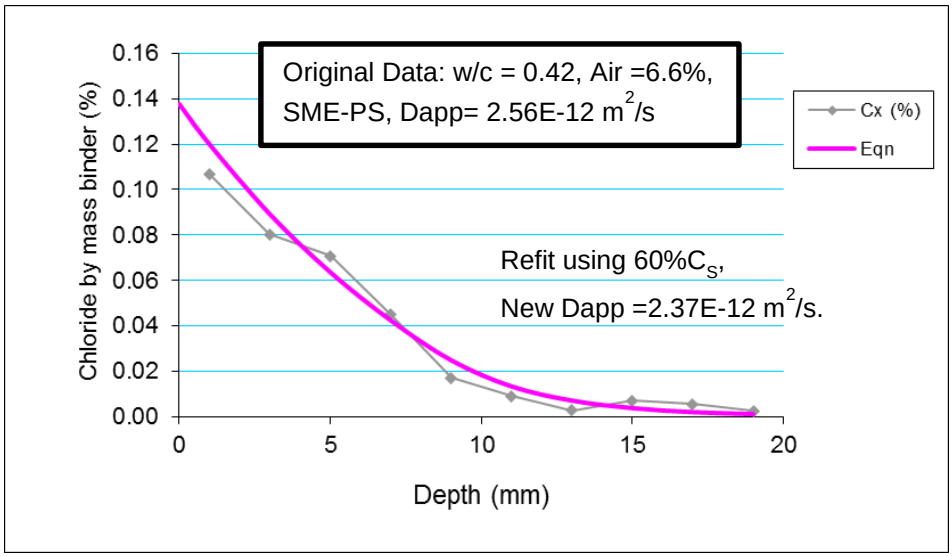

Figure A.39: Chloride profile- w/c =0.42, air content = 6.6%, refit for Dapp using 50% of Cs from a similar plain sample. Note: samples were exposed to NaCl for 4 months

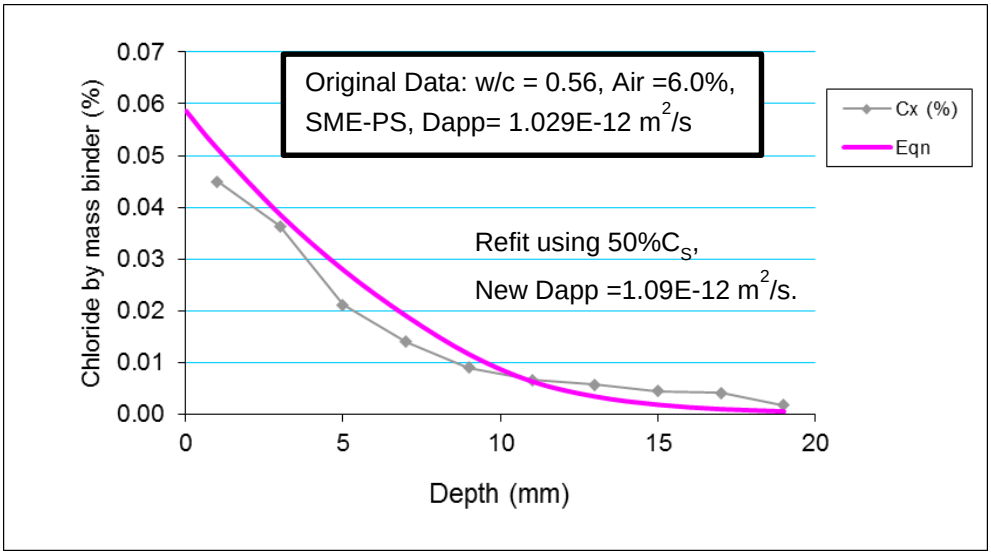

Figure A.40: Chloride profile- w/c =0.56, air content = 6.0%, refit for Dapp using 50% of Cs from a similar plain sample. Note: samples were exposed to $CaCl_2$ for 9 months

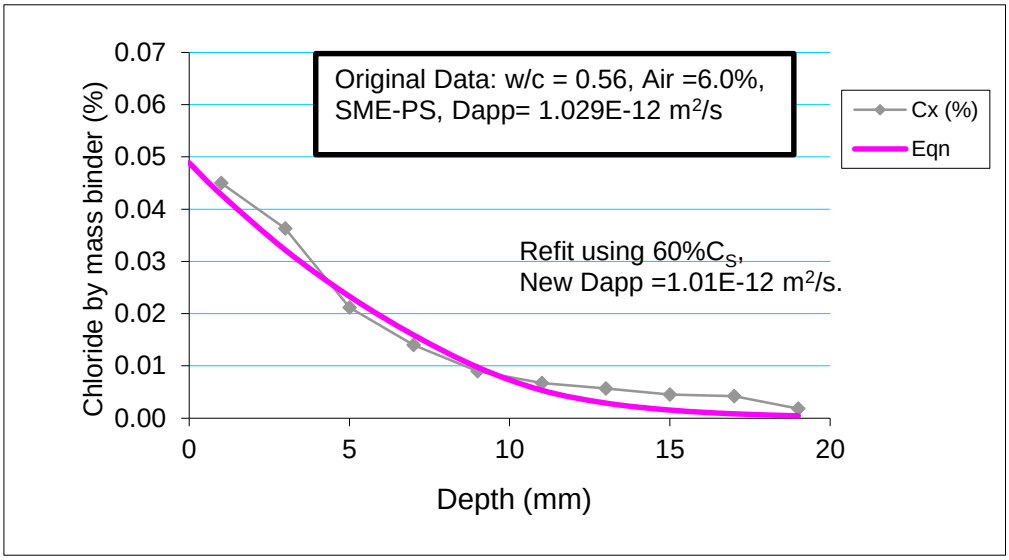

Figure A.41: Chloride profile- w/c =0.56, air content = 6.0%, refit for Dapp using 60% of Cs from a similar plain sample. Note: samples were exposed to $CaCl_2$ for 9 months

Appendix E. Graphical Representation of Data Presented in Tables

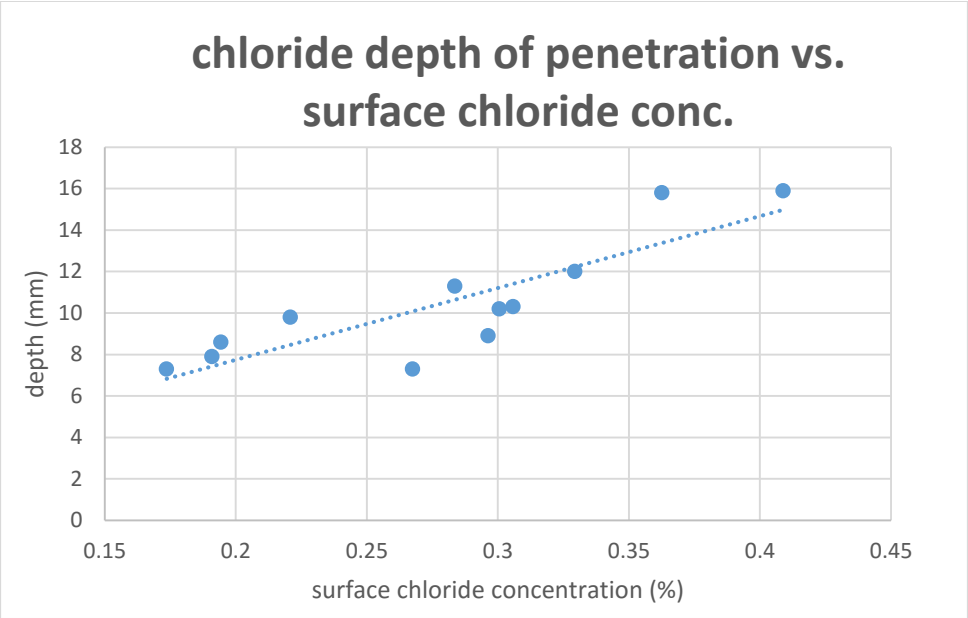

A.42: Graphical Representation of Data Presented in Table 3-10

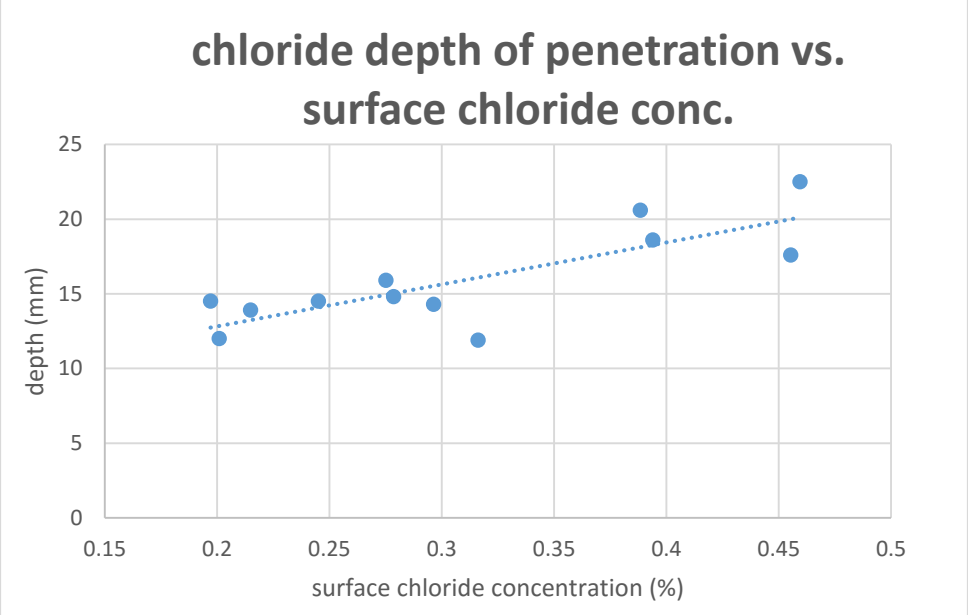

A.43: Graphical Representation of Data Presented in Table 3-11